AD-A133 127 INTERACTIVE MECHANISMS OF SLIDING-SURFACE BEARINGS(U) 1/2
DAVID W TAYLOR NAVAL SHIP RESEARCH AND DEVELOPMENT
CENTER BETHESDA MD T L DAUGHERTY ET AL. AUG 83
UNCLASSIFIED DTNSRDC-82/119 F/G 11/8 NL

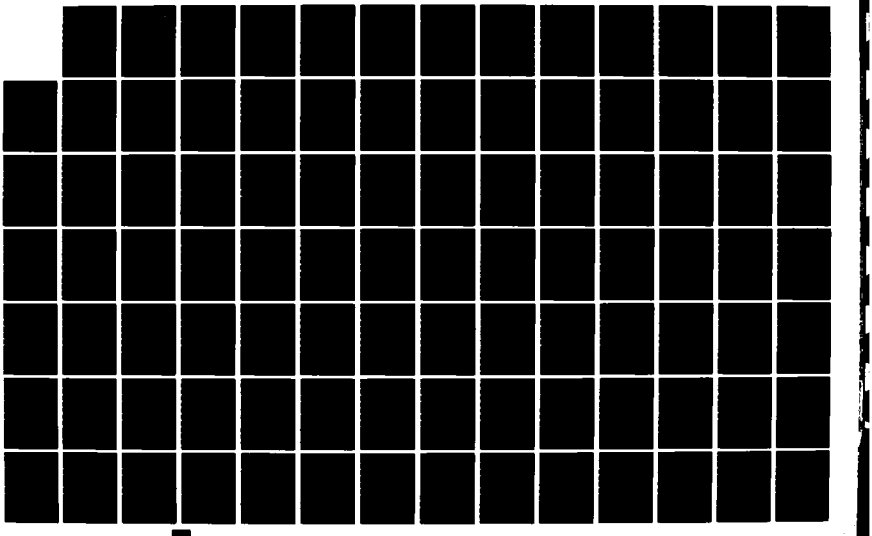

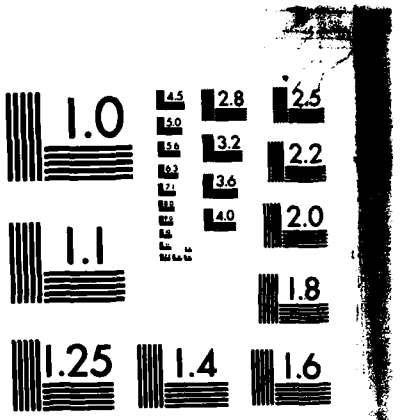

(12)





# DAVID W. TAYLOR NAVAL SHIP RESEARCH AND DEVELOPMENT CENTER

Bethesda, Maryland 20084

## INTERACTIVE MECHANISMS OF SLIDING-SURFACE BEARINGS

by

Thomas L. Daugherty, DTNSRDC

and

Coda H. T. Pan, Columbia University

APPROVED FOR PUBLIC RELEASE:
DISTRIBUTION UNLIMITED



SHIP MATERIALS ENGINEERING DEPARTMENT
RESEARCH AND DEVELOPMENT REPORT



August 1983

DTNSRDC-82/119

## MAJOR DTNSRDC ORGANIZATIONAL COMPONENTS

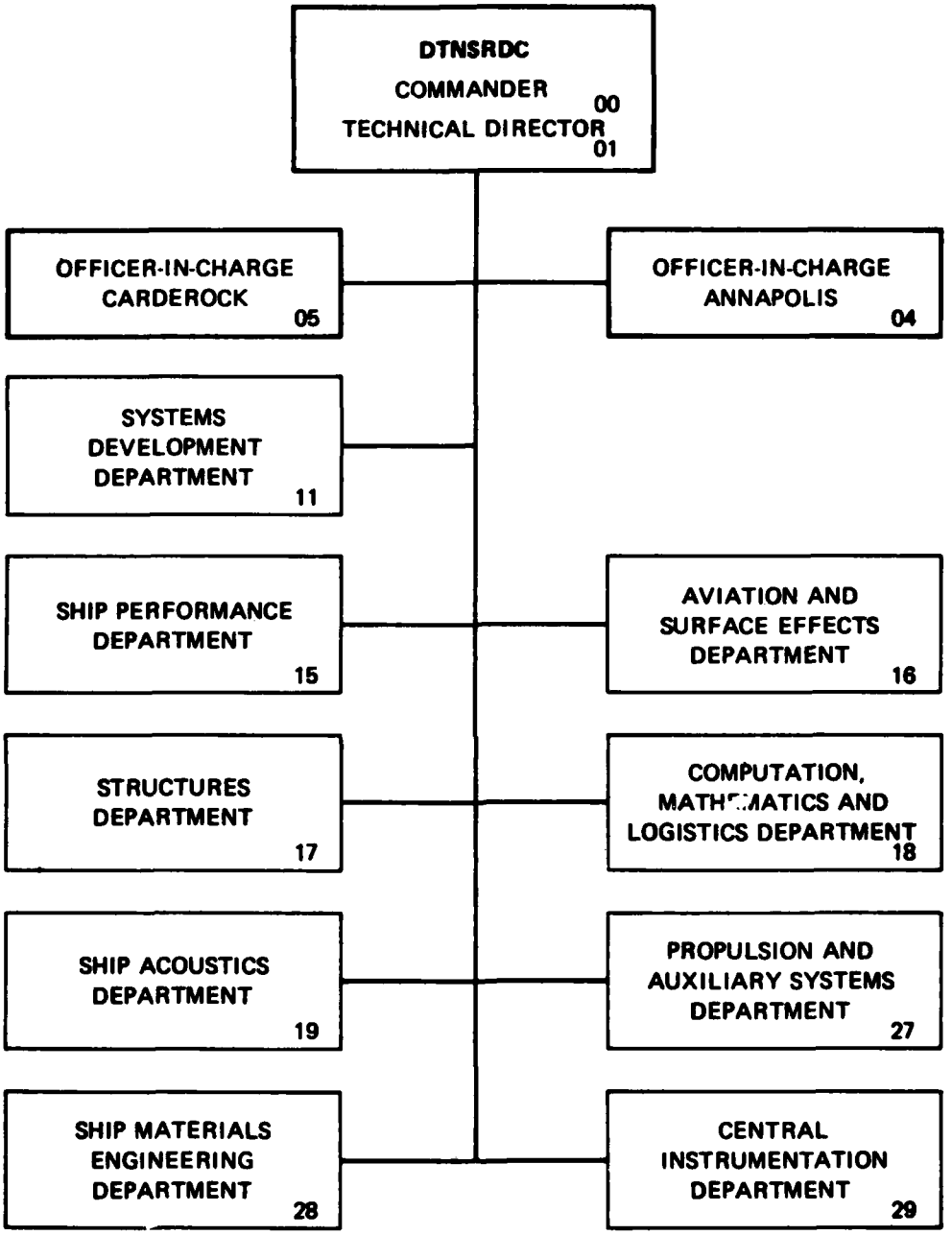

UNCLASSIFIED

SECURITY CLASSIFICATION OF THIS PAGE (When Data Entered)

| REPORT DOCUMENTATION PAGE | READ INSTRUCTIONS BEFORE COMPLETING FORM |
|---|---|
| 1. REPORT NUMBER: DTNSRDC-82/119 | 2. GOVT ACCESSION NO.: AD-A133 127 |
| | 3. RECIPIENT'S CATALOG NUMBER: |
| 4. TITLE (and Subtitle): INTERACTIVE MECHANISMS OF SLIDING SURFACE BEARINGS | 5. TYPE OF REPORT & PERIOD COVERED: Research and Development |
| | 6. PERFORMING ORG. REPORT NUMBER: |
| 7. AUTHOR(s): Thomas L. Daugherty, DTNSRDC<br>Dr. Coda H. T. Pan, Columbia University | 8. CONTRACT OR GRANT NUMBER(s): |
| 9. PERFORMING ORGANIZATION NAME AND ADDRESS: David Taylor Naval Ship R&D Center<br>Annapolis, MD. 21402 | 10. PROGRAM ELEMENT, PROJECT, TASK AREA & WORK UNIT NUMBERS: Program Element 62761N<br>Task Area SF 61-541-502<br>Work Unit 1-2832-101 |
| 11. CONTROLLING OFFICE NAME AND ADDRESS: Naval Sea Systems Command (SEA 05R25)<br>Washington, D. C. 20362 | 12. REPORT DATE: August 1983 |
| | 13. NUMBER OF PAGES: 141 |
| 14. MONITORING AGENCY NAME & ADDRESS(if different from Controlling Office) | 15. SECURITY CLASS. (of this report): UNCLASSIFIED |
| | 15a. DECLASSIFICATION/DOWNGRADING SCHEDULE |

16. DISTRIBUTION STATEMENT (of this Report)

APPROVED FOR PUBLIC RELEASE: DISTRIBUTION UNLIMITED.

17. DISTRIBUTION STATEMENT (of the abstract entered in Block 20, if different from Report)

18. SUPPLEMENTARY NOTES

19. KEY WORDS (Continue on reverse side if necessary and identify by block number)

Hydrodynamic
Mixed Lubrication
Fluid Film Bearings
Cavitation
Surface Roughness
Friction

20. ABSTRACT (Continue on reverse side if necessary and identify by block number)

The theory of hydrodynamic lubrication has been adapted in this report to include surface roughness effects and asperity interactions. This theory becomes a means of studying the behavior of sliding-surface bearings in transition from hydrodynamic into mixed lubrication. A model problem, in the form of a crowned tilt-pad bearing with longitudinal roughness, was solved. In the treatment of the model problem, end-leakage was neglected and a constant lubricant viscosity was assumed. Use of numerical computational

DD FORM 1 JAN 73 1473 EDITION OF 1 NOV 65 IS OBSOLETE
S/N 0102-014-6601

UNCLASSIFIED

SECURITY CLASSIFICATION OF THIS PAGE (When Data Entered)

(Block 20 continued)

methods could readily remove these restrictions.

In real life operating environments of ship components and shipboard machinery, the lubrication process is made more complex by thermo-elastohydrodynamic effects and the likely occurrence of film striation. Because these complicated phenomena are only qualitatively understood, no adequate or comprehensive method exists for designing critical machine components such as face seals, elastomeric sterntube bearings, rudder stock, diving plane bearings, and main shaft thrust bearings. This report

The work presented herein is part of a more comprehensive plan to develop a better understanding of the interactive wear mechanisms of sliding surfaces. The theoretical basis is the application of Reynolds' equation to the mixed lubrication regime. A closed-form solution of Reynolds' equation applied to a crowned tilt-pad thrust bearing in transition from the hydrodynamic to the mixed lubrication region is presented to demonstrate some of the principles of this approach. Associated topics related to the extension of such analyses are also discussed. Concepts developed herein are applicable to a wide variety of bearings and seals. The concepts They provide a basis for future work in tribology of improved machinery design methods.

| Accession For | |
|---|---|
| NTIS GRA&I | X |
| DTIC TAB | ☐ |
| Unannounced | ☐ |
| Justification | |
| By | |
| Distribution/ | |
| Availability Codes | |
| Dist | Avail and/or Special |
| A | |

TABLE OF CONTENTS

## LIST OF FIGURES



## LIST OF TABLES

## NOMENCLATURE

| | |
|---|---|
| $a_0$, $a_1$, $a_2$ | Coefficients in polynominal expansion of $E\{h^3\}$ |
| $A_c$ | Area fraction of asperity contact |
| A, B, C, D | Corners of sector pad |
| $A_i$, $B_i$ | Coefficients at ith mesh point |
| $\vec{A}$ | Arbitrary vector |
| $A_r$, $A_\theta$, $A_z$ | (Radial, circumferential, axial) component of $\vec{A}$ |
| $[A^{(0)}]_j$, $[A^{(-)}]_j$, $[A^{(+)}]_j$ | Matrices in conduction problem [equation (2-34)] |
| $b_0$, $b_1$, $b_2$ | Coefficients in polynominal expansion of $6\eta UE\{H\}$ |
| $[B_I]$ | Influence coefficient matrix of $\{q_I\}$ on $\{T\}_1$ |
| b | Width of bearing pad |
| c | Half total range of the random film thickness variable, $\delta$ |
| $\bar{c}$ | $c/\sigma$ |
| $c_0$, $c_1$, $c_2$ | Coefficients of polynomial expansion |
| C | Nominal bearing clearance |
| $C_E$ | Constant of integration |
| $C_V$ | Specific heat at a constant volume process |
| $C_i$, $D_i$ | Coefficients at ith mesh point |
| D/Dt | Substantive time derivative |
| $E_e$ | Specific internal energy |
| E, F | Mid-points of radial sector sides |
| E { } | Expectation or stochastic average of { } |
| $E_O$ { } | Uninterfered expectation of ( ) |
| $\Delta E$ { } | Expectation deficiency of ( ) due to interference |
| $F_F$ | Frictional force |

| | |
|---|---|
| $F_N$ | Normal force |
| f | A stochastic function |
| F (x, y/h) | Temperature profile as a function of x and $y/h$ |
| G | Symmetrical polynomial generating function for stochastic computations |
| H | Film thickness, including roughness deviations |
| h | Smooth fluid film thickness, $h = h_2 - h_1$ |
| $h_1$, $h_2$ | Distance to (lower, upper) bearing surface from reference bearing surface |
| $h_a$ | Circumferential crown |
| $h_b$ | Radial crown |
| $h_c$ | Crown increment |
| $h_d$ | Edge pitching |
| $h_e$ | Edge rolling |
| $h_f$ | Radial helix |
| $h_s$ | Longitudinal roughness deviation function of one surface |
| $h_T$ | Heat transfer coefficient at exposed surface |
| i | Mesh point index, ranges from 1 to N+1 |
| $\vec{i}_r$, $\vec{i}_\theta$, $\vec{i}_z$ | Unit base vectors of the cylindrical polar coordinate system |
| $I_k$ | kth moment integral of inverse viscosity; k may be 0, 1, or 2 |
| $I_C$ | Viscosity weighted, Couette velocity profile function |
| $I_P$ | Viscosity weighted, Poiseuille velocity profile function |
| $I_n$ | nth moment integral of G |
| $J_C$, $J_P$ | Integral of ($I_C$, $I_P$) |

| | |
|---|---|
| $K_C$, $K_P$ | Viscosity weighted (Couette, Poiseuille) temperature transport integral |
| L | Bearing pad length |
| $m_1$, $m_2$ | Coefficents in Walther-ASTM formula for temperature effect on viscosity |
| M, N | Mid-points of peripheral sector arcs |
| $\vec{n}$ | Unit vector perpendicular to the nominal bearing surface |
| $N_T$ | Total number of mesh intervals |
| O | Origin |
| p | Pressure of fluid film |
| $p_c$ | Cavitation pressure |
| $p_i$ | Pressure of fluid film at $x_i$ |
| P | Center point of sector |
| $P_1$, $P_2$ | Histogram of probability density function of roughness deviations of (lower, upper) bearing surface |
| $P(h_s)$ | Probability distribution function of $h_s$ |
| $q_x$ | x - component of flow flux |
| $q_z$ | z - component of flow flux |
| $\vec{q}$ | Conduction heat flux |
| $\{q_I\}$ | Column vector representing conduction heat flux at bearing surface by body I |
| Q | Specific internal dissipation |
| r | Radial coordinate in polar notation |
| $r_i$ | Inner radius of sector |
| $r_m$ | Mean radius of sector |
| $r_o$ | Outer radius of sector |
| R | Nominal radius |

| | |
|---|---|
| $S$ | Exposed surface of bearing |
| $t$ | Time |
| $T$ | Fluid temperature |
| $T_A$ | Ambient temperature |
| $\{T\}_j$ | Column vector representing temperature in body I at $y_j$ |
| $T_S$ | Temperature of exposed surface |
| $u$ | x Component of fluid velocity |
| $U$ | Sliding speed |
| $\vec{U}$ | Fluid velocity component tangential to the nominal bearing surface |
| $U_1$, $U_2$ | x component of $\vec{U}$ at (lower, upper) bearing surface |
| $\vec{V}$ | Fluid velocity vector |
| $V$ | Reference value of $\vec{V}$ |
| $w$ | Thickness of body I |
| $W_1$, $W_2$ | z component of $\vec{U}$ at (lower, upper) bearing surface |
| $x_c$ | Coordinate of the cavitation or rupture boundary |
| $x_i$ | Coordinate of ith mesh point |
| $x$, $y$, $z$ | Cartesian coordinates |
| $y_j$ | Discretized y coordinate |
| $y'$ | Dummy variable of integration for y |
| $\alpha$ | Arc angle of sector |
| $\beta$ | Bulk coefficient of thermal expansion |
| $\delta$ | Roughness deviation |
| $\delta_0$ | Skew-bias of roughness deviation |
| $\bar{\delta}_0$ | $\delta_0/\sigma$ |

| | |
|---|---|
| $\delta_1, \delta_2$ | Roughness deviations of (lower, upper) bearing surface, $(h_1-H_1,\ h_2-H_2)$ |
| $\delta\ (\ )$ | Increment of ( ) |
| $\Delta x$ | Mesh interval |
| $\Theta$ | Film integral of temperature |
| $\theta$ | Circumferential angular coordinate |
| $\theta_s$ | Root mean third moment stochastic integral of $\delta$ |
| $\overline{\theta}_s$ | $\theta_s/\sigma$ |
| $\kappa$ | Thermal conductivity of fluid |
| $\kappa_I$ | Thermal conductivity of body I |
| $\mu$ | Viscosity coefficient of fluid |
| $\mu_0$ | Reference viscosity coefficient |
| $\nu$ | Kinematic viscosity coefficient of fluid |
| $\xi$ | $x - x_i$ |
| $\rho$ | Fluid density |
| $\sigma$ | Combined roughness |
| $\sigma_1,\ \sigma_2$ | Rms value of $(\delta_1,\ \delta_2)$ |
| $\tau$ | Viscous shear stress |
| $\phi$ | Leakage flux through bearing surfaces |
| $\Phi$ | Film flux (expectation of) |
| $\Phi_0, \Phi_1,\ \Phi_2$ | Coefficients in polynomial expansion of $\phi$ |
| $\vec{\Psi}$ | Film flux vector |
| $\omega$ | Angular rotational speed |
| $\omega_1,\ \omega_2$ | Angular rotational speed of (lower, upper) bearing surface |
| $\nabla$ | Three-dimensional gradient operator |

| | |
|---|---|
| $\nabla$ | Two-dimensional surface gradient operator |
| $( )_f$ | Pertaining to the bearing surface |
| $( )_I$ | Pertaining to body I |

## ABSTRACT

The theory of hydrodynamic lubrication has been adapted in this report to include surface roughness effects and asperity interactions. This theory becomes a means of studying the behavior of sliding-surface bearings in transition from hydrodynamic into mixed lubrication. A model problem, in the form of a crowned tilt-pad bearing with longitudinal roughness, was solved. In the treatment of the model problem, end-leakage was neglected and a constant lubricant viscosity was assumed. Use of numerical computational methods could readily remove these restrictions.

In real-life operating environments of ship components and shipboard machinery, the lubrication process is made more complex by thermo-elastohydrodynamic effects and the likely occurrence of film striation. Because these complicated phenomena are only qualitatively understood, no adequate or comprehensive method exists for designing critical machine components such as face seals, elastomeric sterntube bearings, rudder stock, diving plane bearings, and main shaft thrust bearings.

The work presented herein is part of a more comprehensive plan to develop a better understanding of the interactive wear mechanisms of sliding surfaces. The theoretical basis is the application of Reynolds' equation to the mixed lubrication regime. A closed-form solution of Reynolds' equation applied to a crowned tilt-pad thrust bearing in transition from the hydrodynamic to the mixed lubrication region is presented to demonstrate some of the principles of this approach. Associated topics related to the extension of such analyses are also discussed. Concepts developed herein are applicable to a wide variety of bearings and seals. They provide a basis for future work in tribology of improved machinery design methods.



## ADMINISTRATIVE INFORMATION

This report covers work conducted under the Marine Tribology Block Program (PE62761N, Task Area SF 61-541-502, Work Unit 2832-101). The coauthor, Dr. Coda H. T. Pan, is a consultant with DTNSRDC under Contract N00167-81-0149. Dr. Pan is a Professor of Mechanical Engineering at Columbia University. The Marine Tribology Block program is sponsored by Dr. H. H. Vanderveldt of NAVSEA 05R25.

## INTRODUCTION

Most sliding-surface bearings are designed to operate with the bearing fully separated from its mating surface by a lubricant film. These bearings are referred to as self-acting or hydrodynamic bearings. The lubricant film develops load capacity, primarily due to a wedge effect between the moving surfaces. Various lubrication modes of such bearings can be explained by considering the Stribeck curve shown in Figure 1. The Stribeck curve represents the general characteristics[1*] of lubricated moving surfaces as a function of the lubricant viscosity, $\mu$, the velocity, V, and the normal load, $F_N$ (or pressure, p). As Figure 1 shows, there are three main lubrication regimes: hydrodynamic, mixed, and boundary. The regime of operation depends upon the geometry, the materials, the operating conditions, and the relative geometry of the opposing surfaces.

In the hydrodynamic regime a wedge of lubricant provides a thick enough lubricant film to keep the surfaces completely separate, such that their combined roughness, $\sigma$, is substantially smaller than the local film thickness, h. The frictional resistance results from viscous shearing of the lubricant. Since the surfaces are separated, no contact wear takes place. Under these conditions, analytical techniques for the study of bearing performance are well developed.

Mixed lubrication begins when the local film thickness, h, approaches that of the combined surface roughness, $\sigma$, of the bearing and the mating surfaces. The pressure generated by the hydrodynamic wedge effect and by the asperity contact between the bearing and the mating surface share the load support. Wear occurs at the contact points. Frictional resistance is a result of these asperity interactions plus shearing of the lubricant.

As load is increased and/or speed or lubricant viscosity are decreased, the coefficient of friction and the wear rate increase rapidly. Eventually all load will be supported by asperity contacts. This is the boundary lubrication region. Physico-chemical interactions at the solid-lubricant-solid interface determine the friction and wear behavior.

In a wide variety of sliding surface bearing and seal applications in ships, not enough lubricant film exists under certain operating conditions to completely

---

*References are listed on page 81.

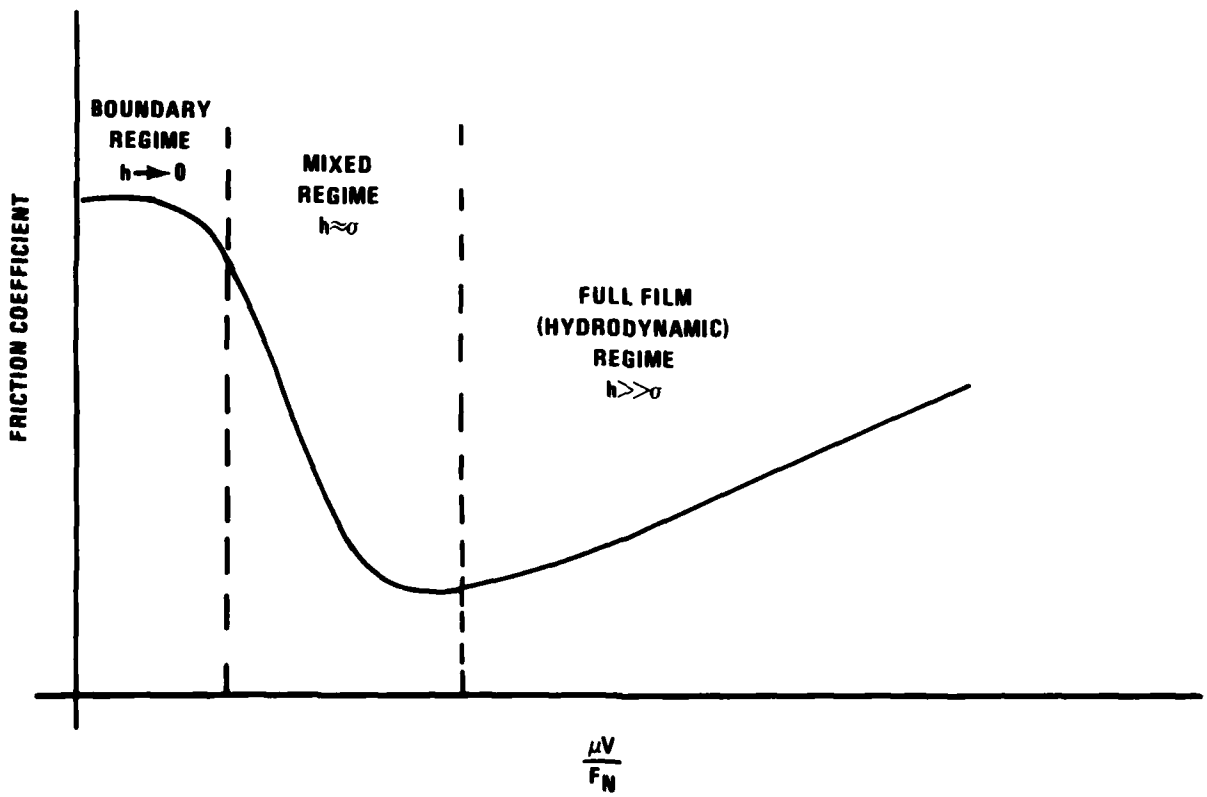


Figure 1 - Stribeck Curve Showing the Three Main Lubrication Regimes. The Characteristics of Moving Lubricated Surfaces are a Function of Lubricant Viscosity, $\mu$, the Velocity, V, and the Normal Load, $F_N$; h is the Fluid Film Thickness and $\sigma$ the Combined Roughness of the Surfaces.

separate the mating surfaces. Such conditions cause mechanical wear. Examples are ship main thrust bearings, lineshaft journal bearings, and compliant-surfaced sterntube and strut bearings. For these bearings, films are often inadequate at slow shaft speeds and under transient conditions of starts and stops. Face seals are unique in having to operate most of their lives in a contact and wear mode, since they are designed to minimize leakage. A good face seal design thus successfully controls wear during normal operation without adequate fluid film.

Even though the design methodology for full-film sliding-surface bearings is relatively well established, tribology laboratories regularly perform friction and wear tests in search of better bearing materials. The challenge is to improve service reliability of ever more complex mechanical systems. A comprehensive knowledge of the interactive wear mechanisms of sliding surfaces is of paramount importance. Because of the multitude of phenomena involved, an interdisciplinary point of view must be maintained. Friction and wear studies, which are traditionally pursued with empirical methods, can and must be vitalized by computer-aided techniques of design, analysis, and research. Theory for mixed lubrication plays a pivotal role in the meaningful study of interactive wear mechanisms. It should address four main issues.

- o How can one predict the start of asperity interactions?
- o What are the important thermo-mechanical consequences of asperity interactions?
- o What are the relevant roles of lubricant chemistry, surface chemistry, and near-surface behavior of materials?
- o How does the wear process alter the topographical and chemical properties of the surface?

Progress in finding answers to these questions will advance design technology for machinery systems in ships.

## BACKGROUND

Reynolds' equation has been used to study hydrodynamics of lubricating films since its development by Professor Osborne Reynolds[2] in 1886. It is a differential equation for the pressure distribution in a lubricant film and takes into account the density and viscosity of the lubricant, the velocities of the

solid surfaces, and the shape of the lubricant film. The most general Cartesian form of Reynolds' equation can be written as:

$$\frac{\partial}{\partial x}\left(\frac{h^3\rho}{\mu}\frac{\partial p}{\partial x}\right)+\frac{\partial}{\partial z}\left(\frac{h^3\rho}{\mu}\frac{\partial p}{\partial z}\right)=6\left\{2\frac{\partial}{\partial t}\left(\rho h\right)+\frac{\partial}{\partial x}\left[\rho h\left(U_1+U_2\right)\right]+\frac{\partial}{\partial z}\left[\rho h\left(W_1+W_2\right)\right]\right\}$$

where: h = smooth fluid film thickness

p = pressure of fluid film

x,z = cartesian coordinates

$\rho$ = fluid density

$\mu$ = fluid viscosity

t = time

$U_1, U_2$ = x-component of fluid velocity component tangential to lower and upper bearing surface, respectively.

$W_1, W_2$ = z-component of fluid velocity component tangential to lower and upper bearing surface, respectively.

The following assumptions are inherent in the development of Reynolds' equation:

- o The lubricant is Newtonian -- that is, the shear stress in the lubricant is proportional to the rate of shear.
- o The flow is laminar.
- o The fluid film thickness is negligibly small in comparison with the overall scale of the bearing.
- o Fluid inertia is negligible.
- o The lubricant adheres to the surfaces (no slip).
- o No external forces act on the lubricant.
- o The lubricant viscosity is uniform across the film.

A thrust bearing usually has sector pads. It is more natural to study the sector pad in cylindrical polar coordinates. The corresponding Reynolds' equation is

$$\frac{\partial}{r\partial\theta}\left(\frac{h^3\rho}{\mu}\frac{\partial p}{r\partial\theta}\right)+\frac{\partial}{r\partial r}\left(\frac{rh^3\rho}{\mu}\frac{\partial p}{\partial r}\right)$$

$$=6\left[2\frac{\partial}{\partial t}\left(\rho h\right)+\frac{\partial}{\partial\theta}\left[\rho h\left(\omega_1+\omega_2\right)\right]\right]$$

where: r = the radial coordinate in polar notation

$\theta$ = the circumferential angular coordinate in polar notation

$\omega_1, \omega_2$ = the angular rotational speed of the lower and upper bearing surfaces

In allowing $(\omega_1, \omega_2)$ to appear as independent quantities, a duo-rotation system can be considered. Often the rectangular form approximation is used, and in the case of an incompressible lubricant, one has

$$\frac{\partial}{\partial x}\left(\frac{h^3}{\mu}\frac{\partial p}{\partial x}\right) + \frac{\partial}{\partial z}\left(\frac{h^3}{\mu}\frac{\partial p}{\partial z}\right)$$

$$= 6\left\{2\frac{\partial h}{\partial t} + (U_1+U_2)\frac{\partial h}{\partial x} + h\frac{\partial}{\partial x}(U_1+U_2)\right\}$$

The terms on the right hand side of the equation are referred to as the squeeze term, the wedge term, and the stretch term, respectively. The stretch term is seldom of any importance. This form of equation can be used to study the two-dimensional tilt pad bearing illustrated in Figure 2. In this particular instance, the surface of the tilt pad does not have a sliding motion ($U_1 = 0$).

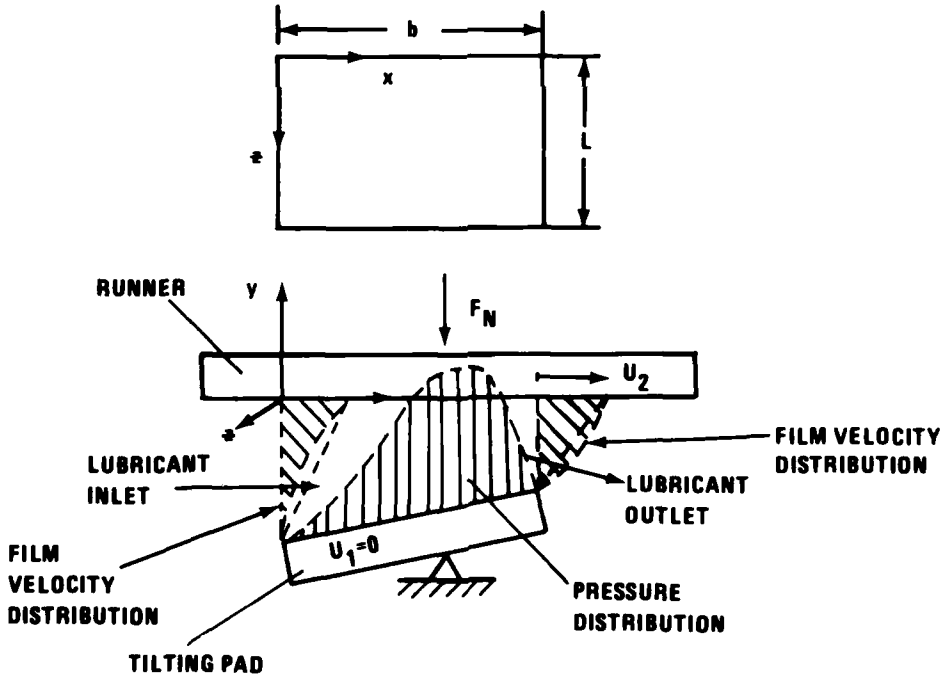


Figure 2 - Two-Dimensional Tilt Pad Bearing; Top View Shows Width, b, and Length, L, of Bearing

The pressure distribution in the lubricant film can be determined by integrating in the x and z direction, yielding the load capacity, $F_N$, as

$$F_N = \int_0^L \int_0^b p(x,z)\, dx\, dz$$

The flow per unit width in the x direction is

$$q_x = (U_1 + U_2)\frac{h}{2} - \frac{h^3}{12\mu}\frac{dp}{dx}$$

and in the z direction

$$q_z = -\frac{h^3}{12}\frac{\partial p}{\partial z}$$

The friction force, $F_F$, in the lubricating film is the sum of the velocity-induced and pressure-induced shear stresses as

$$F_F = \pm \int_0^L \int_0^b \frac{\mu(U_2 - U_1)}{h}\, dx\, dz - \frac{1}{2}\int_0^L \int_0^b h\frac{\partial p}{\partial x}\, dx\, dz$$

where the plus and minus signs are used for the force acting on the lower and upper surfaces, respectively. The film thickness must be describable in terms of x and z for use in Reynolds' equation.

Other simplifications are usually possible in applying Reynolds' equation to hydrodynamic bearings. For steady state conditions the squeeze term, $\partial h/\partial t$, vanishes. If the bearing and mating surfaces are made of rigid material, the stretch term also vanishes. In most applications the bearing speed, $U_1$, is zero. Reynolds' equation now becomes, writing $U = U_2$

$$\frac{\partial}{\partial x}\left(\frac{h^3}{\mu}\frac{\partial p}{\partial x}\right) + \frac{\partial}{\partial z}\left(\frac{h^3}{\mu}\frac{\partial p}{\partial z}\right) = 6\,U\frac{\partial h}{\partial x}$$

If the viscosity can be considered constant over the entire domain, further simplification can be made:

$$\frac{\partial}{\partial x}\left(h^3\frac{\partial p}{\partial x}\right) + \frac{\partial}{\partial z}\left(h^3\frac{\partial p}{\partial z}\right) = 6\,\mu\,U\frac{\partial h}{\partial x}$$

This equation is most commonly used to determine the pressure distribution, from which one can determine the bearing load capacity and the friction for operation that is free of asperity interactions (hydrodynamic conditions).

Reynolds' equation has also been applied to the region of mixed lubrication, where load is supported by both hydrodynamic pressure and asperity contacts. Christensen[3] proposed stochastic models to permit consideration of surface roughness. For the one-dimensional, longitudinal roughness (Figure 3), he recast the Reynolds' equation in terms of mean or expected values of pressure and film thickness parameters[4]:

$$\frac{\partial}{\partial x}\left[E\left\{H^3\right\}\frac{\partial}{\partial x}E\left\{p\right\}\right] + \frac{\partial}{\partial z}\left[\frac{1}{E\{1/H^3\}}\frac{\partial}{\partial z}E\left\{p\right\}\right] = 6\mu U\frac{\partial}{\partial x}E\left\{H\right\}$$

where: H = the fluid film thickness, including roughness deviations

E{ } = the expectation or stochastic average of { }

The corresponding film thickness profile was treated as

$$H = h(x,z) + h_s(z)$$

Where h is the smooth part of the film thickness profile and $h_s(z)$ represents the roughness deviations, which are assumed to be on one of the two surfaces. Independence of $h_s$ on x indicates the longitudinal topography. Stochastic description of the roughness deviations is represented by the probability distribution function, which is assumed to have the polynomial form of

$$P(h_s) = \frac{35\left(c^2 - h_s^2\right)^3}{32c^7} \qquad -c \le h_s \le c$$

where: $P(h_s)$ = the probability distribution function of $h_s$

c = half the total range of the random film thickness variable, $\delta$

E {}is the ensemble average with respect to the assumed probability distribution function. As a model problem, Christensen analyzed in detail the infinitely long, tapered slider.

Christensen's approach was applied to a crowned, tilt-pad bearing (shown in Figure 4) under a David Taylor Naval Ship R&D Center contract. Crowning was introduced to simulate initial pad crown and distortions during operation due to pad loading and thermal gradients. The tilt-pad feature required the pad inclination to be determined by the condition of moment equilibrium about the pivot point. This condition included the contribution of asperity contact friction, which would become prominent in mixed lubrication. The technical report of this analysis is included as Appendix A. Although the predicted frictional

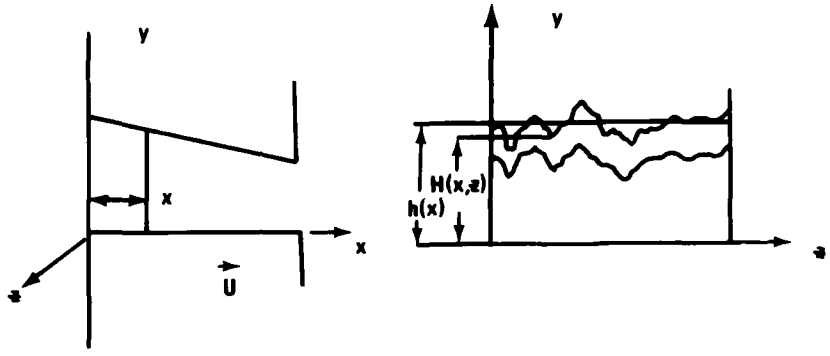


Figure 3 - Christensen's Longitudinal, One-Dimensional Roughness Model

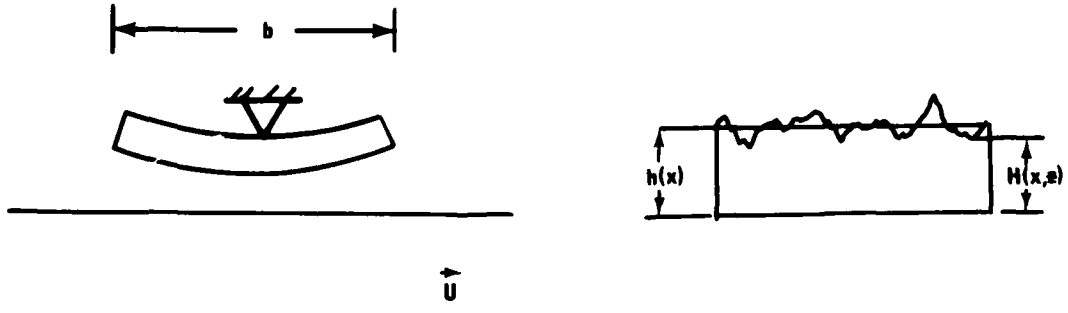


Figure 4 - Crowned Tilt-Pad Bearing with Longitudinal, One-Dimensional Roughness

performance of the tilt-pad thrust bearing in the hydrodynamic and mixed lubrication region resemble experimental results, several theoretical issues remain. These can be grouped as follows:

- o Film striation or cavitation
- o Thermo-elastohydrodynamic effects
- o Computation techniques
- o Surface roughness effects

In the rest of this report we have addressed theoretical approaches to various topics under these headings. These approaches may serve as guidelines for future in-depth studies.

## THEORETICAL TOPICS RELATED TO THE STUDY OF MIXED LUBRICATION OF SLIDING SURFACE BEARINGS

### 1. FILM STRIATION

Film striation often occurs in sliding bearings. Part of the bearing gap is filled with gaseous and/or vaporous constituents at close to ambient pressure. The boundaries of the striation region must be accurately determined for computation of the film pressure, the flow rate, the viscous shear stress, and viscous heating. The following derivations incorporate film rupture into the computation of pressure and shear in a fluid film.

#### Incipience Point of Film Rupture

On page 93 of Appendix A, pressure gradient and pressure of the hydrodynamic film, respectively, are given as

$$\frac{dp}{dx} = 6\mu U[E(H)+C_E]/E\{H^3\} \tag{1-1}$$

$$p = 6\mu U\left[\int_0^x \frac{E\{H\}dx}{E\{H^3\}} + C_E\int_0^x \frac{dx}{E\{H^3\}}\right] \tag{1-2}$$

If a full film is allowed to occupy the entire shoe length, then the constant of integration, $C_E$, is to satisfy the ambient condition imposed at the exit point of the fluid film:

$$p(b) = 0 \tag{1-3}$$

or

$$C_E = -\int_0^b \frac{E\{H\}dz}{E\{H^3\}} \Big/ \int_0^b \frac{dx}{E\{H^3\}} \tag{1-4}$$

as indicated in Appendix A. However, in the case of a converging-diverging film profile, Equations (1-2) and (1-4) can result in a subambient pressure domain immediately preceding the exit edge. The latter circumstance violates common experience. It is generally believed that a subambient pressure condition in a fluid film cannot be sustained; instead, the film ruptures or cavitates somewhere so that the ambient condition will be reached internally with a vanishing pressure gradient. This is known as the Reynolds-Swift-Stieber condition of film rupture or cavitation and is stated as

$$p(x_c) = 0 \tag{1-5}$$

$$\frac{dp}{dx}\bigg|_{x_c} = 0 \tag{1-6}$$

$$0 < x_c < b \tag{1-7}$$

To satisfy Equation (1-6), Equation (1-1) yields

$$C_E = -E\{H\}\Big|_{x_c} \tag{1-8}$$

Substitute Equation (1-8) into Equation (1-2), setting $x=x_c$; one obtains

$$p(x_c) = 6\mu U \left[ \int_0^{x_c} \frac{E\{H\}dx}{E\{H^3\}} - E\{H\} \Big|_{x_c} \int_0^{x_c} \frac{dx}{E\{H^3\}} \right] \tag{1-9}$$

This may be regarded as a transcendental equation, the root of which yields the location of the beginning of film rupture or the cavitation domain.

The necessary steps to determine the root of Equation (1-9) can be readily incorporated into a computer program. Equation (1-9) can be regarded as a residual function and can be obtained within the cycle of numerical quadratures for the two integrals. Sign reversal of the residual function signifies that the beginning of film rupture had just been overtaken, and a simple interpolation would yield its location and the correct value of $C_E$ quite accurately.

In common bearing configurations, the bearing gap continues to diverge until the exit edge of the bearing pad is reached, so that there is no need to consider whether the full-film condition can be re-established. Even the full cylindrical journal bearing usually has a feed-groove or a feed-hole located in the unloaded part of the bearing surface, so that it may be regarded as a circular arc of approximately 360°, and the maximum gap point can be assumed to be the end of the rupture domain or the full-film reestablishment point.

Viscous Shear of a Striated Film

The film flux of a bearing with ruptured film is $\frac{1}{2}UE(H)\big|_{x_c}$. In the domain $x_c < x \leq b$, this film flux is insufficient to fill the local film thickness $E(H)\big|_x$. According to the striation model of film rupture, the local striation length fraction is $E(H)\big|_{x_c}/E(H)$. Accordingly the local viscous shear stress, $\tau$, is

$$\tau \Big|_{x_c \leq x \leq b} = \mu U \frac{E(H)\Big|_{x_c}}{E(H)} E\left(\frac{1}{H}\right) \tag{1-10}$$

The analysis presented in Appendix A is a closed integral solution to Reynolds' equation. End leakage is neglected. During operation lubricant flow occurs not only in the direction of motion (leading edge to trailing edge) but also leaks along ends of the pad. Such end leakage can significantly affect the load capacity of the bearing by bleeding off pressures built up in the film. Fuller[5] presented an approximate procedure to account for end leakage through the use of a correction factor for the load and the minimum film thickness. The correction factor was based on the experimental data for a tapered wedge with bearing width-to-length ratio ranging from ¼ to 5¾. Such an approximate procedure for correcting end leakage can be used in conjunction with the analysis of Appendix A. A later section of this report, Finite Difference Computation of the Infinitely Long Slider (in the section on computation techniques under "High Accuracy Numerical Algorithm for Computing Fluid Film Pressure"), presents approaches for considering the use of finite difference techniques to prepare a more thorough treatment of end leakage.

## 2. THERMO-ELASTOHYDRODYNAMIC EFFECTS

### General Discussion

Thin-film lubrication is prevalent in many critical machine elements in naval propulsion and shipboard machine systems. Trouble-free operation of such machine elements depends on the control of subtle geometrical details of the film, details that are readily influenced by elastic and thermoelastic deformations of the surfaces. Rational design procedures for such machine elements have not been developed. The derivations in the following sections provide general guidance for the development of such analytical engineering tools.

The possibility of adjusting surface geometry for optimization of designs was eloquently demonstrated by Rayleigh's classic paper[5], and elastohydrodynamic and thermo-elastohydrodynamic effects in thin-film machine elements are especially important in naval applications.

For various reasons, lubrication by very thin fluid films in naval machine elements is likely to be associated with pressure distribution that can significantly deflect the lubricated surface. At the same time, the viscous shear stress in the fluid film, which is responsible for the generation of load-carrying film pressure, necessarily also generates heat and accompanying temperature rise and temperature gradients in the machine parts. Important thermal phenomena include reduction of fluid viscosity, differential thermal growths (due to different coefficients of thermal expansion of various materials in the machine structure), and thermal distortions (due to temperature gradients regardless of the temperature level).Three major categories of machine elements deserve particular recognition in relation to studies of thermo-elastohydrodynamic effects. An example in the first category is the thrust bearing in a ship propulsion system, which carries the load caused by sea pressure acting on an unbalanced area and by vessel acceleration. The study of tilting-shoe thrust bearings first revealed the significance of thermo-elastohydrodynamic effects. Thermally induced surface crowning is probably responsible for the stabilization of the pitch-roll motions of the bearing shoes. An example in the second category is the dynamic seal, which not only keeps water out of the ship interior but also prevents lubricants and process fluids from contaminating the cabin environment. Although "contact" operation is often assumed for low-leakage seals, current belief holds that low wear rate is critically dependent on the effective generation of film pressure to maintain a stable, partial separation of the mating surfaces. Several mechanisms have been suggested to explain the likely existence of load-carrying film pressure in low-leakage face seals: namely, hydrodynamic wedge action due to runner misalignment or thermoelastic waviness of the mating surfaces; pressure-induced gap convergence; and evaporation of leakage fluid. An example from the third category of machine elements, one that has fascinated researchers studying probable thermo-elastohydrodynamic effects, is the sterntube bearing, which is constructed of elastomeric staves. A relatively large coefficient of thermal expansion and a relatively small shear modulus make the elastomeric stave bearing a prime subject for study of both the beneficial and the harmful effects that have been attributed to these properties. Table 1 illustrates the essential thermo-elastohydrodynamic phenomena associated with these three machine elements.

TABLE 1 - THERMO-ELASTOHYDRODYNAMIC PHENOMENA IN TYPICAL NAVAL MACHINE ELEMENTS

| Machine Element and Load Type | Film Parameters | | | | | | Load-Related Elastic Distortion | Thermal Growth | Material Mismatch | Thermal Distortion | Catastrophic Thermal Phenomena |
|---|---|---|---|---|---|---|---|---|---|---|---|
| | Minimum Gap | Crowning | Convergence | Tilt | Local Deformation | Waviness | | | | | |
| Thrust Bearing Speed-Dependent Propulsive Force | X | X | | X | | | | | | X | X |
| Face Seal Pressure-Dependent Closing Force | X | | X | | | X | X | | X | X | X |
| Sterntube Bearing Speed-Dependent Gravity and Maneuver Force | X | | | X | X | | X | X | | | X |

The generic machine element of interest consists of two bodies, which are respectively designated as (1) and (2), and a thin fluid film that permits low friction relative sliding between the two bodies. The internal mutual action between the two bodies is transmitted, for the most part, through the enveloping surfaces of the thin film in the form of distributed traction. Friction heating in the thin film is due to viscous dissipation and may also be associated with asperity contact sliding. The latter can precipitate tribological trauma and thus cause catastrophic failure. Under ordinary circumstances, friction heating is converted into sensitive heat, raising the temperature of the two bodies and the circulating fluid.

Conservation laws of mass, momentum, and energy as applied to each of the three parts of the system and as applied to the overall system are the foundation for the thermo-elastohydrodynamic analysis of machine elements. The essential elements of the mathematical statements of this problem are derived below.

## Conservation Laws for the Fluid Film

The significance of thermo-elastohydrodynamic analysis for machine elements was broadly discussed above in connection with naval machine systems. The generic machine element is a system consisting of two bodies separated by a thin film of a viscous fluid. The functional behavior of the machine element depends on the dynamic and thermal interactions between the thin fluid film and the two surrounding bodies. The present section summarizes the applicable equations specifically pertaining to the thin fluid film.

For an incompressible Newtonian lubricant, the mathematical theory of lubrication is usually presented in terms of the Reynolds' equation, which is summarized in the contemporary form as follows:

$$\vec{\Psi} = \vec{U}_1 h + (\vec{U}_2 - \vec{U}_1) J_C - (\nabla p) J_P \qquad (2\text{-}1a)$$

$$\nabla \cdot \vec{\Psi} + \frac{\partial h}{\partial t} + \Sigma \phi = 0 \qquad (2\text{-}1b)$$

where: $\vec{\Psi}$ = the film flux vector

$J_C$ = the integral of the viscosity weighted Couette velocity profile function

$J_P$ = the integral of the viscosity weighted Poiseuille velocity profile function

$\nabla$ = the two-dimensional surface gradient operator

$\phi$ = leakage flux through bearing surfaces

In the "surface" vector form presented here, these expressions are valid for all flat and moderately curved surfaces. Figure 5 illustrates a generic representation of such a pair of surfaces. The film geometry has two length scales; R is the size scale of the bearing while C is the separation scale representing the nominal bearing clearance.

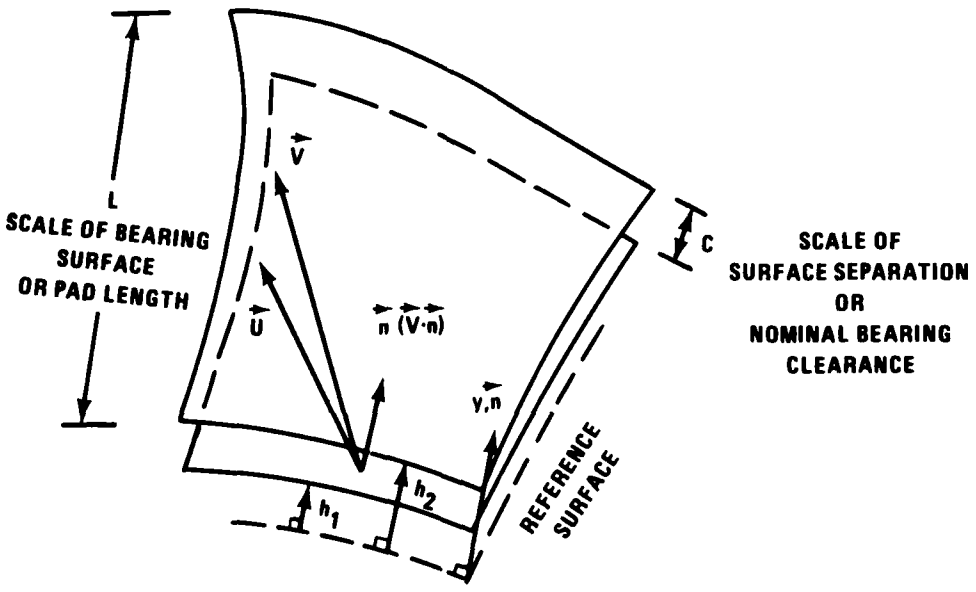


Figure 5 - Thin Film Between Nearly Parallel Surfaces

A suitably chosen reference surface is used to define the geometry of lower and upper bearing surfaces in terms of their respective normal distances ($h_1$, $h_2$). A unit normal, $\vec{n}$, can be defined at every point of the reference surface; it can be regarded to be also perpendicular to either bearing surface and is usually "outwardly" directed by convention. The three-dimensional fluid velocity $\vec{V}$ is described by its normal component $\vec{V}\cdot\vec{n}$ and its tangential component $\vec{U}$; the latter can further be decomposed into appropriate surface components according to the representation of the reference surface. $\nabla$ is the surface gradient operator, which is constrained to exclude the normal component of the conventional three-dimensional gradient operator.

The radius of curvature of the reference surface is, by definition, of the same order as the size scale. The separation to size ratio C/L, is typically $10^{-4}$ to $10^{-3}$. A necessary, but sometimes overlooked, assumption is

$$\left|\nabla(h_1,h_2)\right| = 0\left\{\frac{C}{L}\right\} \tag{2-2}$$

Where O{ }means "order of { }." Any discontinuities in ($h_1$, $h_2$) will require special attention. $\vec{\Psi}$ is the tangential (to the reference surface) flux vector and is obtained by integrating the tangential velocity component with respect to the separation between the two surfaces:

$$\vec{\Psi} = \int_{h_1}^{h_2} \vec{U}\, dy \tag{2-3}$$

Subscripts (1, 2) as applied to $\vec{U}$ and h refer to the lower and upper surfaces, respectively. The film pressure p is regarded as invariant with respect to the film thickness coordinate y in the lubrication theory. $h = h_2 - h_1$ is the local separation between the surfaces. $\Sigma\phi$ accounts for porosity of the bearing surfaces and is the sum of the (wall) penetration flow rate per unit area of the two surfaces.

Simplification of the Navier-Stokes' equations to the lubrication theory, as represented by Equations (2-1a) and (2-1b), requires a number of prior assumptions. Let V be the scale of fluid velocity. The necessary assumptions to ensure validity of the lubrication theory include the following:

(1) Components of the dyad $\nabla \vec{V}$ are dominated by the term $(\vec{n}\cdot\nabla)\vec{U}$ which is of O {V/C}. Consequently, the stress tensor enters into the momentum conservation law through the term

$$\nabla\cdot\iota = -\nabla p + (\vec{n}\cdot\nabla)\,[\mu(\vec{n}\cdot\nabla)\vec{U}]$$

where: $\nabla$ = the three-dimensional gradient operator

$\nabla\cdot\iota$ = the dot product of the three-dimensional gradient operator and the viscous shear stress

$\vec{n}$ = the unit vector perpendicular to the nominal bearing surface

$\vec{V}$ = the fluid velocity vector

$$\nabla\cdot\iota = O\left\{\frac{\mu_0 V}{C^2}\right\}$$

$\mu_o$ is the nominal viscosity coefficient; the actual viscosity coefficient may vary throughout the lubricant film.

(2) The film Reynolds' number $(\rho VC/\mu_o)$ (C/L) is of negligible magnitude.

(3) Mass conservation is satisfied with $\nabla\cdot\vec{U}$ and $(\vec{n}\cdot\vec{V})$ $(\vec{n}\cdot\vec{V})$, cancelling out each other so that

$$|\vec{U}| = O\{V\};\quad |\vec{n}\cdot\vec{V}| = O\left\{\frac{CV}{L}\right\}$$

(4) The flow field is laminar. Consistent with these assumptions, the fluid pressure can be shown to have negligible variation in the normal direction. The momentum conservation law is reduced to

$$\nabla p = \frac{\partial}{\partial y}\left(\mu\frac{\partial\vec{U}}{\partial y}\right) \qquad (2\text{-}4)$$

which can be integrated with respect to y twice; upon imposing nonslip conditions at the surfaces, one obtains

$$\vec{U} = \vec{U}_1 + (\vec{U}_2 - \vec{U}_1)\ I_C - (\nabla p) I_P \tag{2-5}$$

where: $I_C = I_0(y)/I_0(h_2)$

$I_P = I_1(h_2)\ I_C - I_1(y)$

$$I_k(y) = \int_{h_1}^{y} \frac{y'^k dy'}{\mu} \tag{2-6a,b,c}$$

$I_k$ is the kth moment integral of inverse viscosity. $I_C$ and $I_P$ are, respectively, velocity profile functions associated with shear and pressure effects.

The lubricant viscosity, at common operating environments of fluid film bearings, should be regarded as temperature dependent. If, however, one chooses to accept the isoviscous approximation, $\mu = \mu_o$ = const., then

$$(I_C)_{isoviscous} = \frac{(y-h_1)}{(h_2-h_1)}$$

$$(I_P)_{isoviscous} = \frac{(h_2-y)(y-h_1)}{2\mu_o} \tag{2-7a,b}$$

These functions are seen to describe the Couette and Poiseuille velocity profiles, respectively. The coefficients ($J_C$, $J_P$) in Equation (2-1a) are obtained by substituting Equations (2-5) and (2-6a, b) into Equation (2-3) and carrying out suitable integrations formally:

$$J_C = \int_{h_1}^{h_2} I_C\, dy; \quad J_P = \int_{h_1}^{h_2} I_P\, dy \tag{2-8a,b}$$

And for the isoviscous approximation,

$$(J_C)_{isoviscous} = \frac{1}{2}(h_2 - h_1) = \frac{1}{2}h$$

$$(J_P)_{isoviscous} = \frac{(h_2 - h_1)^3}{12\mu_0} = \frac{h^3}{12\mu_0}$$

(2-9a,b)

Accurate determination of the film pressure requires a suitable allowance for the temperature dependence of viscosity, so that Equation (2-8a,b) instead of (2-9a,b) can be used. Therefore, it is of interest to examine the energy conservation law as applied to the lubricant film flow process. The complete governing equation of energy in a liquid is

$$\rho \frac{DE_e}{Dt} + \beta p \frac{DT}{Dt} = Q + \nabla\cdot(\kappa\nabla T)$$

(2-10)

where $E_e$ is the specific internal energy, $\beta$ is the bulk coefficient of thermal expansion, Q is the internal dissipation, $\kappa$ is the thermal conductivity, and T is the fluid temperature. (D/Dt) is the substantive time derivative which includes the convective derivative to account for fluid motion. For common conditions in fluid film bearings, the second term on the left hand side of Equation (2-10) can be neglected. Also, consistent with the approximations already invoked in the lubrication theory, the terms on the right hand side may be simplified as

$$Q = \mu\left(\frac{\partial\vec{U}}{\partial y}\right)\cdot\left(\frac{\partial\vec{U}}{\partial y}\right)$$

$$\nabla\cdot(\kappa\nabla T) = \frac{\partial}{\partial y}\left(\kappa\frac{\partial T}{\partial y}\right)$$

(2-11a,b)

If asperity contacts occur because of surface roughness, the dissipation term, Equation (2-11a), should be increased to reflect sliding friction effects.

Also, writing $DE_e = C_v DT$, $C_v$ being the specific heat for a constant volume process, then the applicable energy equation which defines the temperature field in the fluid film is

$$\rho C_v \frac{DT}{Dt} = \mu\left(\frac{\partial \vec{U}}{\partial y}\right)\cdot\left(\frac{\partial \vec{U}}{\partial y}\right) + \frac{\partial}{\partial y}\left(\kappa \frac{\partial T}{\partial y}\right) \tag{2-12}$$

For the steady-state problem,

$$\rho C_v (\vec{V}\cdot\nabla) T$$

$$= \mu\left(\frac{\partial \vec{U}}{\partial y}\right)\cdot\left(\frac{\partial \vec{U}}{\partial y}\right) + \frac{\partial}{\partial y}\left(\kappa \frac{\partial T}{\partial y}\right) \tag{2-13}$$

This equation is of the parabolic type and its rigorous field solution is to satisfy an inlet temperature profile and suitable continuity conditions of heat flux at the surfaces. Equation (2-13) can also be expressed in the thin film integral form:

$$\rho C_v \nabla\cdot \int_{h_1}^{h_2} (\vec{U}T)\, dy$$

$$= \int_{h_1}^{h_2} \mu\left(\frac{\partial \vec{U}}{\partial y}\right)\cdot\left(\frac{\partial \vec{U}}{\partial y}\right) dy + \left(\kappa \frac{\partial T}{\partial y}\right)\Bigg|_1^2 \tag{2-14}$$

Equation (2-14) can be utilized to seek an approximate temperature field without dealing with the full complexity of Equation (2-13). Both the convective term on the left hand side and the dissipation term, the first term on right hand side, need to be known as integrals across the surface separation; they can tolerate crude approximations without introducing very serious errors. The last term is to be matched with conduction heat flux entering the bodies which surround the fluid film.

The cylindrical polar coordinate system can be used for the three-dimensional, geometrical representation of either the cylindrical journal bearing or the thrust bearing. The complete three-dimensional gradient operator is

$$\nabla = \vec{i}_r \frac{\partial}{\partial r} + \vec{i}_\theta \frac{1}{r} \frac{\partial}{\partial \theta} + \vec{i}_z \frac{\partial}{\partial z}$$

The components of a vector $\vec{A}$ are designated by the subscripts (r,θ,z) respectively. The divergence operation takes on the form

$$\nabla \cdot \vec{A} = \frac{1}{r} \frac{\partial}{\partial r} (rA_r) + \frac{1}{r} \frac{\partial A_\theta}{\partial \theta} + \frac{\partial A_z}{\partial z}$$

The sliding velocity is due to rotation:

$$\vec{U} = \vec{i}_\theta \omega r$$

If both surfaces slide, then subscripts (1,2) would be associated with the rotational speed, $\omega$. In the case of the counter-rotating shafting, ($\omega_1$, $\omega_2$) would have opposite signs.

For the cylindrical journal bearing, the nominal reference surface is a circular cylinder. The normal direction is radial. Equations (2-1a,b) thus become

$$\vec{\Psi} = \vec{i}_\theta \left\{ \left[ \omega_1 h + (\omega_2 - \omega_1) J_C \right] r - \frac{J_P}{r} \frac{\partial p}{\partial \theta} \right\} + \vec{i}_z \left( - J_P \frac{\partial p}{\partial z} \right)$$

$$O = \frac{1}{r^2} \frac{\partial}{\partial \theta} \left\{ \left[ \omega_1 h + (\omega_2 - \omega_1) J_C \right] r^2 - J_P \frac{\partial p}{\partial \theta} \right\} - \frac{\partial}{\partial z} \left( J_P \frac{\partial p}{\partial z} \right) + \frac{\partial h}{\partial t} + \Sigma \phi$$

(2-15a,b)

The radial coordinate r can, within the accuracy of the lubrication theory, be regarded as a constant and be equated to the nominal journal radius, R.

For the thrust bearing, the nominal reference surface is a radial plane. The normal direction is axial. Reynolds' equation takes on the form

$$\vec{\Psi} = \vec{i}_\theta \left\{ \left[ \omega_1 h + (\omega_2 - \omega_1) J_C \right] r - \frac{J_P}{r} \frac{\partial p}{\partial \theta} \right\} + \vec{i}_r \left( - J_P \frac{\partial p}{\partial r} \right)$$

$$O = \frac{1}{r^2}\frac{\partial}{\partial\theta}\left\{\left[\left|\omega_1 h + (\omega_2 - \omega_1) J_C\right| r^2 - J_P \frac{\partial p}{\partial\theta}\right\} - \frac{1}{r}\frac{\partial}{\partial r}\left(r J_P \frac{\partial p}{\partial r}\right) + \frac{\partial h}{\partial t} + \Sigma\phi\right.$$

(2-16a,b)

In contrast to Equation (2-15), in which r=R is a constant, r in Equation (2-16) is the radial coordinate.

To restate the energy equation in a more usable form, each term in Equation (2-14) will be separately examined. For either bearing type, the integrated dissipation can be rewritten as

$$\int_{h_1}^{h_2} Q\, dy = \frac{(\omega_2 - \omega_1)^2 r^2}{I_0(h_2)} + \left|\nabla p\right|^2 I_2(h_2)$$

(2-17)

$I_0$ and $I_2$ are moment integrals, respectively of the 0th and 2nd orders, of the inverse of the viscosity coefficient as given previously by Equation (2-6c).

The surface conduction terms do not need further attention. The convective heat transfer terms differ slightly in form for the two bearing types, mainly in the divergence operator:

$$\rho C_v \nabla\cdot \int_{h_1}^{h_2} (\vec{U}T)\, dy$$

$$= \rho C_v \left\{\frac{\partial}{\partial\theta}\left[\left|\omega_1\Theta + (\omega_2 - \omega_1) K_c\right| - \nabla\cdot(K_p \nabla p)\right\}\right.$$

(2-18)

where,

$$\Theta = \int_{h_1}^{h_2} T\, dy$$

$$K_C = \int_{h_1}^{h_2} \Pi_C\, dy$$

$$K_P = \int_{h_1}^{h_2} \Pi_P\, dy$$

(2-19a,b,c)

For the cylindrical journal bearing,

$$\nabla\cdot(K_P\nabla p) = \frac{1}{r^2}\frac{\partial}{\partial\theta}\left(K_P\frac{\partial p}{\partial\theta}\right) + \frac{\partial}{\partial z}\left(K_P\frac{\partial p}{\partial z}\right)$$

(2-20)

while for the thrust bearing,

$$\nabla\cdot(K_P\nabla p) = \frac{1}{r^2}\frac{\partial}{\partial\theta}\left(K_P\frac{\partial p}{\partial\theta}\right) + \frac{1}{r}\frac{\partial}{\partial r}\left(K_P r\frac{\partial p}{\partial r}\right)$$

(2-21)

The fluid film is not a closed system regarding the conservation laws. The following are sources of interactions between the fluid film and the two surrounding bodies:

(1) Global equilibrium of the machine element requires that the internal load and moment transmitted through the fluid film be related to the kinematics of the two surrounding bodies and the externally imposed constraints.

(2) The surface separation, $h = h_2 - h_1$, which is the dominant factor in the generation of the film pressure, is significantly affected by thermoelastic deformations of the two bodies. Thermoelastic deformations, in turn, result from temperature fields caused by viscous heating which is moderated by convective and conductive cooling effects as described by Equations (2-14,17,18). A major computational difficulty is associated with the accurate determination of the temperature field with its simultaneous conduction-convection effects.

(3) The surface separation is also affected by elastic deformations caused by film pressure. This aspect is quite important in sterntube bearings because of the compliant elastomeric staves. It is also important for high-pressure face seals. Load-induced cross-sectional twisting of the seal ring can be considerable in comparison with the thickness of the film formed by leakage flow. Elastic deformation from film pressure is less important for tilting-shoe thrust and tilting-shoe journal bearings, where pitch-roll equilibrium becomes an inherent feature of the overall analysis.

(4) Temperature distribution across the film thickness, in addition to the surface temperature fields, influence the film pressure because of the temperature dependence of lubricant viscosity. Equations (2-6a,b,c) pertain to this issue.

(5) Surface permeability due to material porosity can also affect film pressure. It can be important in the friction behavior of the retainer-roller contact of rolling element bearings.

Thermal Effects

Thermal coupling between the fluid film and surrounding bodies stems from two independent physical causes: (1) temperature dependence of lubricant; and (2) thermal distortion of bearing surfaces.

The Walther-ASTM formula may be used to determine the kinematic viscosity, $\nu$, from two data points:

$$\log\log(\nu + 0.6) = m_1 \log T + m_2 \qquad (2\text{-}22)$$

where $\nu$ and T are, respectively, in units of centistokes and degrees Rankine and $m_1$ and $m_2$ are coefficients which depend upon the oil. If the temperature distribution within the fluid film is known, then the weighted integrals of the reciprocal of viscosity coefficient can be accordingly calculated:

$$I_k(y) = \int_{h_1}^{y} \frac{y'^k dy'}{\mu(T)} \tag{2-23}$$

where y' is a dummy variable of integration for y

$$I_C(y) = I_0(y)/I_0(h_2)$$

$$I_P(y) = I_1(h_2)\, I_C(y) - I_1(y) \tag{2-24a,b}$$

$$J_c = \int_{h_1}^{h_2} I_C\, dy$$

$$J_p = \int_{h_1}^{h_2} I_P\, dy \tag{2-25a,b}$$

Subsequently, the film pressure can be found by solving the generalized Reynolds' equation for a fluid contained between nonpermeable, smooth walls:

$$\nabla \cdot \vec{\psi} + \frac{\partial h}{\partial t} = 0$$

$$h = h_2 - h_1$$

$$\vec{\psi} = \vec{U}_1 h + (\vec{U}_2 - \vec{U}_1) J_C - (\nabla p) J_P \tag{2-26a,b,c}$$

$\vec{U}_1$ and $\vec{U}_2$ are sliding velocity vectors of the lower and upper surfaces, respectively. The film velocity profile is

$$\vec{U} = \vec{U}_1 + (\vec{U}_2 - \vec{U}_1) I_C - (\nabla p) I_P \tag{2-27}$$

The temperature field itself is to be found by solving the thin-film energy equation:

$$\rho C_v (\vec{V}\cdot\nabla)T = \mu\left(\frac{\partial\vec{U}}{\partial y}\right)\cdot\left(\frac{\partial\vec{U}}{\partial y}\right) + \frac{\partial}{\partial y}\left(\kappa\frac{\partial T}{\partial y}\right) \tag{2-28}$$

$\vec{V}$ is the three-dimensional velocity vector. $\partial\vec{U}/\partial y$ can be found by differentiating Equation (2-27), yielding

$$\frac{\partial\vec{U}}{\partial y} = \frac{(\vec{U}_2 - \vec{U}_1)}{\mu I_0(h_2)} - (\nabla p)\left(\left[\frac{I_1(h_2)}{I_0(h_2)} - y\right]\left(\frac{1}{\mu}\right)\right) \tag{2-29}$$

Equation (2-28) is truly three-dimensional; it is of the parabolic type, being first order in the tangential direction and second order in the normal direction. Needless to say, its complete solution is a formidable task. Thus, it is often desirable to accept the compromise of tackling the integral form of the energy equation:

$$\rho C_v \nabla\cdot\int_{h_1}^{h_2}(\vec{U}T)\,dy = \frac{(\omega_2-\omega_1)^2 r^2}{I_0(h_2)} + \left|\nabla p\right|^2\left\{I_2(h_2) - \frac{\left[I_1(h_2)\right]^2}{I_0(h_2)}\right\} + \kappa\frac{\partial T}{\partial y}\Big|_1^2 \tag{2-30}$$

Analysis of the Temperature Field

The fluid-film is coupled to the two surrounding bodies through the equilibrium conditions (both static and dynamic), elasticity effects, and thermal coupling. The thermal coupling problem will be treated here.

Consider the schematic illustration given in Figure 6. Bodies I and II are separated by the thin fluid film. Flow through the thin film is maintained by a supply through a manifold arrangement in Body I. The exposed surfaces of Body I, marked "S," are submerged in a fluid bath that is maintained at a constant ambient temperature. The thermal environment is similar for Body II. Subsequent discussion will refer specifically to Body I only.

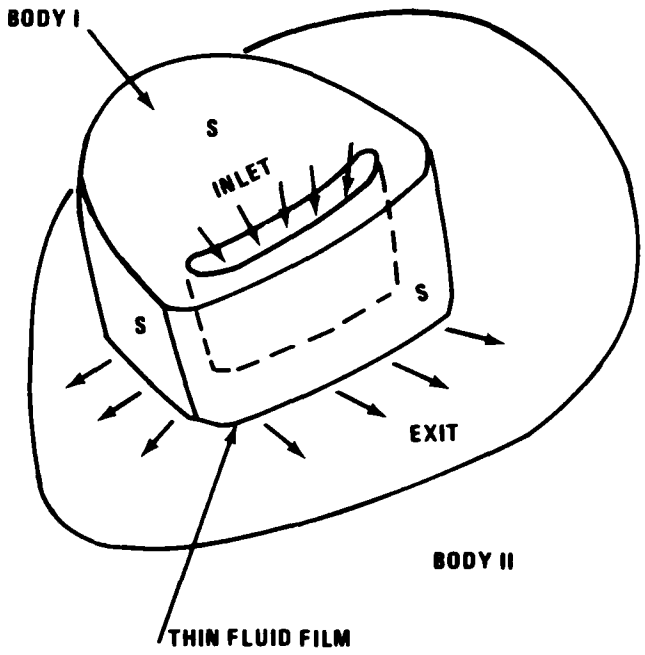


Figure 6 - Schematic Thermal System

The steady-state temperature field in Body I would obey the classical potential theory:

$$\vec{q} = -\kappa_I \nabla T$$

$$\nabla \cdot \vec{q} = -\nabla \cdot (\kappa_I \nabla T) = 0$$

(2-31a,b)

where: q = the conductor heat flux

$\kappa_I$ = the thermal conductivity of Body I

If the body is moving, for example the runner of a thrust bearing, the divergence law should be replaced by the diffusion law, which allows for the contribution of convection. Nevertheless, because of the large thermal capacity of the moving material, an isothermal condition is approximately maintained along its interface with the fluid film. Thus Equation (2-31b) in a two-dimensional form, would remain applicable even to the runner. The coefficient of thermal conductivity should be spatially uniform; consequently, the divergence law is equivalent to the Laplace's equation $\nabla^2 T = 0$.

Three types of thermal boundary conditions are to be imposed:

(1) At the surface of the thin fluid film there is a yet unknown distribution of normal heat flux.

(2) At each of the exposed surfaces, a suitable heat transfer coefficient can be assigned to relate the local surface temperature rise above the ambient to the heat flux:

$$-\kappa_I \vec{n} \cdot (\nabla T) = h_T (T_S - T_A) \tag{2-32}$$

where: $h_T$ = the heat transfer coefficient at the exposed surface

$T_S$ = the temperature at the exposed surfaces S

$T_A$ = the temperature of the ambient fluid

(3) At the walls of the supply manifold, an adiabatic condition could be assumed. On an actual bearing, however, a feed groove, instead of a closed manifold, is more typical. Because circulation between the feed flow and the ambient fluid is not inhibited, part of the overall cooling would take place at the walls of the feed groove. The fluid in the feed groove should be somewhat hotter than the ambient fluid. Thus, the adiabatic supply model would overestimate the temperature rise of Body I. The other extreme model would assume that an ambient condition prevails in the feed groove and would select a suitable heat transfer coefficient for the feed groove. This model thus would underestimate the temperature rise of Body I. These two extreme models may be regarded as upper and lower bounds of the thermal situation.

Standard methods are available for solving the conduction problem. The boundary condition at the exposed surfaces, as given by Equation (2-32), can accommodate a full range of possibilities, which include the extremes of a fully chilled condition

$$T_S = T_A \text{ at } S \quad \text{if } h_T/\kappa_I \to \infty$$

and also the insulated condition

$$\vec{n} \cdot (\nabla T) = 0 \text{ at } S \quad \text{if } h_T/\kappa_I \to 0$$

At the interface with the fluid film, the conduction heat flux should be continuous; therefore

$$\vec{q_I} = -\kappa_I \vec{n} \cdot (\nabla T)_I$$

$$= -\kappa \vec{n} \cdot (\nabla T)_f \qquad \textit{at the interface.}$$

Here, the subscript "I" refers to body I and the subscript "f" refers to the fluid film. The temperature also should be continuous at the interface; or

$$(T)_I = (T)_f \qquad \textit{at the interface.}$$

If Body I is moving and is also well chilled, then $(T)_I$ would be a known constant and the conduction problem of Body I merely serves to impose a temperature boundary condition at the interface with the fluid film. It is no longer necessary to treat the conduction problem. The heat flux across the interface can be calculated only from the temperature field in the fluid film.

To illustrate the relationship between the temperature and the heat flux at the interface with the fluid, consider a model two-dimensional problem for the domain ($0 \leq x \leq b$, $0 \leq y_I \leq w$). Discretization is accomplished by dividing the sides a and b respectively into M and N uniform intervals. The mesh index i has the range of (1 to M+1) in the x-direction while j has the range of (1 to N+1) in the $y_I$-direction. Let j=1 be the interface with the fluid film, while the convectively cooled boundary condition is imposed for the sides (i=1, i=M+1, and j=N+1). The entire temperature field is represented by the column vectors

$$\{T\}_j$$

for (j=1,2,3,...N+1). Each vector has a rank of M+1 and contains the elements $T_{i,j}$ for (i=1,2,3,...M+1). The conduction heat flux at the interface directed into the fluid film is the vector

$$\{q_I\}$$

which is also of rank M+1. The conduction problem of Body I can thus be described in terms of the following system of matrix equations:

$$[A^{(o)}]_1 \{T\}_1 + [A^{(+)}]_1 \{T\}_2 = -\{q\}_1 \qquad (2\text{-}33)$$

$$[A^{(-)}]_j \{T\}_{j-1} + [A^{(o)}]_j \{T\}_j + [A^{(+)}]_j \{T\}_{j+1} = \{0\}$$

for j=2,3,...N (2-34)

$$[A^{(-)}]_{N+1} \{T\}_N + [A^{(o)}]_{N+1} \{T\}_{N+1} = \{0\}$$

(2-35)

This system can be solved by the method of forward-elimination-and-backward-substitution, resulting in

$$\{T\}_1 = [B_I] \{q_I\}$$

(2-36)

In turn, this last expression can be inverted to yield

$$\{q_I\} = [B_I]^{-1} \{T\}_1$$

(2-37)

In this manner, the conduction problem is reduced to a pair of reciprocal influence matrices $[B_I]$ and $[B_I]^{-1}$ which relate the interface temperature $\{T\}_1$ linearly with the heat flux $\{q\}_I$ and vice versa according to Equations (2-36) and (2-37).

Next, the energy equation of the fluid film will be treated for the domain ($0 \leq x \leq a$, $0 \leq y_f \leq h$). Equation (2-28) can be written as

$$\rho C_v \left[ \frac{\partial}{\partial x}(uT) + \frac{\partial}{\partial y}(vT) \right] = \kappa \frac{\partial^2 T}{\partial y^2} + \mu \left( \frac{\partial u}{\partial y} \right)^2$$

(2-38)

The subscript "f" has been dropped from $y_f$ to simplify notation. The velocity components (u,v) are regarded to be given. The interface with Body I, temperature and heat flux are continuous. Thus

$$T(x,h) = T_I(x)$$

(2-39)

$T_I(x)$ in the discretized representation is simply $\{T\}_1$. And

$$\kappa\left(\frac{\partial T}{\partial y}\right)_{y=h} = q_I$$

(2-40)

Note that the sign in Equation (2-40) is consistent with the definition of $q_I$, which is directed into the fluid film. In the above pair of equations, neither $T_I$ nor $q_I$ is fully specified. However, they are related to each other according to Equation (2-36) or (2-37). To complete the physical description of the model problem let the inlet fluid-film temperature be a known constant

$$T(x=0,y) = T_{inlet}$$

(2-41)

and the surface temperature of Body II be also a given constant to represent a runner face:

$$T(x,y=0) = T_{runner}$$

(2-42)

Although the above statements are sufficient to allow computation of the temperature field in the fluid film, one may observe that Equation (2-38), which contains the convective terms on the left-hand side and conduction-dissipation terms on the right-hand side, is a troublesome partial differential equation from the standpoint of numerical analysis. A special scheme, which consists of iterative successive approximations, is proposed to simplify the method of computation. Essential steps of the proposed iterative scheme are outlined below for the model problem.

(1) Postulate the transverse temperature profile to be of the form

$$T(x,y) = T_{runner} + (T_I - T_{runner})\, F(x,y/h)$$

(2-43)

to satisfy Equations (3-39) and (2-42), profile function F(x,y/h) should be unity at y=h and vanish at y=0. To start the iterative computation, let

$$F(x,y/h) = y/h$$

(2-44)

for the first time.

(2) Consider the integral form of Equation (2-38) with the profile function:

$$\rho C_v \frac{d}{dx} \int_0^h \left[ UF\left(\frac{y}{h}\right) T_I \right] dy - \kappa T_I \left[ \left(\frac{\partial F}{\partial y}\right)_{y=h} - \left(\frac{\partial F}{\partial y}\right)_{y=0} \right]$$

$$= -\rho C_v \frac{d}{dx} \int_0^h \left[ U(1-F) T_{runner} \right] dy - \kappa T_{runner} \left[ \left(\frac{\partial F}{\partial y}\right)_{y=h} - \left(\frac{\partial F}{\partial y}\right)_{y=0} \right]$$

$$+ \frac{V^2}{I_0(h)} + \left(\frac{dp}{dx}\right)^2 \left\{ I_2(h) - \frac{\left[I_1(h)\right]^2}{I_0(h)} \right\}$$

(2-45)

Note that this is an ordinary differential equation for $T_I$ (x).

(3) Having obtained $T_I$ (x), use Equation (2-37) to compute $q_I$, which then yields $\kappa \partial T/\partial y$ at y=h.

(4) Integrate Equation (2-38) across, beginning from y=h, with

$$\left(\frac{\partial T}{\partial y}\right)_{y=h} = \frac{q_I}{\kappa}$$

(2-46)

as a boundary condition. For the terms in the left hand side of Equation (2-38), the profile function F(x,y/h) is same as before. The value of $T_I$(x), however, is left to satisfy the other boundary condition as specified by Equation (2-42). Completion of the integration process from y=h to y=0 would yield the improved temperature field.

(5) Revise the profile function according to the improved temperature field. F now depends on both x and y/h. Repeat the iteration process from step (2).

Successful convergence of the iteration scheme would be indicated by a stationary trend of $T_I(x)$ and $q_I(x)$.

Iterative improvement on the film pressure calculation and on the convective heat transport, presently approximated by Equation (2-38), can be implemented if desired. The temperature field in the fluid film would directly affect the fluid viscosity in the hydrodynamic analysis. At the same time the film geometry should also reflect thermal distortions of the surrounding bodies. With tilting pad bearings, the tilt position and motion should also be adjusted and be included in the hydrodynamic analysis in a manner consistent with the static and dynamic equilibrium conditions of the pad.

The above proposed iteration scheme can be extended to the three-dimensional case as is required to analyze a realistic problem. For the three-dimensional problem $T_I$ and $q_I$ depend upon two spatial variables, x and z. Step (2) would be a marching type two-dimensional integration. Step (4) remains a one-dimensional computation.

## 3. COMPUTATION TECHNIQUES

For approximately 25 years, researchers on fluid film lubrication have made use of electronic digital computers to numerically analyze various bearing types. Theoretical analysis of lubrication can be formulated as a two-dimensional partial differential equation of the elliptic type. Accordingly, the applicable computation methods are always based on a discretized approximation, which may be induced by either a finite difference formulation or a variational argument. More recently, the finite-element method has become very popular because it adapts to the description of complicated geometry quite conveniently. As a computation algorithm, the finite-element method achieves discretization through a variational formalism within the domain of a finite, although small, element.

Interest in the study of sliding surface bearings with a very small local film thickness, and with the inclusion of surface roughness and wear effects, makes it particularly challenging to have a universally accurate computation algorithm for the lubrication theory. Furthermore, inherent physical features make it necessary to consider elastic compliance of the bearing parts, thermal

distortion of the bearing surfaces, and the temperature dependence of lubricant viscosity. These issues were discussed in the preceding sections. In the mixed lubrication regime the film thicknesses are on the order of the surface roughness of the mating parts. Emphasis must be placed upon the accuracy of the film pressure and thickness for precise considerations of surface interactions.

In the following sections, the basis for implementation of a highly accurate algorithm will be outlined. First, the problem considered in Appendix A, which neglects end leakage and thus possesses closed form solution for the film pressure, will be recast in terms of a numerical procedure so that numerical accuracy may be directly verified in terms of this particular model problem. Next, a procedure is provided whereby the actual metrology record can be used to describe the surface of a sector pad in the as-manufactured state. And finally, a high accuracy algorithm, which accounts for end-leakage effects, which requires a minimum of fine mesh treatment to describe film thickness variation, and which permits intermesh interpolation for extrema, is documented.

## Finite Difference Computation of the Infinitely Long Slider

Appendix A treats the infinitely long slider problem by formally integrating the governing differential equation

$$\frac{d}{dx}\left[E(H^3)\frac{dp}{dx} - 6\mu U E(H)\right] = 0 \tag{3-1}$$

yielding

$$p(x) = 6\mu U\left[\int_0 \frac{E(H)dx}{E(H^3)} + C_E \int_0 \frac{dx}{E(H^3)}\right] \tag{3-2}$$

$C_E$ is an integration constant that is fixed by the exit condition

$$p(b) = 0 \tag{3-3}$$

Or, in the case of a converging-diverging film geometry, if the rupture condition

$$\int_0^b \frac{E(H)\,dx}{E(H^3)} - E(H)\Big|_b \int_0^b \frac{dx}{E(H^3)} < 0 \tag{3-4}$$

is satisfied, then

$$C_E = -E(H)\Big|_{x_c} \tag{3-5}$$

and

$$\int_0^{x_c} \frac{E(H)dx}{E(H^3)} + C_E \int_0^{x_c} \frac{dx}{E(H^3)} = 0 \tag{3-6}$$

together satisfy the Reynolds-Swift-Stieber condition for film rupture. To address end leakage or a slider of finite length, it is expected that closed form integrals such as Equation (3-2) will no longer be available so that a numerical procedure of the finite-difference or finite-element type will be needed. As a preparatory effort, the infinitely long slider problem will be re-examined in terms of numerical computation formalism, which subsequently can be generalized to deal with the finite length slider.

Consider that the slider width be divided into $N_T$ equal intervals such that

$$\Delta x = b/N_T \tag{3-7}$$

And the mesh points are designated by the index i, which represents the set of integers between and inclusive of (1, $N_T$+1). Note that $x_i = (i-1)\Delta x$. Equation (3-1) will next be recast into

$$\phi = -E(H^3)\frac{dp}{dx} + 6\mu U E(H) \tag{3-8}$$

$$\frac{d\phi}{dx} = 0 \tag{3-9}$$

Consider these equations between mesh points (i, i+1). Define the local coordinate

$$\xi = x\text{-}x_i \tag{3-10}$$

Assume that, upon making $\Delta x$ suitably small, $\Phi$ can be approximated by the series expansion

$$\phi = \phi_0 + \xi\phi_1 + \frac{1}{2}\xi^2\phi_2 + \ldots \tag{3-11}$$

To the same order of approximation, $E(H^3)$ and $E(H)$ can be similarly expressed as

$$E(H^3) = a_0 + \xi a_1 + \frac{1}{2}\xi^2 a_2 + \ldots \tag{3-12}$$

$$6\mu UE(H) = b_0 + \xi b_1 + \frac{1}{2}\xi^2 b_2 + \cdots \tag{3-13}$$

Note that the coefficients of Equation (3-11) are unknown constants associated with point i, whereas those of Equations (3-12) and (3-13) can be determined from their respective mesh point values. Since attention is directed exclusively between points (i, i+1), the above series expansions will be truncated beyond $O\{\xi\}$.

Equation (3-8) can now be rewritten as

$$\frac{dp}{d\xi} = \frac{(b_0 - \phi_0) + \xi(b_1 - \phi_1)}{a_0 + \xi a_1} \tag{3-14}$$

which has the exact solution

$$(p-p_i)=\left(\frac{b_1-\phi_1}{a_1}\right)\xi+\left[\left(\frac{b_0-\phi_0}{a_1}\right)-\left(\frac{a_0}{a_1}\right)\left(\frac{b_1-\phi_1}{a_1}\right)\right]ln\left(\frac{a_0+\xi a_1}{a_0}\right)$$

(3-15)

Setting $\xi = \Delta x$, one obtains

$$p_{i+1}-p_i=\left(\frac{b_1}{a_1}\right)\Delta x+\left[\left(\frac{b_0}{a_1}\right)-\left(\frac{a_0}{a_1}\right)\left(\frac{b_1}{a_1}\right)\right]ln\left(\frac{a_0+a_1\Delta x}{a_0}\right)$$

$$-\left(\frac{\phi_0}{a_1}\right)ln\left(\frac{a_0+a_1\Delta x}{a_0}\right)-\left(\frac{\phi_1}{a_1}\right)\left[\Delta x-\left(\frac{a_0}{a_1}\right)ln\left(\frac{a_0+a_1\Delta x}{a_0}\right)\right]$$

(3-16)

Equation (3-9), however, also requires

$$\Phi_1 = 0$$

(3-17)

Thus, one obtains

$$\phi_0=\frac{a_1}{ln\left(\frac{a_0+a_1\Delta x}{a_0}\right)}\left\{\left(\frac{b_1}{a_1}\right)\Delta x+\left[\left(\frac{b_0}{a_1}\right)-\left(\frac{a_0}{a_1}\right)\left(\frac{b_1}{a_1}\right)\right]ln\left(\frac{a_0+a_1\Delta x}{a_0}\right)-p_{i+1}+p_i\right\}$$

(3-18)

Note that $\Phi_0$ is a "universal constant" which applies to all i. Equation (3-18) can thus be rewritten as

$$p_{i+1} = p_i + A_i\Phi_0 + B_i$$

(3-19)

($A_i$, $B_i$) are coefficients which can be computed at each i. At the leading edge, i=1, the boundary condition is

$$p_1 = 0$$

(3-20)

Therefore,

$$p_2 = A_1 \phi_0 + B_1 \tag{3-21}$$

Upon setting i=2 in Equation (3-19) and making use of Equation (3-21), one obtains

$$p_3 = (A_2 + A_1)\phi_0 + (B_2 + B_1) \tag{3-22}$$

Equations (3-20) through (3-22) can be given the generic form

$$p_i = C_i \phi_0 + D_i \tag{3-23}$$

with $C_1=D_1=0$; $C_2=A_1$, $D_2=B_1$; $C_{i+1}=A_i+C_i$; $D_{i+1}=B_i+D_i$. (3-24a,b,c)

Equation (3-24c) can be implemented repeatedly until $i=N_T$ so that ($C_{N_T+1}$, $D_{N_T+1}$) are regarded as known. But at the exit, $p_{N_T+1} = 0$; therefore,

$$\Phi_0 = -D_{N_T+1}/C_{N_T+1} \tag{3-25}$$

whereupon, since ($C_i$, $D_i$) are now known at all i's, Equation (3-23) allows $p_i$ to be computed also at all i's.

Now Equation (3-14) allows one also to compute

$$\left(\frac{dp}{dx}\right)_i = \left[\left(b_0 - \phi_0\right)/a_0\right]_i \tag{3-26}$$

noting that ($a_0$, $b_0$) are known constants at each i. Also

$$\left(\frac{dp}{dx}\right)_{N_T+1} = \left[\frac{b_0 + b_1\Delta x - \phi_0}{a_0 + a_1\Delta x}\right]_{N_T} \tag{3-27}$$

If the last value is positive, then the computed set of $p_i$ may include a subset $p_j$, j being inclusive of ($N_c$ +1, $N_T$-1), whose values are negative. One can then compute $(\phi_0)j$ such that $(dp/dx)_j = 0$, i.e.

$$(\phi_0)_j = (b_0)_j$$

(3-28)

Accordingly (p)j can be calculated by Equation (3-23). As j steps up from ($N_c$+1), (p)j will be initially positive. Let j = $M_c$ + 1 be the first point where $(p)_{M_c + 1}$ is negative, then the rupture point had been established to be in the interval ($M_c$, $M_{c+1}$). Whereupon Equation (3-14) yields

$$\phi_0 = (b_0)_{M_c} + (b_1)_{M_c}\xi_c$$

(3-29)

Substituting into Equation (3-15), with $\Phi_1$=0 and Equation (3-23) used for $P_{M_c}$, one finds

$$0 = (a_1)_{M_c}\left[C_{M_c}\left\{(b_0)_{M_c} + (b_1)_{M_c}\xi_c\right\} + D_{M_c}\right] + (b_1)_{M_c}\xi_c$$

$$- (b_1)_{M_c}\left[(a_0)_{M_c}/(a_1)_{M_c} + \xi_c\right] ln\left(\frac{a_0 + a_1\xi_c}{a_0}\right)_{M_c}$$

(3-30)

which is the characteristic equation for $\xi_c$ and can be solved numerically. Subsequently Equation (3-29) yields $\Phi_0$ and Equation (3-23) can be used to calculate all $p_i$.

To determine load and pressure center, one must seek the integrals

$$\int p d\xi \; and \int p\xi d\xi$$

Explicit expressions can be obtained by using Equation (3-15) for p and integrating formally. In a similar manner, the viscous friction can be computed.

The crowned tilt-pad bearing analysis of Appendix A assumes a constant lubricant viscosity and includes no coupling, either to pad distortions caused by elastic deformations from load or to thermally induced deformations. Consideration of these topics adds considerable complexity to the required analyses.

Description of Thrust Bearing Film Profile

The film profile of a sector thrust bearing pad, as measured from a nominal runner surface, can be described as the sum of the following components:

(1) warpage;

(2) pitch and roll of the sector pad;

(3) displacement (axial) and misalignment of the runner; and

(4) waviness of the runner

Consider the sector pad shown in Figure 7. Point "P" is the intersection of the bisecting radius and the mean circumference. The four vertices are marked (A,B,C,D). M is the midpoint of the inner arc and N is the midpoint of the outer arc. E and F are midpoints of the sides. For the nominal flat surface, all nine points are on the same plane. Note that each of these nine points is designated by an upper case letter.

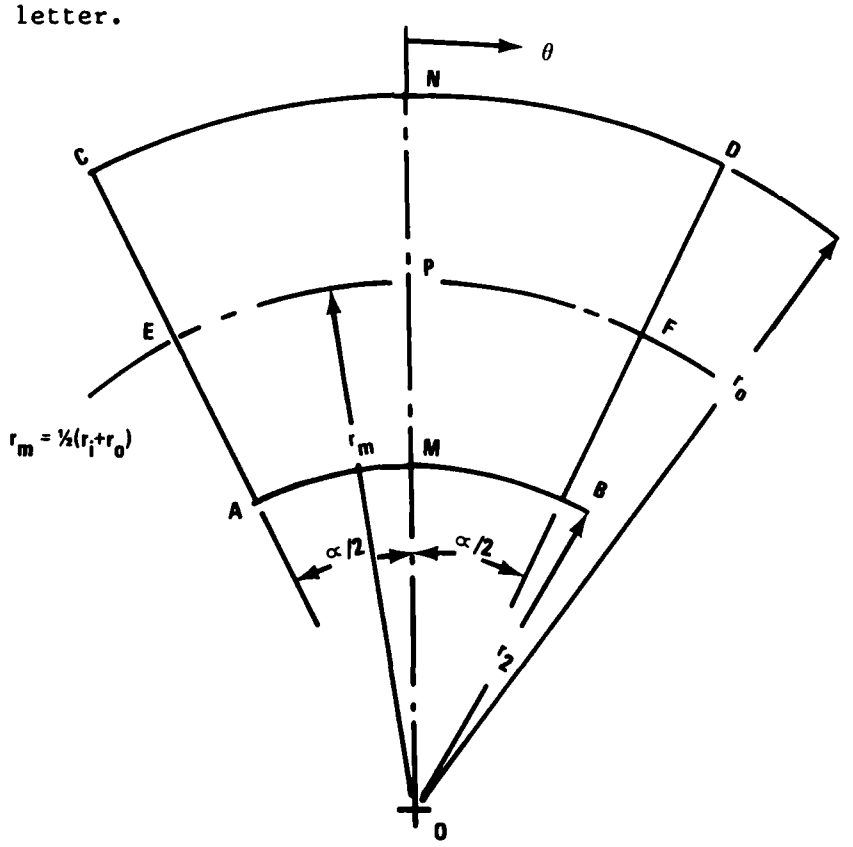


Figure 7 - Sector Pad of a Thrust Bearing

If the bearing surface is warped, the warpage can further be defined in terms of the following components:

Radial Crown -

$$4\left(\frac{r-r_m}{r_o-r_i}\right)^2 h_b$$

Circumferential Crown -

$$4\left(\frac{\theta}{\alpha}\right)^2 h_a$$

These can be respectively measured from P at (M,N) and at (E,F); i.e.

$$h_M - h_P = h_N - h_P = h_b$$

$$h_E - h_P = h_F - h_P = h_a$$

Note that the definitions of ($h_a$, $h_b$) in essence fixes the metrological setup.

The heights of the corner points remain to be defined. The following additional relations can be specified:

$$h_A + h_B + h_C + h_D = 4(h_a + h_b + h_c)$$

$$h_A - h_B + h_C - h_D = 4h_d$$

$$-h_A - h_B + h_C + h_D = 4h_e$$

$$h_A - h_B - h_C + h_D = 4h_f$$

$h_c$ is crown increment; $h_d$ is edge pitching; $h_e$ is edge rolling; and $h_f$ is radial helix. A lower case letter is used as a subscript to indicate a type of surface deviation from the nominal plane. Combining these effects.

$$h_{warpage} = 4\left(\frac{r-r_m}{r_o-r_i}\right)\left(\frac{\theta}{\alpha}\right)\left[h_f - 2\left(\frac{r-r_m}{r_o-r_i}\right)h_d + 2\left(\frac{\theta}{\alpha}\right)h_e\right]$$

$$+ 4\left(\frac{r-r_m}{r_o-r_i}\right)^2 h_b + 4\left(\frac{\theta}{\alpha}\right)^2 h_a$$

$$+ 16\left(\frac{r-r_m}{r_o-r_i}\right)^2\left(\frac{\theta}{\alpha}\right)^2 h_c$$

## High Accuracy Numerical Algorithm for Computing Fluid Film Pressure

The load capacity of a fluid-film bearing (sliding surface type) depends on the development of the film pressure. The film pressure results from the hydrodynamic wedge effect, which is caused by the spatial variation in the film thickness. Operating the bearing near the mixed lubrication condition is usually desirable. The film pressure is then concentrated upstream of and near the minimum film thickness location. The minimum film thickness at the initiation of mixed lubrication would be typically one order of magnitude smaller than the prevailing maximum film thickness. Since the wedge effect is inversely proportional to the third power of the local film thickness, numerical computation of the film pressure requires special care to achieve the desired accuracy. The conventional algorithms of either the finite element or the finite difference type, which attempt to describe the film pressure by simple polynomial functions, may not be accurate enough unless a very fine computation mesh network is used. Since a fine computation network usually means a high computation cost, one often has to resort to use of a nonuniform mesh. As a result, the overall accuracy realizable by such computation schemes is unreliable at best. Therefore, a consistently accurate computation method for the fluid film pressure remains to be developed. Here, a new algorithm to allow high precision in pressure field computation will be outlined.

Strategy. The proposed new algorithm addresses two somewhat independent issues in numerical field computations: the sizing of the computation meshes and the derivation of the high accuracy algorithm. The two are covered in separate sections.

Background. Christensen's[4] mixed lubrication theory for longitudinal roughness was followed for the derivation of governing equations in a form that is valid for both journal bearings (of either the full cylindrical or the partial arc variety) and the sector-type thrust bearing pads. Anticipating eventual consideration of

thermo-elastohydrodynamic coupling, the Couette and the Poiseuille flux components are presented in a form that allows for viscosity variation across the fluid film. However, since the mixed-lubrication theory has not yet been advanced enough to treat variable viscosity conjunctively with surface roughness, any symbolic reference to the stochastic evaluation of a variable viscosity cannot be executed in reality except for the limiting case of smooth surfaces.

Following Christensen's lead, variables are expressed according to the stochastic point of view in terms of values of expectation; e.g., E {p} is the expected value of film pressure and is its ensemble average. The ensemble averaging process, however, is to be executed in the two-dimensional probability space, with the roughness distributions of the two surfaces furnishing independent stochastic states except when asperity interference occurs. The applicable governing equations are

$$E\{\overline{\Psi}_x\} = y^{2n}\left[\overline{\omega}_1 E\{\overline{h}\} + (\overline{\omega}_2 - \overline{\omega}_1) E\{\overline{J}_C\} - E\{\overline{J}_P\}\frac{\partial}{\partial \overline{x}} E\{p\}\right] \tag{3-31}$$

$$E\{\overline{\Psi}_y\} = -\frac{\overline{y}^n}{E\{1/\overline{J}_P\}}\frac{\partial}{\partial y} E\{\overline{p}\} \tag{3-32}$$

$$\frac{\partial}{\partial x} E\{\overline{\Psi}_x\} + \overline{y}^n \frac{\partial}{\partial \overline{y}} E\{\overline{\Psi}_y\} + \overline{y}^{2n} \frac{\partial}{\partial \overline{t}} E\{\overline{h}\} = 0 \tag{3-33}$$

Where index n is (0 or 1), respectively, for the cylindrical journal and thrust bearings.

($\overline{\Psi}_x$, $\overline{\Psi}_y$) are dimensionless, radius-weighted flux components in the sliding and in the transverse directions, respectively. ($\overline{\omega}_1$, $\overline{\omega}_2$) are rotational speeds of the lower and upper surfaces normalized with a suitable reference rate $\omega$.

($\overline{x}$, $\overline{y}$) are dimensionless spatial coordinates; $\overline{x}$ is normalized by the local radius r and is actually the angular coordinate, and the transverse coordinate is normalized by a nominal radius R. $\overline{t}$ is time multiplied by $\omega$.

$\overline{p}$ is the film pressure normalized by $\mu_0\ \omega\ (R/C)^2$. $\mu_o$ is a reference viscosity coefficient. ($\overline{J_C}$, $\overline{J_P}$) are normalized, viscosity-weighted Couette and Poiseuille flow coefficients; they are defined as follows:

$$\overline{J_C} = \frac{1}{C}\int_{h_1}^{h_2}\left[\int_{h_1}^{y}\frac{\mu_0}{\mu}dy'\right]dy \Big/ \left[\int_{h_1}^{h_2}\frac{\mu_0}{\mu}dy\right] \tag{3-34}$$

$$\overline{J_P} = \frac{1}{C^3}\int_{h_1}^{h_2}\left\{\int_{h_1}^{y}\left[\left(\int_{h_1}^{h_2}\frac{\mu_0}{\mu}ydy\right)\Big/\left(\int_{h_1}^{h_2}\frac{\mu_0}{\mu}dy\right) - y'\right]\frac{\mu_0}{\mu}dy'\right\}dy \tag{3-35}$$

$\mu$ is the local viscosity coefficient and is dependent on the temperature profile. C is the nominal gap.

$h_1$ and $h_2$ are heights of the lower and upper surfaces, including roughness profiles on each surface, as measured from a fixed reference surface. $h = h_2 - h_1$ is the local gap. For the isoviscous approximation,

$$\left(\overline{J_C}, \overline{J_P}\right) = \left(\frac{h}{2C}, \frac{h^3}{12C^3}\right) \tag{3-36}$$

For the present discussion, the ambient condition, $\overline{p} = 0$ is assumed at all edges.

Mesh Sizing. Selecting the proper mesh size to achieve the desired computation accuracy involves a number of considerations.

1. Structure of the equation - The governing equation is second order. The simplest nontrivial field distribution would be a parabolic profile that can be defined numerically by no less than three points in each direction.

2. Field coefficients - The field coefficients are mainly associated with the film thickness profile and may also be temperature dependent through Equations (3-34) and (3-35). If crowning of the surface is present, again a minimum of three points are needed to permit unambiguous numerical definition of the field coefficients in the corresponding direction.

3. Slenderness ratio - The slenderness ratio for the cylindrical journal bearing is $L/(\alpha R)$; that of the sector thrust pad is $[(\ln (R_O/R_i)]/\alpha^*$. If the slenderness ratio is very large, variation along the transverse direction is minimal except near either end. If the slenderness ratio is very small, the short bearing solution[6] applies, except near the leading and trailing edges. For a finite but large slenderness ratio, a reasonable rule to follow is to maintain equidistant mesh spacings in the end-edge regions while requiring the mesh aspect ratio to stay within the range of 0.75-2.0. For a small slenderness ratio, mesh points are to be spaced evenly near the inlet and exit edges. Table 2 illustrates the direct application of this rule, assuming three mesh points are equally spaced along the smaller dimension.

TABLE 2 - MINIMUM RECOMMENDED MESH POINTS

| Slenderness Ratio | Mesh Points | | Mesh Aspect Ratio | |
|---|---|---|---|---|
| | x | y | Central | End-Edge |
| 1/4 | 7 | 3 | 2.0 | 1.0 |
| 1/3 | 6 | 3 | 2.0 | 1.0 |
| | 7 | 3 | 1.0 | 1.0 |
| 1/2 | 4 | 3 | 2.0 | 1.0 |
| | 5 | 3 | 1.0 | 1.0 |
| 1 | 3 | 3 | 1.0 | 1.0 |
| 4/3 | 4 | 5 | 1.33 | 1.0 |
| 3/2 | 4 | 3 | 1.0 | 1.0 |
| | 4 | 3 | 1.5 | 0.75 |
| 2/1 | 3 | 4 | 2.0 | 1.0 |
| | 3 | 5 | 1.0 | 1.0 |
| 3/1 | 3 | 6 | 2.0 | 1.0 |
| | 3 | 7 | 1.0 | 1.0 |

* $\alpha$ is the pad arc; for a full cylindrical journal $\alpha = 2\pi$

In order to realize good accuracy, the number of mesh points in either direction probably should be no less than four.

Overall Accuracy. The purpose of an accurate algorithm is to seek a numerical approximation to Equations (3-1) and (3-3) so that the residue of the approximation vanishes uniformly. If one presumes that the convergence of the residue to zero can be achieved by the limiting process of an infinitesimal mesh set ($\Delta\bar{x}$, $\Delta\bar{y}$), then such an approximation can be constructed by the following scheme.

Let

$$E\{\bar{\psi}_x\} = F(\bar{x},\bar{y}) + 0\,\{residue\} \tag{3-37}$$

$$E\{\bar{\psi}_y\} = G(\bar{x},\bar{y}) + 0\{residue\} \tag{3-38}$$

Then F and G may be replaced by their respective truncated Taylor expansions from a suitable mesh point ($\bar{x}_i$, $\bar{y}_j$); i.e.,

$$F(\bar{x},\bar{y}) = F(\bar{x}_i,\bar{y}_j) + (\bar{x}-\bar{x}_i)\frac{\partial F}{\partial \bar{x}_i} + (\bar{y}-\bar{y}_j)\frac{\partial F}{\partial \bar{y}_j} + \ldots \tag{3-39}$$

$$G(\bar{x},\bar{y}) = G(\bar{x}_i,\bar{y}_j) + (\bar{x}-\bar{x}_i)\frac{\partial G}{\partial \bar{x}_i} + (\bar{y}-\bar{y}_j)\frac{\partial G}{\partial \bar{y}_j} + \ldots \tag{3-40}$$

Similarly, one can write

$$\frac{\partial}{\partial \bar{t}}E\{\bar{h}\} = H(\bar{x}_i,\bar{y}_j;\bar{t}) + (\bar{x}-\bar{x}_i)\frac{\partial H}{\partial \bar{x}_i} + (\bar{y}-\bar{y}_j)\frac{\partial H}{\partial \bar{y}_j} + \ldots \tag{3-41}$$

Substituting the above expansions into Equation (3-33) and collecting terms of like order, one obtains

$$\frac{\partial F}{\partial \bar{x}_i} + \bar{y}_j^n\frac{\partial G}{\partial \bar{y}_j} + \bar{y}_j^{2n}H(\bar{x}_i,\bar{y}_j;\bar{t})$$

$$+ (\bar{x}-\bar{x}_i)\left(\frac{\partial^2 F}{\partial \bar{x}_i^2} + \bar{y}_j^n\frac{\partial^2 G}{\partial \bar{x}_i\partial \bar{y}_j} + \bar{y}_j^{2n}\frac{\partial H}{\partial \bar{x}_i}\right) + (\bar{y}-\bar{y}_j)\left(\frac{\partial^2 F}{\partial \bar{x}_i\partial \bar{y}_j} + \bar{y}_j^n\frac{\partial^2 G}{\partial \bar{y}_j^2} + \bar{y}_j^{2n}\frac{\partial H}{\partial \bar{y}_j} + n\bar{y}_j^{n-1}\frac{\partial G}{\partial \bar{y}_j}\right.$$

$$+ 2n\bar{y}_j^{2n-1}H\Big) + \ldots = 0 \tag{3-42}$$

Listing separately in progressively higher orders, the approximation requires

$$0\{1\}: \frac{\partial F}{\partial \bar{x}_i} + \bar{y}_j^n \frac{\partial G}{\partial \bar{y}_j} + \bar{y}_j^{2n} H = 0 \tag{3-43a}$$

$$0\{(x-x_i)\}: \frac{\partial^2 F}{\partial \bar{x}_i^2} + \bar{y}_j^n \frac{\partial^2 G}{\partial \bar{x}_i \partial \bar{y}_j} + \bar{y}_j^{2n} \frac{\partial H}{\partial \bar{x}_i} = 0 \tag{3-43b}$$

$$0\{(\bar{y}-\bar{y}_j)\}: \frac{\partial^2 F}{\partial \bar{x}_i \partial \bar{y}_j} + \bar{y}_j^n \frac{\partial^2 G}{\partial \bar{y}_j^2} + \bar{y}_j^{2n} \frac{\partial H}{\partial \bar{y}_j} + n\bar{y}_j^{n-1} \frac{\partial G}{\partial \bar{y}_j} + 2n\bar{y}_j^{2n-1} H = 0 \tag{3-43c}$$

Since ($\partial F/\partial \bar{x}_i$, $\partial G/\partial \bar{y}_j$, H; etc.) are fixed at the mesh point ($\bar{x}_i$, $\bar{y}_j$), these expresssions are algebraic constraints; they are not differential equations.

In a conventional finite difference algorithm, the truncated series expansions are extended to $E\{\bar{p}\}$ such that Equations (3-31) and (3-32) are directly reduced to algebraic constraints. In the proposed approach, Equations (3-31) and (3-32) are retained as ordinary differential equations so that $E\{\bar{p}\}$ is not required to be equally smooth as $E\{\overline{\Psi}_x\}$ and $E\{\overline{\Psi}_y\}$. Thus, the effects of variable field coefficients can be naturally accommodated in the locally exact field of $E\{\bar{p}\}$. In this sense, mesh sizing is used to ensure the validity of the approximation imposed by Equation (3-43); meanwhile, within the domain of convergence permitted by the mesh sizes, $E\{\bar{p}\}$ is determined as accurately as possible through analytical means.

Polynomial Approximations of Field Coefficients. In the isoviscous case of smooth surface problems,

Polynomial Approximations of Field Coefficients. In the isoviscous case of smooth surface problems,

$$E\{\bar{h}\} = (h/C);\ E\{\overline{J}_c\} = \frac{1}{2}(h/C)$$

$$E\{\bar{J}_p\} = \frac{1}{12}(h/C)^3;\ \frac{1}{E\{1/\bar{J}_p\}} = \frac{1}{12}(h/C)^3$$

(h/C) can usually be adequately approximated by a second order polynomial within the domain of two consecutive mesh intervals, even when the surfaces are nearly in contact. Note that, consistent with a second order polynomial for $E\{\bar{h}\}$, $E\{\bar{J}_p\}$. should be regarded as a sixth order polynomial. Such functional behaviors of the field coefficients will be retained. Specifically, one shall accept

$$\bar{\omega}_1 E\{\bar{h}\} + (\bar{\omega}_2 - \bar{\omega}_1) E\{\bar{J}_c\} = a_0 + a_1(\bar{x} - \bar{x}_i) + \frac{a_2}{2}(\bar{x} - \bar{x}_i)^2 \tag{3-44}$$

$$E\{\bar{J}_p\}^{\frac{1}{3}} = b_0 + b_1(\bar{x} - \bar{x}_1)^2 + \frac{b_2}{2}(\bar{x} - \bar{x}_i)^2 \tag{3-45}$$

$$\left[\frac{1}{E\{1/\bar{J}_p\}}\right]^{\frac{1}{3}} = c_0 + c_1(\bar{y} - \bar{y}_j) + \frac{c_2}{2}(\bar{y} - \bar{y}_j)^2 \tag{3-46}$$

$(a_0, a_1, a_2)$ is a set of coefficients applicable to the known data of $E\{\bar{h}\}$ and $E\{\bar{J}_C\}$ for $\bar{x}_{i-1} \le \bar{x} \le \bar{x}_{i+1}$ and $\bar{y} = \bar{y}_j$ . $(b_0, b_1, b_2)$ is similarly related to $[E\{\bar{J}_p\}]^{\frac{1}{3}}$ along the same line element. $(c_0, c_1, c_2)$ represents the second order curve fit of $[E\{1/\bar{J}_p\}]^{-\frac{1}{3}}$ for $\bar{x} = \bar{x}_i$, $\bar{y}_{j-1} \le \bar{y} \le \bar{y}_{j+1}$.

Locally Exact Ordinary Differential Equation Solutions. Consider the 2 x 2 mesh cluster around point $(x_i, y_j)$ shown for the general case in Figure 8. Uniform mesh intervals are not assumed. Based on the known numerical data of the field coefficients, $(a_0, a_1, a_2; b_0, b_1, b_2; c_0, c_1, c_2)$ can be obtained by second order curve fitting.

Substituting Equation (3-39) for $E\{\overline{\Psi}_x\}$ in Equation (3-31) and making use of Equations (3-44) and (3-45), one obtains

$$\frac{\partial E\{\bar{p}\}}{\partial \bar{x}} = \frac{\left(\bar{y}_j^{2n} a_0 - F_{i,j}\right) + \left(\bar{y}_j^{2n} a_1 - \frac{\partial F_{i,j}}{\partial \bar{x}_i}\right)(\bar{x} - \bar{x}_i) + \ldots}{[b_0 + b_1(\bar{x} - \bar{x}_1) + \frac{1}{2} b_2(\bar{x} - \bar{x}_i)^2]^3} \tag{3-47}$$

Similarly, substituting Equation (3-40) for $E\{\bar{\psi}_y\}$ in Equation (3-32) and making use of Equation (3-46), one obtains

$$\frac{\partial E\{\bar{p}\}}{\partial \bar{y}} = \frac{-G_{i,j} - \dfrac{\partial G_{i,j}}{\partial \bar{y}_j}(\bar{y}-\bar{y}_i) - \dots}{[\bar{y}_j + (\bar{y}-\bar{y}_j)]^n [c_0 + c_1(\bar{y}-\bar{y}_j) + \frac{1}{2}c_2(\bar{y}-\bar{y}_j)^2]^3} \tag{3-48}$$

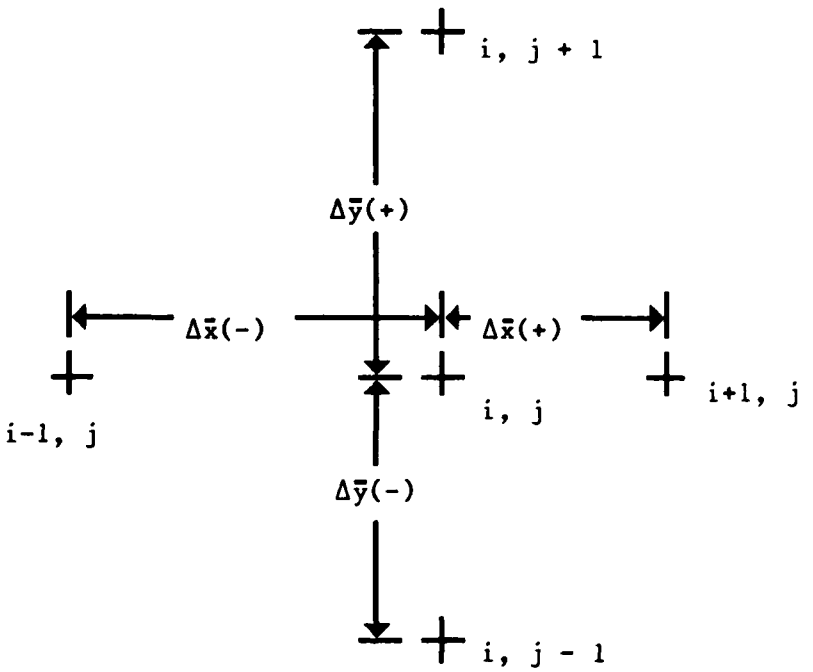


Figure 8 - Schematic of a Nonuniform Mesh Cluster

Closed form integration of Equation (3-47) along $\bar{y} = \bar{y}_i$ from $\bar{x} = \bar{x}_i$ yields

$$E\{\bar{p}\}_j - E\{p\}_j = [A_0(\bar{x}) - A_0(\bar{x}_i)](\bar{y}_j^{2n} a_0 - F_{i,j}) + [A_1(\bar{x}) - A_1(\bar{x}_i)]\left(\bar{y}_j^{2n} a_1 - \frac{\partial F_{i,j}}{\partial \bar{x}_i}\right) + \ldots \tag{3-49}$$

where,

$$A_0(\bar{x}) = \int \frac{d\bar{x}}{\left| b_0 + b_1(\bar{x} - \bar{x}_i) + \frac{b_2}{2}(\bar{x} - \bar{x}_i)^2 \right|^3} \tag{3-50a}$$

$$A_1(\bar{x}) = \int \frac{(\bar{x} - \bar{x}_i)d\bar{x}}{\left| b_0 + b_1(\bar{x} - \bar{x}_i) + \frac{b_2}{2}(\bar{x} - \bar{x}_i)^2 \right|^3} \qquad \text{etc.} \tag{3-50b}$$

The detailed expressions for ($A_0$, $A_1$) are given in Appendix B. Similarly, closed forms integration of Equation (3-48) along $\bar{x} = \bar{x}_i$ from $\bar{y} = \bar{y}_j$ results in

$$E\{\bar{p}\}_i - E\{\bar{p}_j\}_i = -[B_0(\bar{y}) - B_0(\bar{y}_j)]G_{i,j} - [B_1(\bar{y}) - B_1(\bar{y}_j)]\frac{\partial G_{i,j}}{\partial \bar{y}_j} - \ldots \tag{3-51}$$

where,

$$B_0(\bar{y}) = \int \frac{d\bar{y}}{(\bar{y})^n \{c_0 + c_1(\bar{y} - \bar{y}_j) + c_2(\bar{y} - \bar{y}_j)^2/2\}^3} \tag{3-52a}$$

$$B_1(\bar{y}) = \int \frac{(\bar{y} - \bar{y}_j)\, d\bar{y}}{(\bar{y})^n \{c_0 + c_1(\bar{y} - \bar{y}_j) + c_2(\bar{y} - \bar{y}_j)^2/2\}^3} \tag{3-52b}$$

Details of ($B_0$, $B_1$) are given in Appendix C.

The Central Algorithm. Truncating the expansion of $E\{\bar{\psi}_x\}$ at the first order term, (3-49) can be regarded as containing two undetermined coefficients ($F_{i,j}$ and $\partial F_{i,j}/\partial \bar{x}_i$). The data of $E\{\bar{p}\}$ at (i-1, j) and (i + 1, j) can be utilized so that

$$\begin{bmatrix} 1 & -1 & 0 \\ & & \\ 0 & -1 & 1 \end{bmatrix} \begin{Bmatrix} E\{\bar{p}_{i-1,j}\} \\ E\{\bar{p}_{i,j}\} \\ E\{\bar{p}_{i+1,j}\} \end{Bmatrix} = \begin{bmatrix} A_0(\bar{x}_{i-1}) - A_0(\bar{x}_i) & A_1(\bar{x}_{i-1}) - A_1(\bar{x}_1) \\ & \\ A_0(\bar{x}_{i+1}) - A_0(\bar{x}_i) & A_1(\bar{x}_{i+1}) - A_1(\bar{x}_1) \end{bmatrix} \begin{Bmatrix} \bar{y}_j^{2n} a_0 - F_{i,j} \\ \\ \bar{y}_i^{2n} a_1 - \partial F_{ij}/\partial \bar{x}_i \end{Bmatrix} \tag{3-53}$$

The matrix equation can be inverted to yield

$$|A| \{\bar{y}_j^{2n} a_0 - F_{i,j}\} = \{A_1(\bar{x}_{i+1}) - A_1(\bar{x}_i)] E\{\bar{p}_{i-1,j}\} - [A_1(\bar{x}_{i+1}) - A_1(\bar{x}_{i-1}) E\{\bar{p}_{i,j}\} - [A_1(\bar{x}_{i-1}) - A_1 \bar{x}_i)\} E\{\bar{p}_{i+1,j}\}$$

(3-54)

and

$$|A| \{\bar{y}_j^{2n} a_1 - \partial F_{i,j}/\partial \bar{x}_j\} = -[A_0(\bar{x}_{i+1}) - A_0(\bar{x}_i)] E\{\bar{p}_{i-1,j}\} + [A_0(\bar{x}_{i+1}) - A_0(\bar{x}_{i-1})] E\{\bar{p}_{i,j}\} + [A_0(\bar{x}_{i-1}) - A_0(\bar{x}_i)] E\{\bar{p}_{i+1,j}\}$$

(3-55)

where

$$|A| \equiv \begin{vmatrix} A_0(\bar{x}_{i-1}) - A_0(\bar{x}_i) & A_1(\bar{x}_{i-1}) - A_1(\bar{x}_i) \\ A_0(\bar{x}_{i+1}) - A_0(\bar{x}_i) & A_1(\bar{x}_{i+1}) - A_1(\bar{x}_i) \end{vmatrix} \tag{3-56}$$

Similarly, making use of the data of $E\{\bar{p}\}$ at (i, j-1) and (i, j+1) would lead to

$$G_{i,j} = |B|^{-1} \left\{ -[B_1(\bar{y}_{j+1}) - B(\bar{y}_j)] E\{\bar{p}_{i,j-1}\} + [B_1(\bar{y}_{j+1}) - B(\bar{y}_{j-1})] E\{\bar{p}_{i,j}\} + [B_1(\bar{y}_{j-1}) - B(\bar{y}_j)] E\{\bar{p}_{i,j+1}\} \right\} \tag{3-57}$$

$$\frac{\partial G_{i,j}}{\partial \bar{y}_j} = |B|^{-1} \left\{ [B_0(\bar{y}_{j+1}) - B_0(\bar{y}_j)] E\{\bar{p}_{i,j-1}\} - [B_0(\bar{y}_{j+1}) - B_0(\bar{y}_{j-1})] E\{\bar{p}_{i,j}\} - [B_0(\bar{y}_{j-1}) - B_0(\bar{y}_j)] E\{\bar{p}_{i,j+1}\} \right\} \tag{3-58}$$

with

$$|B| \equiv \begin{vmatrix} B_0(\bar{y}_{j-1}) - B_0(\bar{y}_j) & B_1(\bar{y}_{j-1}) - B_1(\bar{y}_j) \\ B_0(\bar{y}_{j+1}) - B_0(\bar{y}_j) & B_1(\bar{y}_{j+1}) - B_1(\bar{y}_j) \end{vmatrix} \tag{3-59}$$

To simplify symbolics further, define

$$A_{0,1(\pm)} = \frac{1}{|A|}[A_{0,1}(\bar{x}_{i\pm1}) - A_{0,1}(\bar{x}_i)]$$

$$B_{0,1(\pm)} = \frac{1}{|B|}[B_{0,1}(\bar{y}_{j\pm1}) - B_{0,1}(\bar{y}_j)]$$

(3-60a,b)

Combining ($\partial F_{i,j}/\partial \bar{x}_i$, $\partial G_{i,j}/\partial \bar{y}_j$) respectively from Equations (3-55) and (3-58) into Equation (3-43a), using the new notation, it is found that

$$B_{0(+)}E\{\bar{p}_{i,j-1}\} + [A_{0(+)} \quad -A_{0(+)}+A_{0(-)}-B_{0(+)}+B_{0(-)} \quad -A_{0(-)}]\begin{Bmatrix} E\{\bar{p}_{i-1,j}\} \\ E\{\bar{p}_{i,j}\} \\ E\{\bar{p}_{i+1,j}\} \end{Bmatrix} - B_{0(-)}E\{\bar{p}_{i,j+1}\} = \bar{y}_j^{2n}[a_1 - H_{i,j}]$$

(3-61)

This is the high-accuracy central difference algorithm. It is to the variable viscosity lubrication theory for surfaces with longitudinal roughness as the relaxation formula is to the classical potential theory. Its inherent accuracy is not affected by the presence of localized small film thickness provided the surface profile is accurately described by a second order polynomial.

Equation (3-61) applies to all (i, j). If one chooses a fixed i, the total system encompassing all j can be written as

$$[U_i]\{p_{i-1}\} + [V_i]\{p_i\} + [W_i]\{p_{i+1}\} = \{Q_i\}$$

(3-62)

$\{p_i\}$ is a column vector with elements of $E\{\bar{p}_{i,j}\}$ (fixed i, all j). $(U_i)$ is a diagonal matrix with the element $A_{0(+)}$. $(V_i)$ is a tri-diagonal matrix with the elements $(B_{0(+)}, -A_{0(+)} + A_{0(-)} - B_{0(+)} + B_{0(-)}, -B_{0(-)})$. $(W_i)$ is another diagonal matrix with the elements $-A_{0(-)}$. $\{Q_i\}$ is a column vector containing the elements $(y_j)^{2n}(a_1 - H_{i,j})$.

The rank of the system represented by Equation (3-62) is the number of mesh points in the $\bar{y}$-direction. Inversion of this system is the bulk of the computation effort. For a bearing with a large slenderness ratio, there are fewer mesh points in the $\bar{x}$-direction. Therefore it would be more advantageous to treat

the alternative representation (fixed j, all i), which can be written in the form

$$(U_j)\{p_{j-1}\} + (V_j)\{p_j\} + (W_j)\{p_{j+1}\} = \{Q_j\} \tag{3-63}$$

Determination of the Rupture Boundary. The presence of film rupture is indicated by

$$E\{\bar{p}\} \leq \bar{p}_c \tag{3-64}$$

whereupon the rupture boundary is located by the condition

$$E\{\bar{p}\} = \bar{p}_c \tag{3-65}$$

From the standpoint of numerical computation, where $E\{\bar{p}\}$ is represented by mesh arrays, a sufficient condition for the inequality (3-64) is

$$E\{\bar{p}\}_{i,j} < \bar{p}_c \tag{3-66}$$

Equation (3-65) can be solved iteratively, in accordance with Equation (3-49) or (3-51), to establish the intermesh location of the rupture boundary. Once the rupture boundary is located, then one may seek to impose the Reynolds-Swift-Stieber condition as the criterion for subsequent global iterations.

If the inequality (3-64) occurs in the interior of four surrounding mesh points then a more elaborate scheme is needed to determine the rupture boundary. Since this situation is not likely to be associated with the thin-film operating condition of sliding surface bearings, it will not be given further attention.

## 4. SURFACE ROUGHNESS EFFECTS

When a sliding surface bearing operates with a minimum film thickness, which is of a similar order as the surface roughness, the classical lubrication theory is no longer adequate. Allowance must now be made for asperity interactions -- load is shared between hydrodynamic pressure and asperity contacts. At asperity contacts, friction behaves according to the principles of boundary lubrication, and attendant heating and wear inevitably lead to alterations in the surface texture. The role of surface topography in tribological functions cannot be

expected to be uniquely associated with a single decriptive parameter, e.g., C.L.A. (center line average) or R.M.S. (root-mean square) roughness. Researchers are beginning to bring together topics that had been regarded as isolated issues to examine the detailed mechanisms of these complicated interactions.

Christensen's theory of mixed lubrication for longitudinal roughness has been selected as the analytical point of view, since the longitudinal orientation of topographical features seems to be a reasonable model for machined and worn-in surfaces.

In Appendix A, as in Christensen's "A Theory of Mixed Lubrication,"[4] the model concentrates on the behavior of the bearing with longitudinal roughness on one surface only. Christensen points out that if both the surfaces in a bearing are rough, then the probability density function used will be considered as a description of the combined roughness. The roughness distribution functions used by Christensen were symmetrical and approximated the Normal or Gaussian distribution.[3,4] There remain areas for theoretical improvement such that more realistic characterization of the interacting surfaces may be considered. The subsequent discussions will deal with two specific aspects of conceptual generalizations that are related to the stochastic description of the topographs. First, the roughness deviations on each surface are recognized as an independent set of statistical data; consequently a two-dimensional representation of the stochastic model would have to be used. Second, a machined surface or one that had experienced prior wear would have fewer peaks than valleys; thus the roughness deviations should have skewed distribution functions. If these improvements were incorporated into mixed lubrication theory, all stochastic operations used in the theory would have to be consistently revised.

Mixed Lubrication of Sliding Surface Bearings with Longitudinal Roughness

Background. Christensen[3] has proposed stochastic models for hydrodynamic lubrication of rough surfaces and has applied this technique to study the mixed lubrication problem using the one-dimensional flat slider for illustration.[4] Christensen's theoretical models include striated roughness of both transverse and longitudinal orientations as well as a uniform isotropic roughness.[7] He considered the hydrodynamic aspect using the thin film model, which is strictly applicable only with roughness on the stationary surface.

Elrod[8] considered striated roughness, again using the thin film model, from the deterministic point of view. The latter approach is a direct extension of the lubrication theory for bearings with shallow, narrow grooves on one surface only.[9,10] In the most general form, both surfaces may be rough; however, their respective striations must be parallel.[11] Using a multiple-scale expansion method,[12] it was shown that the flow across the striations would not follow the rapid gap fluctuations associated with surface roughness. If the surface motion has a component that is transverse to the striations, then the moving roughness would contribute to an additional squeeze-film effect, which has a nonvanishing temporal average. Patir and Cheng,[13] concerned mainly with transverse striations, arrived at similar conclusions. More recent efforts on lubrication analysis for rough surfaces are reported in References 14,15 and 16. In Reference 17, Elrod gave a comprehensive review of theoretical ideas on roughness effects, including deterministic considerations of two-dimensional Reynolds roughness (thin film), Stokes roughness (short wavelength), as well as molecular slip (very thin gas films).

The purpose of this section is to consolidate relevant approaches to form the basis for studying mixed lubrication on both stationary and moving surfaces to allow for longitudinal roughness. Specifically, equations suitable for the study of cylindrical journal and sector type thrust bearings will be developed.

Description of Surfaces, Roughness Functions, and Film Thickness. Subscripts 1 and 2 will be used to designate the lower and upper bearing surfaces, respectively. Each point on the surface is measured as the height from an

appropriate nominal surface; and each surface is described as the sum of a geometrical part (which is "smooth") and a topographical part (which is "rough"). Thus

$$h_1 = H_1(x/b, y/L, t) + \delta_1(y/\lambda_1)$$

$$h_2 = H_2(x/b, y/L, t) - \delta_2(y/\lambda_2)$$

(4-1a, b)

(x,y) are local Cartesian coordinates, x being aimed in the sliding direction; t is the time. $\delta_1$ and $\delta_2$ are topographical descriptions of the roughness features. Their sign conventions depict elevation above the respective mean surfaces as positive values. ($\lambda_1$, $\lambda_2$) are roughness scales for the respective surfaces. It will be assumed that

$$(\varepsilon_1, \varepsilon_2) = (\lambda_1, \lambda_2)/L << 1$$

(4-2)

($\sigma_1$, $\sigma_2$) are rms values of ($\delta_1, \delta_2$); i.e.,

$$\sigma_1^2 = \int_{y_o - \frac{1}{2}\Delta y}^{y_o + \frac{1}{2}\Delta y} \delta_1^2 \frac{dy}{\Delta y}; \quad \sigma_2^2 = \int_{y_o - \frac{1}{2}\Delta y}^{y_o + \frac{1}{2}\Delta y} \delta_2^2 \frac{dy}{\Delta y}$$

(4-3a, b)

It is assumed that

$$(\lambda_1, \lambda_2) << \Delta y << L$$

(4-4)

($\sigma_1, \sigma_2$) can be dependent upon (x, y), if desired, to allow for spatial variation of roughness features.

Separation of the surfaces is

$$h = h_2 - h_1$$

$$= H - \delta_1 - \delta_2$$

(4-5)

where

$$H = H_2 - H_1 \tag{4-6}$$

is the usual film thickness upon neglecting roughness. $\delta_1$ and $\delta_2$ may be regarded as definable through their respective profilometry data. However, the coordinates $(y/\lambda_1, y/\lambda_2)$ can not be related to each other. In this sense $(\delta_1, \delta_2)$ should be regarded as stochastically independent of each other; that is, the probability for $\delta_1$ to assume any particular value is independent of the particular value of $\delta_2$. This point of view is crucially important to the development of a consistent stochastic analysis.

Stochastic Computations. The stochastic descriptions of the topographic functions $(\delta_1, \delta_2)$ will be assumed to be known in terms of their respective surface height histograms $P_1$ $(\delta_1)$ and $P_2$ $(\delta_2)$. $P_1 d\,\delta_1$ can be regarded as the infinitesimal area fraction on the lower surface that has the (roughness) height of $\delta_1$. $(P_1, P_2)$ are sometimes called probability density functions. By the nature of this definition, the following identities hold:

$$\int_{-\infty}^{\infty} P_1 d\delta_1 = 1; \quad \int_{-\infty}^{\infty} P_2 d\delta_2 = 1 \tag{4-7a, b}$$

$$\int_{-\infty}^{\infty} P_1 \delta_1 d\delta_1 = 0; \quad \int_{-\infty}^{\infty} P_2 \delta_2 d\delta_2 = 0 \tag{4-8a, b}$$

$$\sigma_1^2 = \int_{-\infty}^{\infty} P_1 \delta_1^2 d\delta_1; \quad \sigma_2^2 = \int_{-\infty}^{\infty} P_2 \delta_2^2 d\delta_2 \tag{4-9a, b}$$

The upper and lower limits of all real roughness profiles are finite; therefore, the integration limits of Equations (4-7) to (4-9) should be replaced accordingly. $(\delta_1, \delta_2)$ are independent variables of the phase space in the stochastic analysis of a problem involving two rough surfaces. The expected value of a function f that is stochastically dependent on $(\delta_1, \delta_2)$ is computed by ensemble averaging

(integrating with probability weighting) in the two-dimensional stochastic phase space. Formally this is written as

$$E(f) = \int\int (P_1 P_2)\ f(d\delta_1\ d\delta_2)$$

(4-10)

The applicable domain excludes the condition $\delta_1 + \delta_2 \geq H$, since H is the separation of the mean surfaces. The area fraction of asperity contact is

$$A_c = \int\int (P_1 P_2)\ (d\delta_1\ d\delta_2) \geq 0$$
$$\delta_1 + \delta_2 \geq H$$

(4-11)

General Equations. The isoviscous, laminar film theory of lubrication will be accepted for the present treatment. In vector notation, this is

$$\vec{\Psi} = \frac{h}{2}\vec{V} - \frac{h^3}{12\mu}\nabla p$$

(4-12)

$$div\,\vec{\Psi} + \frac{\partial h}{\partial t} = 0$$

(4-13)

$\vec{\Psi}$ is the volume flux vector. $\vec{V}$ is the sum of the sliding vectors. This form can be used for a counter-rotating bearing. For cylindrical journal and sector type thrust bearings, these equations can be rewritten in the component form with a common representation.

$$x = r\theta; \quad r = R\,(y/R)^n$$

(4-14a, b)

$$\Psi_x = \frac{h(\omega_1 + \omega_2)r}{2} - \frac{h^3}{12\mu r}\frac{\partial p}{\partial y};$$

$$\Psi_y = -\frac{h^3}{12\mu}\frac{\partial p}{\partial y}$$

(4-15a, b)

$$div\,\vec{\Psi} = \frac{1}{r}\frac{\partial \Psi_x}{\partial \theta} + \frac{1}{r}\frac{\partial}{\partial y}(r\Psi_y)$$

(4-16)

n=(0,1) respectively for the cylindrical journal and thrust bearings.

For a dimensionless formulation, the spatial coordinates are

$$\overline{x} = \theta = x/r \quad \overline{y} = y/R$$

(4-17a, b)

A nominal clearance C is used to scale the composite film thickness while the two roughness profiles are respectively scaled by their rms roughness values $(\sigma_1, \sigma_2)$:

$$\overline{h} = h/C = \overline{H} - \overline{\sigma}_1\overline{\delta}_1 - \overline{\sigma}_2\overline{\delta}_2$$

(4-18)

where,

$$\overline{H} = (H_2 - H_1)/C$$

$$(\overline{\delta}_1, \overline{\delta}_2) = (\delta_1/\sigma_1, \delta_2/\sigma_2); \qquad (\overline{\sigma}_1, \overline{\sigma}_2) = (\sigma_1/C, \sigma_2/C)$$

(4-19a, b, c)

The rotational speeds are scaled by a nominal rotational rate

$$(\overline{\omega}_1, \overline{\omega}_2) = (\omega_1/\omega, \omega_2/\omega)$$

(4-20)

The flux components are scaled by the nominal Couette flux

$$(\overline{\Psi}_x, \overline{\Psi}_y) = 2(\Psi_x, \Psi_y)/(\omega RC)$$

(4-21)

The film pressure, as measured above ambient pressure, is scaled by

$$\overline{p} = \frac{p\,C^2}{6\,\mu\,\omega\,R^2}$$

(4-22)

Equations (4-15, 4-13) can thus be rewritten in the dimensionless form:

$$\overline{\Psi}_x = (\overline{\omega}_1 + \overline{\omega}_2)\overline{h}\,\overline{y}^n - \frac{\overline{h}^3}{\overline{y}^n}\frac{\partial \overline{p}}{\partial \overline{x}}; \quad \overline{\Psi}_y = -\overline{h}^3\frac{\partial \overline{p}}{\partial \overline{y}}$$

(4-23a, b)

$$\frac{1}{\overline{y}^n}\frac{\partial \overline{\Psi}_x}{\partial \overline{x}} + \frac{1}{\overline{y}^n}\frac{\partial}{\partial \overline{y}}(\overline{y}^n\,\overline{\Psi}_y) + \frac{\partial \overline{h}}{\partial t} = 0$$

(4-24)

The natural dimensionless time is

$$\overline{t} = \omega\, t/2$$

(4-25)

Multiple-Scale Analysis of Striated Reynolds Roughness. After Elrod,[12] one recognizes that the roughness function is more appropriately described in terms of a local coordinate of a fine structure; i.e.,

$$(\zeta_1, \zeta_2) = \left(\frac{1}{\lambda_1}, \frac{1}{\lambda_2}\right)(y - y_o)$$

(4-26)

Therefore, partial spatial derivative with respect to the transverse coordinate must also make allowance for these fine scales, which play the role of amplification in the differentiation process. In other words

$$\frac{\partial}{\partial \overline{y}}\bigg|_{\overline{x}} = \frac{\partial}{\partial \overline{y}}\bigg|_{\overline{x},\zeta_1,\zeta_2} + \left(\frac{R}{\lambda_1}\right)\frac{\partial}{\partial \zeta_1}\bigg|_{\overline{x},\overline{y},\zeta_2} + \left(\frac{R}{\lambda_2}\right)\frac{\partial}{\partial \zeta_2}\bigg|_{\overline{x},\overline{y},\zeta_1}$$

(4-27)

$(R/\lambda_1, R/\lambda_2)$ can be regarded as roughness amplification factors associated with transverse (relative to the direction of striation) spatial differentiation.

One may also reasonably postulate that longitudinal spatial differentiation and temporal differentiation do not introduce roughness amplifications. A simple idea is used in the narrow groove lubrication theory and is known to be valid in all areas remote from the edges. Equation (4-24) can thus be rewritten, treating $\overline{y}_1$, $\zeta_1$, $\zeta_2$ as independent variables, and be regrouped according to various degrees of roughness amplification:

$$\left[\left(\frac{R}{\lambda_1}\right)\frac{\partial}{\partial\zeta_1}+\left(\frac{R}{\lambda_2}\right)\frac{\partial}{\partial\zeta_2}\right]\overline{\Psi}_y+\frac{1}{\overline{y}^n}\left[\frac{\partial\overline{\Psi}_x}{\partial\overline{x}}+\frac{\partial}{\partial\overline{y}}\left(\overline{y}^n\,\overline{\Psi}_y\right)\right]+\frac{\partial\overline{h}}{\partial\overline{t}}=0 \tag{4-28}$$

This expression suggests the usefulness of constructing the solution in terms of a double power-series expansion with respect to the two smallness parameters $(\lambda_1/R,\ \lambda_2/R)$.

Neglecting $0\{\lambda_1/R,\ \lambda_2/R\}$, since Equation (4-28) is to be valid for the independent limits $(\lambda_1\to 0,\ \lambda_2\to 0)$, one concludes that

$$\frac{\partial\overline{\Psi}_y}{\partial\zeta_1}=0;\quad\frac{\partial\overline{\Psi}_y}{\partial\zeta_2}=0 \tag{4-29}$$

These expressions are the essence of the theory of striated Reynolds' roughness. The flux component transverse to the roughness striations does not respond to the fine-scale fluctuations of the surface topography. This general conclusion is independent of the orientation of the striations relative to the sliding direction, but does require the striations on one surface be parallel to those on the other.

Stochastic Analysis of Film Flux and Film Pressure. The ultimate interest of lubrication analysis is concerned with the spatial integrals of film flux and film pressure. In the statistical studies, these are really ergodic averages as opposed to ensemble averages. Thus for a specific rough surface, spatial integration is the real objective, and stochastic analysis is conceptually irrelevant. If, however, the surface topography can be defined only in statistical terms, then the results are valid for all surfaces that are statistically similar to the sample topography. In this sense, the statistical point of view begins to have meaning. However, the use of ensemble averaging instead of spatial integration is mainly a matter of convenience. When both surfaces are rough, because the relative location of the two roughness profiles is not certain, the actual composite roughness cannot be uniquely constructed from the individual roughness profiles in a deterministic manner. Accordingly, the stochastic point of view becomes a matter of necessity. In the following,

stochastic analysis will always refer to ensemble averaging (expectation) and the deviation.

Symbolicly every function will be so treated; i.e.,

$$f = E(f) + \tilde{f} \tag{4-30}$$

The expectation operation has already been defined by Equation (4-10), in which the roughness heights $(\delta_1, \delta_2)$ were used to define the probability density functions $(P_1, P_2)$. Consistent with the dimensionless notations adopted above, the expectations operation on a dimensionless variable will be defined in terms of the dimensionless probability density functions.

$$\overline{P}_1(\overline{\delta}_1) \equiv \sigma_1 P_1 \quad (\delta_1 = \sigma_1 \overline{\delta}_1);$$

$$\overline{P}_2(\overline{\delta}_2) \equiv \sigma_2 P_2 \quad (\delta_2 = \sigma_2 \overline{\delta}_2) \tag{4-31a, b}$$

Clearly, expectations of the film fluxes and the film pressure are of particular interest. Equation (4-29) is equivalent to a null condition of the deviation component of $\overline{\Psi}_v$, i.e.,

$$\tilde{\overline{\Psi}}_y = \overline{\Psi}_y - E(\overline{\Psi}_y) = 0 \tag{4-32}$$

Equation (4-23b) now can be rewritten as

$$\frac{\partial \overline{p}}{\partial \overline{y}} = -\frac{\overline{\Psi}_y}{\overline{h}^3} \tag{4-33}$$

Taking the ensemble average,

$$\frac{\partial}{\partial \overline{y}} E(\overline{p}) = -E\left(\frac{1}{\overline{h}^3}\right) \overline{\Psi}_y \tag{4-34}$$

or,

$$\overline{\Psi}_y = E(\overline{\Psi}_y) = -\frac{\partial E(\overline{p})}{\partial \overline{y}} \Big/ E\left(\frac{1}{\overline{h}^3}\right)$$

(4-35)

Equation (4-33) can be differentiated with respect to $\overline{x}$, yielding

$$\frac{\partial}{\partial \overline{x}}\left(\frac{\partial \overline{p}}{\partial \overline{y}}\right) = -\frac{\partial}{\partial \overline{x}}\left(\frac{\overline{\Psi}_y}{\overline{h}^3}\right)$$

(4-36)

The order of differentiation of the left-hand side can be written in reverse; therefore,

$$\frac{\partial}{\partial \overline{y}}\left(\frac{\partial \overline{p}}{\partial \overline{x}}\right) = -\frac{\partial}{\partial \overline{x}}\left(\frac{\overline{\Psi}_y}{\overline{h}^3}\right)$$

(4-37)

The last relation means, neglecting $0\{\lambda_1/R, \lambda_2/R\}$, that $\partial\overline{p}/\partial\overline{x}$ also has a null deviation component; i.e.

$$\frac{\partial \tilde{p}}{\partial \overline{x}} = 0$$

(4-38)

Consequently, from Equation (4-23a), the ensemble average of $\overline{\Psi}_x$ can be derived as

$$E(\overline{\Psi}_x) = (\overline{\omega}_1 + \overline{\omega}_2)\,\overline{y}^n\,E(\overline{h}) - \frac{1}{\overline{y}^n}\,E(\overline{h}^3)\,\frac{\partial E(\overline{p})}{\partial \overline{x}}$$

(4-39)

Finally, taking the ensemble average of Equation (4-24) term by term, one obtains

$$\frac{1}{\bar{y}^n}\left\{\frac{\partial}{\partial\bar{x}}\left[(\bar{\omega}_1+\bar{\omega}_2)\bar{y}^n E(\bar{h})-\frac{1}{\bar{y}^n}E(\bar{h}^3)\frac{\partial}{\partial\bar{x}}E(\bar{p})\right]-\frac{\partial}{\partial\bar{y}}\left[\frac{\bar{y}^n}{E\left(\frac{1}{\bar{h}^3}\right)}\frac{\partial}{\partial\bar{y}}E(\bar{p})\right]\right\}+\frac{\partial}{\partial\bar{t}}E(\bar{h})=0$$

(4-40)

This is the analog of Reynolds' equation for longitudinal roughness. Typical boundary conditions are

$$E(\bar{p})=0\ at\ \bar{x}_{inlet}$$

(4-41)

$$E(\bar{p})=0\ at(\bar{x}_{exit},\ \bar{y}=1,\ \bar{y}=1-L/R)$$

(4-42)

Equation (4-42) is subject to the ambient-rupture constraint

$$E(\bar{p})\geq 0$$

(4-43)

Where appropriate, Equation (4-42) is to be replaced by the Swift-Stieber rupture condition:

$$E(\bar{p})=\frac{\partial}{\partial\bar{x}}E(\bar{p})=0$$

(4-44)

at the rupture boundary $x_r$ (y).

Computation of Ensemble Averages. To solve (4-40) for E ($\bar{p}$), ensemble averages of ($\bar{h}$, $\bar{h}^2$, $1/\bar{h}^3$) are needed. The procedures of these computations depend on whether or not asperity contacts would take place. Let ($-a_1$, $b_1$) be, respectively, the (lower, upper) limits of the roughness profile of the lower surface, and ($-a_2$, $b_2$) be those of the upper surface. Then the condition for asperity contact is

$$\bar{\sigma}_1 b_1+\bar{\sigma}_2 b_2>\bar{H}$$

(4-45)

This inequality marks the boundary of a forbidden domain in the two-dimensional phase space; this domain must be excluded from all ensemble average calculations. Figure 9 illustrates these ideas.

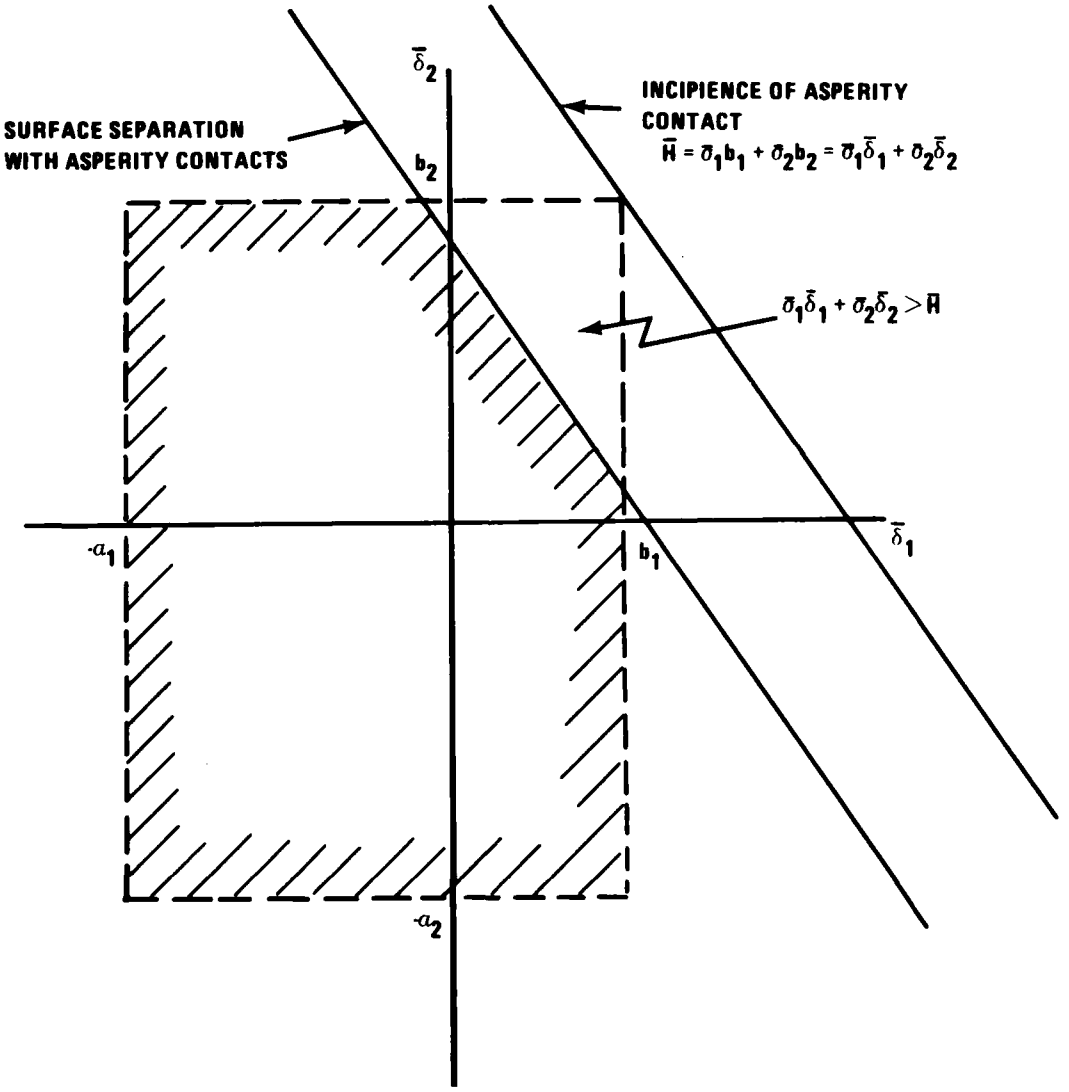


Figure 9 - Applicable Domain for Ensemble Averaging

It is convenient to define the unrestricted expectation as the ensemble integration over the entire rectangular domain:

$$E_o(f) = \int_{-a_1}^{b_1} \overline{P}_1 \, d\overline{\delta}_1 \int_{-a_2}^{b_2} \overline{P}_2 f \, d\overline{\delta}_2$$

(4-46)

Then, if the inequality (4-45) is satisfied, also define the expectation deficiency as

$$\Delta E(f) = \int_{\frac{(\overline{H}-\overline{\sigma}_2 b_2)}{\sigma_1}}^{b_1} \overline{P}_1 \, d\overline{\delta}_1 \int_{\frac{(\overline{H}-\overline{\sigma}_1\overline{\delta}_1}{\sigma_2}}^{b_2} \overline{P}_2 f \, d\overline{\delta}_2$$

(4-47)

The net expectation is

$$E(f) = E_o(f) - \Delta E(f)$$

(4-48)

For the various functions of interest, the unrestricted expectations are

$$E_o(\overline{h}) = \overline{H}$$

$$E_o(\overline{h}^3) = \overline{H}^3 + 3(\overline{\sigma}_1^2 + \overline{\sigma}_2^2)\overline{H} - \overline{\sigma}_1^3 E_o(\overline{\delta}_1^3) - \overline{\sigma}_2^3 E_o(\overline{\delta}_2^3)$$

(4-49a, b)

$E_o(1/\overline{h}^3)$ is much more complicated and will be given attention separately.

Expectation deficiency functions of $(\overline{h}, \overline{h}^3)$ require computation of the type

$$\int \overline{\delta}^n \overline{P} \, d\overline{\delta}; \quad n = 0,1,2,3$$

(4-50)

through appropriate ranges as defined in Equation (4-47). In particular

$$\Delta E(1) = \int_{\frac{(\overline{H}-\overline{\sigma}_2 b_2)}{\overline{\sigma}_1}}^{b_1} \overline{P}_1 \, d\overline{\delta}_1 \int_{\frac{(\overline{H}-\overline{\sigma}_1 \overline{\delta}_1)}{\overline{\sigma}_2}}^{b_2} \overline{P}_2 \, d\overline{\delta}_2$$

(4-51)

yields the area fraction of contact.

Hydrodynamic Shear. The hydrodynamic shear stress in the sliding direction is of interest because it contributes to the drive torque. Depending on the particular circumstance, the shear stress on either the upper or the lower surface is of interest; they are

$$\tau = \frac{\mu(w_2 - \omega_1) r}{h} \pm \frac{h}{2} \frac{\partial p}{\partial x}$$

(4-52)

The upper sign is to be used for the shear stress on the upper surface; and the lower sign, for the shear stress on the lower surface.

Scaling with $\mu\omega R/C$

$$\overline{\tau} = \frac{(\overline{\omega}_2 - \overline{\omega}_1)}{\overline{h}} \overline{y}^n \pm 3 \frac{\overline{h}}{\overline{y}^n} \frac{\partial \overline{p}}{\partial \overline{x}}$$

(4-53)

Carrying out ensemble averaging,

$$E(\overline{\tau}) = (\overline{\omega}_2 - \overline{\omega}_1) \overline{y}^n \, E(1/\overline{h}) \pm 3 \frac{E(\overline{h})}{\overline{y}^n} \frac{\partial \overline{p}}{\partial \overline{x}}$$

(4-54)

$E(1/\overline{h})$ is the additional expression that did not appear in the analysis of film pressure.

Stochastic Computations for Mixed Lubrication with Skewed Roughness Distribution Function

The theory of mixed lubrication -- for example, the original treatment by Christensen[3] -- was developed with a symmetrical roughness distribution function. The bearing roughnesses in practical applications are not likely to be symmetrically distributed, rather, they are skewed. Most likely, there are more valleys of a certain magnitude than peaks of the same magnitude. The necessary analysis to accommodate an unsymmetrical roughness distribution function is given below.

Background. The mixed lubrication theory of Christensen[4] requires the computation of ensemble averages of the following quantities:

Longitudinal Poiseuille Flow Admittance

$$h^3 = (H - \delta_1 - \delta_2)^3 \tag{4-55}$$

Couette Flow Admittance

$$h = H - \delta_1 - \delta_2 \tag{4-56}$$

Transverse Poiseuille Flow Resistance

$$h^{-3} = (H - \delta_1 - \delta_2)^{-3} \tag{4-57}$$

Couette Shear Function

$$h^{-1} = (H - \delta_1 - \delta_2)^{-1} \tag{4-58}$$

Transverse Poiseuille Shear Function

$$h^{-2} = (H - \delta_1 - \delta_2)^{-2} \tag{4-59}$$

Ensemble averaging (as the expectation) of a stochastic function that depends on two random variables, f ($\delta_1$, $\delta_2$), is defined as the probability-weighted integral in the two-dimensional phase space; namely.

$$E(f) = \iint [P_1(\delta_1) P_2(\delta_2)] f(d\delta_1\, d\delta_2)$$

(4-60)

With a finite separation, H, the domain of integration should exclude the condition of interference, which is

$$\delta_1 + \delta_2 > H$$

(4-61)

Consequently, the ensemble average can be treated as the sum of the unrestricted expectation and an expectation deficiency;

$$E(f) = E_o(f) - \Delta E(f)$$

(4-62)

where,

$$E_o(f) = \int_{-\infty}^{+\infty} \int (P_1 P_2) f(d\delta_1\, d\delta_2)$$

(4-63)

$$\Delta E(f) = \iint P_1 P_2 f\, d\delta_1\, d\delta_2$$

$$\delta_1 + \delta_2 > H$$

(4-64)

The probability density functions ($P_1$, $P_2$) should be based on actual topographical records of the surfaces. However, to facilitate the computation procedure, an empirical function, which shares the same overall characteristics of the actual function, may be used. Christensen[3] proposed a symmetrical sixth order polynomial, which contains a single free parameter that can be directly associated with the rms roughness, $\sigma$, defined by

$$\sigma^2 = \int P \delta^2\, d\delta$$

(4-65)

Christensen's empirical formula is

$$P = \frac{35}{32(3\sigma)^7}[(3\sigma)^2 - \delta^2]^3$$

$$P(\delta^2 > (3\sigma)^2) = 0 \; for \; \delta^2 < (3\sigma)^2$$

(4-66)

Note that this function has vanishing derivatives up to the second order at the extreme points ($\delta = \pm 3\sigma$). Furthermore, the distribution of asperity height is symmetrical, so that there are as many protrusions as there are depressions. For real surfaces, however, due to the inherent features of machining processes and possible run-in effects, there always are fewer protrusions than depression. Therefore, the centroid of the distribution function should be skewed to the negative side (depressions). It should be possible to modify Equation (4-66) slightly, so that a second parameter becomes available to describe skewness in the topography. A seventh-order polynomial will be examined as a proposed basis for the computation of ensemble averages of interest.

Basic Properties of the Distribution Function. The distribution function is always positive, and must satisfy two contraints due to the very nature of its definition. The first is the convention of normalization in probability theory:

$$\int_{-\infty}^{+\infty} P \, d\delta = 1$$

(4-67)

The second is the condition of null-biasing, which must be satisfied because the stochastic function itself must have a null value for its ensemble average, i.e.,

$$\int_{-\infty}^{+\infty} P \delta \, d\delta = 0$$

(4-68)

The rms deviation, sometimes called the standard deviation, σ, was previously given by Equation (4-65). These are moment integrals of P(δ) of order (0, 1, 2) for Equations (4-67, 68, and 65), respectively. One way to examine the skewness of the distribution is to consider the third order moment integral as given by

$$\theta_s^3 = \int_{-\infty}^{+\infty} P\delta^3 \, d\delta \tag{4-69}$$

Note that for a symmetrical probability density function such as Equation (4- 66), and all odd orders, the moment integrals vanish identically.

Derivation of a New Probability Distribution Function. Instead of using Equation (4-66) as the probability distribution function, its basic form is adopted as a generating function.

$$G(\delta) = (c^2 - \delta^2)^3 \text{ for } \delta^2 \leq c^2$$

$$G(\delta) = 0 \text{ for } \delta^2 > c^2 \tag{4-70}$$

The indefinite moment integral of G is defined as

$$\Gamma_n(\delta) = \int G\,\delta^n \, d\delta = \left( \frac{c^6}{n+1} - \frac{3\,c^4\delta^2}{n+3} + \frac{3\,c^2\delta^4}{n+5} - \frac{\delta^6}{n+7} \right) \delta^{n+1} \tag{4-71}$$

One may postulate that

$$P(\delta) = [A+B\ (\delta + \delta_o)]\ [c^2 - (\delta + \delta_o)^2]^3 \text{ for } (\delta + \delta_o)^2 \leq c^2 \tag{4-72}$$

For Equation (4-67) to be satisfied

$$1 = 2\,A\,I_o(c) = \frac{32\,A\,c^7}{35}$$

Or,

$$A = \frac{35}{32\,c^7} \tag{4-73}$$

To satisfy Equation (4-68), one finds

$$0 = \int_{-(c+\delta_o)}^{(c-\delta_o)} [A + B(\delta + \delta_o)][c^2 - (\delta + \delta_o)^2]^3 \delta \, d\delta$$

$$= \int_{-c}^{+c} [A + B(\delta + \delta_o)][c^2 - (\delta + \delta_o)^2]^3 [(\delta + \delta_o) - \delta_o] \, d(\delta + \delta_o)$$

$$= -\delta_o + 2B I_2(c) = -\delta_o + \frac{32 B c^9}{315}$$

Or

$$B = \frac{315 \delta_o}{32 c^9} \tag{4-74}$$

Thus the desired two-parameter distribution function is

$$P(\delta) = \frac{35}{32 c^9} [c^2 + 9 \delta_o (\delta + \delta_o)][c^2 - (\delta + \delta_o)^2]^3 \tag{4-75}$$

The two parameters, c and $\delta_o$, remain to be determined from $\sigma$ and $\theta_s$. By substituting Equation (4-74) into Equations (4-65) and (4-69) one finds that

$$\left(\frac{3\sigma}{c}\right)^2 = 1 - \left(\frac{3\delta_o}{c}\right)^2 \tag{4-76}$$

$$\left(\frac{3\theta_s}{c}\right)^3 = -2\left[\frac{3}{11} - \left(\frac{3\delta_o}{c}\right)^2\right]\left(\frac{3\delta_o}{c}\right) \tag{4-77}$$

It is customary to present topographical data by normalizing the roughness height with the rms roughness, $\sigma$. Thus, the normalized roughness height is

$$\delta = \frac{\delta}{\sigma}$$

(4-78)

Accordingly, the various statistical parameters, all normalized with σ, are

Half maximum Height $\quad \overline{c} = (c/\sigma)$

Skew-Bias Parameter $\quad \overline{\delta}_o = (\delta_o/\sigma)$

Root Mean Third Moment $\quad \overline{\theta}_s = (\theta_s/\sigma)$ (4-79a,b,c)

The corresponding probability distribution function is

$$\overline{P}(\overline{\delta}) = \sigma \overline{P}(\delta)$$

(4-80)

Recasting Equation (4-75) in the new notation, one can write

$$\overline{P}(\overline{\delta}) = \left(\frac{35}{32}\right)\left(\frac{1}{\overline{c}}\right)\left[1 + \left(\frac{3}{\overline{c}}\right)^2 \overline{\delta}_o(\overline{\delta} + \overline{\delta}_o)\left\{1 - [(\overline{\delta} + \overline{\delta}_o)/\overline{c}\right|^2\right\}^3 \quad for \; -\overline{c} - \overline{\delta}_o \le \overline{\delta} \le \overline{c} - \overline{\delta}_o$$

(4-81)

Equations (4-81) and (4-77) can be rewritten as

$$\overline{c} = 3\sqrt{1 + \overline{\delta}_o^2}$$

(4-82)

$$\overline{\theta}_s^3 = \left(\frac{2}{11}\right)\overline{\delta}_o\left(8\,\overline{\delta}_o^2 - 3\right)$$

(4-83)

These expressions provide an easy-to-use single parameter ($\overline{\delta}_o$) for the statistical characterization of skewed topography.

From the specific profilometry data, the value of $\overline{\theta}_s$ can be calculated. Thus, according to Equation (4-83), the skew-bias parameter can be determined as the root of

$$R(\overline{\delta}_o) = \overline{\theta}_s^3 - \left(\frac{2}{11}\right)\overline{\delta}_o(8\,\overline{\delta}_o^2 - 3) = 0$$

(4-84)

However, because this solution is not unique, the appropriate branch must be identified. Equation (4-84) lacks a unique root because $\theta_s$ has a stationary point at $\delta_o^2 = 1/8$. Fortunately, in the range

$$o \leq \delta_o^2 \leq \frac{1}{8} \tag{4-85}$$

$(\theta, \delta_o)$ have a one-to-one correspondence. In fact the upper bound of $\delta_o^2$ makes certain that p is non-negative in the full range of $\delta$. This constraint is obviously due to the relatively simple functional form of Equation (4-81), and limits its applicability to

$$\left| \overline{\theta}_s^3 \right| < \frac{\sqrt{2}}{11} \tag{4-86}$$

If a larger numerical value of $\overline{\theta}_s$ should be indicated by actual profilometry data, then the upper-bound condition, $(\overline{\delta}_o^2 = 1/8)$, would have to be used in lieu of solving Equation (4-84) for $\overline{\delta}_o$.

If the last inequality is satisfied, the root of Equation (4-83) can be rapidly found by the Newton-iteration method. Given an initial estimate $\overline{\delta}'_o$, the residue $R' = R(\overline{\delta}'_o) \neq 0$ can be readily calculated. Then an improved estimate of $\overline{\delta}_o$ is

$$\overline{\delta}_o = \overline{\delta}'_0 - \frac{R'}{dR/d\overline{\delta}'_o} = \overline{\delta}'_o + \left(\frac{11}{6}\right)\frac{R'}{[8(\overline{\delta}'_o)^2 - 1]} \tag{4-87}$$

Table 3 shows $\overline{\theta}_s^3$ and $\overline{c}^2$ tabulated for the full range of $\overline{\delta}_o$. Note that $\overline{c}^2$ changes only slightly and therefore would not be an accurate means of reflecting skewness. By comparison, the relative sensitivity of $\overline{\theta}_s^3$ for indicating skewness is quite evident.

TABLE 3 - DEPENDENCE OF THIRD MOMENT AND SQUARE OF HALF MAXIMUM HEIGHT ON THE SKEW-BIAS PARAMETER

| $\overline{\delta}_o$ | $\overline{\theta}_s^3$ | $\overline{c}^2$ |
|---|---|---|
| 0 | 0 | 9 |
| 0.018 | -0.009810 | 9.002916 |
| 0.036 | -0.019569 | 9.011664 |
| 0.054 | -0.029226 | 9.026244 |
| 0.072 | -0.038730 | 9.046656 |
| 0.090 | -0.048031 | 9.072900 |
| 0.108 | -0.057077 | 9.104976 |
| 0.126 | -0.065818 | 9.142884 |
| 0.144 | -0.074202 | 9.186624 |
| 0.162 | -0.082180 | 9.246196 |
| 0.180 | -0.089699 | 9.291600 |
| 0.198 | -0.096709 | 9.352836 |
| 0.216 | -0.103160 | 9.419904 |
| 0.235 | -0.108999 | 9.492804 |
| 0.252 | -0.114177 | 9.571536 |
| 0.270 | -0.118643 | 9.656100 |
| 0.288 | -0.122345 | 9.746496 |
| 0.306 | -0.125233 | 9.842724 |
| 0.324 | -0.127255 | 9.944784 |
| 0.342 | -0.128361 | 10.052676 |
| 0.3538132 | -0.128565 | 10.125000 |

## CONCLUSIONS

Knowledge of the mixed lubrication process and the associated interactive wear mechanisms is vital in the engineering of a variety of machine components for reliable service in the operational environment of naval ships. The thermo-mechanical interactions can be effectively studied by computer-aided analysis techniques. However, any accurate theoretical model must penetrate the traditional boundaries that isolate classical disciplines from one another. The analytical technique presented here required methodologies to be combined that were developed in the fields of numerical computations, statistics, heat transfer, continuum mechanics, and topographic analysis of surfaces, in addition to the theory of hydrodynamic lubrication. Experimental verification of theoretical predictions presented will be necessary to prove that such an assemblage of analytical tools is valid, so that these tools can eventually be used with confidence in the engineering of actual hardware.

## RECOMMENDATIONS

Because the study of mixed lubrication is inherently an interdisciplinary undertaking, a well-focused overview must be balanced by commensurate stimulation of the constituent disciplines which play the pacing roles. At present, it is timely to demonstrate the possibility of quantitative analysis of the mixed lubrication process in the realistic operational environment of a machine component.

A recent endeavor (Appendix A) yielded a reasonable analytical prediction of friction behavior of the tilt-pad bearing in the one-dimensional approximation. Such an analysis procedure can be readily upgraded to consider a full complement tilt-pad thrust bearing. Specifically, we recommend that a computer-aided analysis procedure for the tilt-pad thrust bearing be developed to include the following features:

- variable sliding speed due to radius change,
- side leakage flows,
- surface roughness effects,

- o film cavitation (Swift-Stieber condition),
- o moment balance about the pivot point, and
- o thermo-elastohydrodynamic interactions as they affect temperature-dependent fluid viscosity and film profile distortions.

We concede that certain aspects of surface roughness effects can be theoretically modelled only rather crudely at present. Although such crude approximations appear adequate to describe the friction behavior, not enough is known about surface deterioration when hydrodynamic lubrication is incomplete. Traditional wear rate estimation based on empirical test data is suitable only for low speed machine elements for which the relative fit and conformance to a nominal geometrical profile determine the functional performance. For high speed machine elements, lack of full film lubrication usually precipitates violent thermomechanical events that rapidly lead to catastrophic failure. Our goal is to control processes in mixed lubrication so that inevitable surface deterioration proceeds at a benign pace. A quantitative understanding is imperative of the closely coupled phenomena of surface chemistry, material moduli and hardness, local heat transfer, material behaviors in the presence of severe thermal gradients, thermal distortions and dynamics, form and size of wear debris, and the topographical changes occurring at the sliding contact, for these phenomena interact and govern the capability of the machine element to endure and to recover from tribological overload that exceeds the full film lubrication capacity. Progress in this area can be fostered by a well-coordinated effort which encompasses:

- o friction and wear tests,
- o surface mechanics, including superficial and near-surface failure processes,
- o topographical analysis for corroboration and correlation with mixed-lubrication analysis and wear tests,
- o testing of a full complement thrust bearing, and
- o the formulation of a cohesive theoretical model of the evolutionary dynamics of topographical changes.

Because of the possible synergistic interactions of various processes, the knowledge of mixed lubrication for one set of machine components and environmental conditions may not directly apply to another machine component or to substantially different environmental conditions, even though the same fundamental processes are involved. However, the general approach to acquiring the knowledge is applicable to many other machine elements that are vital in naval ship systems. The face seal and the elastomeric sterntube bearings are candidate topics worthy of attention when resources are available.

## ACKNOWLEDGEMENTS

The authors acknowledge the support of Dr. H. H. Vanderveldt, NAVSEA 05R25, who sponsors the Marine Tribology Block Program under which this work was accomplished. The authors also acknowledge the work conducted under DTNSRDC contract N00600-78-D-1302 (HW-22) by Dr. B. H. Carson of CADCOM, a division of ManTech International Corporation. Dr. Carson's work is included herein as Appendix A. Professor H. G. Elrod, Jr., reviewed an early manuscript of this document. His constructive comments were gratefully appreciated.

## REFERENCES


1. Czichos, H., "TRIBOLOGY - A Systems Approach to the Science and Technology of Friction, Lubrication, and Wear," Elsevier Scientific Publishing Company, New York, Second ed., p. 131 (1979).

2. Reynolds, O., "On the Theory of Lubrication and its Application to Mr. Beauchamp Tower's Experiments, Including an Experimental Determination of the Viscosity of Olive Oil," Philosophical Transactions, 177, p. 157 (1886).

3. Christensen, H., "Stochastic Models for Hydrodynamic Lubrication of Rough Surfaces," Proc. Instn. Mech. Engrs., 184 (Pt. 1), pp. 1013-1022 (1969-1970).

4. Christensen, H., "A Theory of Mixed Lubrication," Proc. Instn. Mech. Engrs., 186 (41/72), pp. 421-430 (1972).

5. Fuller, D., "Theory and Practice of Lubrication for Engineers," John Wiley and Sons (1956).

6. Dubois, G. B. and F. W. Ocvirk, "Analytical Derivation of Short Bearing Approximation for Full Journal Bearings," NACA Report 1157 (1953).

7. Christensen, H. and K. Tonder, "The Hydrodynamic Lubrication of Rough Journal Bearings," Journal of Lubrication Technology, Trans. ASME, April 1973, pp. 166-172.

8. Elrod, H. G., "Thin-Film Lubrication Theory for Newtonian Fluids with Surfaces Possessing Striated Roughness or Grooving," Journal of Lubrication Technology, Trans. ASME, Series F, pp. 484-489 (Oct 1973).

9. Vohr, J. H. and C. H. T. Pan, "On the Spiral-Grooved Self Acting Gas Bearing," Mechanical Technology Incorporated, Latham, N.Y., USA, MTl Tech. Rept. MTl 63-52, prepared under ONR Contract Nonr-373(00), Task NR 061-031.

10. Elrod, H. G., "A Generalized Narrow Groove Theory Including Ambient Edge Corrections," 5th Bi-Annual Gas Bearing Symposium, Univ. of Southampton, England (1974).

11. Rhow, S. K. and H. G. Elrod, "The Effects on Bearing Load Carrying Capacity of Two-Sided Striated Roughness," Journal of Lubrication Technology, Trans. ASME, Series F, Vol. 96, No. 4, pp. 554-560 and 640 (Oct 1974).

12. Rhow, S. K. and H. G. Elrod, "Effects of Surface Roughness or Grooving on Thin, Laminar Lubricating Films," Columbia University, Lubrication Research Laboratory, Report No. 23 (Nov 1973).

13. Patir, N. and H. S. Cheng, "An Average Flow Model for Determining Effects of 3-D Roughness on Partial Hydrodynamic Lubrication," Journal of Lubrication Technology, Trans. ASME, pp. 12-17 (Jan 1978).

14. Elrod, H. G., "A General Theory for Laminar Lubrication with Reynolds Roughness," Journal of Lubrication Technology, Trans. ASME, pp. 8-14 (Jan 1979).

15. Teal, J. L. and A. O. Lebeck, "An Evaluation of the Average Flow Model for Surface Roughness Effects in Lubrication," Journal of Lubrication Technology, Trans. ASME, pp. 360-367 (July 1980).

16. Sun, D. C., Discussion on "A General Theory for Laminar Lubrication with Reynolds Roughness," by H. G. Elrod, Journal of Lubrication Technology, Trans. ASME, pp. 537-539 (Oct 1979).

17. Elrod, H. G., "A Review of Theories for the Fluid Dynamic Effects of Roughness on Laminar Lubricating Films," Columbia University, Lubrication Research Laboratory, Report No. 27 (Dec 1977).

APPENDIX A

# THE CROWNED, MOMENT BALANCED TILT PAD BEARING IN MIXED LUBRICATION

CADCOM Report No. 81-11, Reproduced in Entirety

prepared by B. H. Carson, Ph.D., P.E. for

David Taylor Naval ship R&D Center

Contract No. N00600-78-D-1302 (HW-22)

C O P Y

TABLE OF CONTENTS

AD-A133 127 INTERACTIVE MECHANISMS OF SLIDING-SURFACE BEARINGS(U) 2/2
DAVID W TAYLOR NAVAL SHIP RESEARCH AND DEVELOPMENT
CENTER BETHESDA MD T L DAUGHERTY ET AL. AUG 83
UNCLASSIFIED DTNSRDC-82/119 F/G 11/8 NL

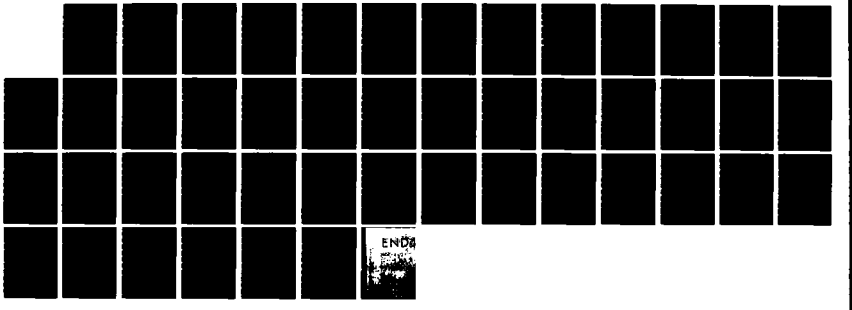

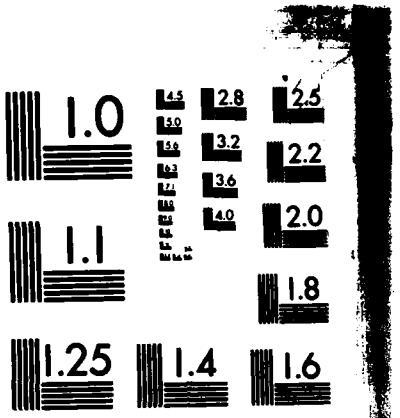

C O P Y

LIST OF FIGURES

C O P Y

## ABSTRACT

The term "mixed lubrication" is used to describe regions of hydrodynamic lubrication in which part of the load carried by a bearing results from actual metallic contact between mating bearing surfaces. Past bearing design practice has been to size bearings to avoid this phenomenon. However, recent interest in reducing size and weight in shipboard machinery has led to a reassessment of this mode of bearing operation. This report presents a computational scheme, based on a stochastic model of roughness distribution, for the determination of bearing performance in the mixed regime. The model also considers "crowning", or convex deformation of the bearing surface that arises due to thermal or mechanical deformations while in service. This is known to cause a significant rearrangement of the pressure profile on the bearing surface. Allowance is also made in the determination of bearing performance for the frictional moment that acts on a tilt-pad bearing, which may assume sizeable proportions in the mixed regime. The results are presented in the form of an interactive computer program.

C O P Y

## I. INTRODUCTION

As the steam engine came of age in the nineteenth century, the need for dependable bearings grew, and journal bearings were successfully developed. But it was not until nearly the turn of the century that the scientific theories of Petrov, Tower, and Reynolds revealed how such bearings operated. Prior to their efforts it was believed that bearing friction depended on material properties, but theory showed that this was not the case, and that friction was merely the consequence of viscous shearing stresses developed in the thin lubricant film that separated the mating bearing surfaces.

Application of these theories led eventually to the development of practical thrust bearings. Working independently, Kingsbury in the United States, and Mitchell in Australia invented the tilt-pad thrust bearing, which had far reaching consequences. Among other things, their invention greatly facilitated the conversion of the world's navies and commercial fleets from sail to steam.

In the intervening years a vast literature dealing with various aspects of hydrodynamic lubrication has emerged, and it seems safe to say that lubrication mechanics is well understood, at least when viewed from the standpoint of lightly loaded bearings. However, in recent years an interest has developed in weight and size reduction in steam propulsion plants designed for shipboard use dictating significant increases in bearing load capacity beyond that which has been previously regarded as good engineering practice. Such bearings typically exhibit phenomena that cannot be explained by classical hydrodynamic lubrication theory. Essentially, at higher loads, the minimum film thickness is reduced to the extent that certain amounts of metal-to-metal contact take place between microscopic surface irregularities, or asperities, that to some extent exist on all bearing

surfaces. This is known as "mixed lubrication." Interest in this regime stems from the fact that bearings can give quite satisfactory performance while operating in mixed lubrication, providing that the load carried by metallic contact is relatively small as compared with the total load. But at higher loadings, complete breakdown of the film occurs, friction rapidly increases, and the bearing fails. Predicting this point of departure is a primary goal of mixed lubrication theory. Material properties play an important role in this prediction, indicating that earlier theorizers may not have been completely wrong.

While the breakdown phenomenon has been observed experimentally for many years, it has only been in recent times that serious attempts have been made to model this process mathematically. Christensen[1] has presented a stochastic theory of mixed lubrication in which the asperities are distributed in a near-Gaussian way and examines a plane slider bearing according to this rationale. His results are illuminating in that the model gives both qualitative and quantitative performance closely matching observed behavior.

Classical bearing theory, when applied to a plain slider bearing, also fails to account for the operation of a centrally pivoted bearing, becoming mathematically degenerate for this case. Despite this frustration, centrally pivoted bearings give fully satisfactory operation and are in widespread use in applications requiring thrust to be carried regardless of rotational direction. A good explanation of this evident paradox has been given by Abramovitz[2], who showed that an exceedingly small amount of crowning, or convex surface curvature on a slider face (which may result from elastic or thermal deformations, or polishing operations) radically alters the pressure distribution on the slider in a way that results in an upstream migration of the pressure center.

Finally, we call attention to another shortcoming of classical theory when applied to a bearing that is free to pivot, and that is the essential "static" nature of the theory, in that the inclination angle of the bearing pad and the ratio of leading to trailing edge film heights are specified a priori and the bearing is then analyzed under conditions of varying load and speed. It is further assumed that the center of pressure and the pivot center are coincident, based on the practical assumption that the offset distance of the center of pressure from the pivot center required to compensate for the moment due to tangential shearing stresses is negligible. While this simplification appears to be fully justified in the pure hydrodynamic regime, it becomes highly suspect in the mixed regime, where frictional moments can reach sizeable proportions. A real bearing pad responds to variations in load and speed within its operating capability by altering its inclination angle and mean film height so that the load is automatically developed and the moment about its pivot center cancelled, regardless of operating regime.

## I-1 Purpose of this Study

The present study was undertaken to explore performance boundaries of tilt pad bearings in a fashion that is unencumbered by restrictions of classical theory previously discussed. Considering the large number of variables in this class of problem, it is not practicable to present performance in customary graphical (generalized) formats. In the final analysis, it is much more convenient to compute performance for each specific example of interest. In the following, we present the rationale leading to a computational scheme that permits numerical

experimentation for a class of curved slider bearings operating in the mixed lubrication regime, having arbitrary pivot coordinates.

## II APPROACH

We adopt the stochastic model of Christensen for a slider bearing free to tilt about some arbitrarily specified point. The macroscopic film height distribution is assumed to be that which results when the slider surface is parabolically crowned, having a maximum crown height at the midpoint of the bearing face. Upon the macroscopic height distribution is superimposed a randomly distributed series of linear roughness asperities, aligned so that the peaks and valleys thus formed lie in the direction of motion. Thus, at any point along the surface, the film height H is represented as

$$H = h(x) + h_s(x,z) \tag{1}$$

where h is the macroscopic film height and $h_s$ is a randomly distributed roughness, or asperity height.

In regions along the bearing surface where the film height is greater than the asperity height, the load and friction are assumed to be purely hydrodynamic in nature, whereas in regions where the film height is less than the asperity height, both the load and friction are carried by separate contributions of hydrodynamic forces, and other forces that depend on the mechanical properties of the bearing material, in linear combination. Viscosity is assumed constant, and side leakage is neglected. Regarding side leakage, it should be noted that in regions of mixed lubrication, the lubricant is effectively trapped in the valleys between asperities, a fact which tends to mitigate the otherwise sweeping

assumption of no side leakage. The model is also two-dimensional, and does not include centrifugal effects.

The general arrangement and nomenclature are indicated in Figure 1.

## III FORMULATION

### III-1. Basic Relationships

Under the stated assumptions, the steady, two-dimensional form of the Reynolds equation is[1]

$$(d/dx)\{E(H^3)\,dp/dx\} = 6\eta U dE(H)/dx \tag{2}$$

where $E(\alpha)$ is the expected value of $\alpha$, and $H = h(x) + h_s(x,z)$, the hydrodynamic film thickness. The value of p in the above expression is taken to be the mean hydrodynamic pressure at any location x, U is the slider speed and $\eta$ is the viscosity of the lubricant, assumed constant.

The random roughness distribution is assumed to be well represented by the near-Gaussian function

$$f(h_s) = (35/32c^7)(c^2 - h_s^2)3$$

where 2c is the maximum peak-to valley height of the roughness. Then the expection of any quantity g(x) is obtained from the expression

$$E(g(x)) = \int g(x) f(h_s) dh_s, \tag{3}$$

where the upper limit of integration is always c, and the lower limit either -c, or -h, depending on whether the film thickness is greater or less than c. This corresponds to regions of pure hydrodynamic and mixed lubrication. In particular, in regions of pure hydrodynamic lubrication, it is readily shown that

$$E(K) = K, \text{a constant}$$

$$E(H) = h,$$

$$\text{and } E(H^3) = h^3 + hc^2/3,$$

whereas, in mixed lubrication regions, more detailed calculations show that

$$E(K) = (K/32c^7)\{16c^7 + 35c^6h - 35c^4h^3 + 21c^2h^5 - 5h^7\},$$

$$E(H) = (35/32c^7)\{c^8/8 + (16/35)c^7h + (1/2)c^6h^2 - (1/4)c^4h^4 + (1/10)c^2h^6 - (1/56)h^8\}, \quad (4)$$

and

$$E(H^3) = (35/32c^7)\{(1/40)c^{10} + (16/105)c^9h + (3/8)c^8h^2 + (16/35)c^7h^3 + (1/4)c^6h^4 - (1/20)c^4h^6 + (3/280)c^2h^6 - (1/840)h^{10}\}.$$

The nominal film height h(x) for a crowned slider bearing (see F-1) is given by the expression [2]

$$h = h_2(a + (1-a)((1 + 4H_c/mB^2)x - (4Hc/mB^3)x^2), \quad (5)$$

where $h_2$ is the trailing edge film height, $a = h_1/h_2$, $h_1$ is the leading edge film height, m is the bearing inclination angle, measured in radians from the direction of motion, and B is the slider length. A useful relationship between a, m, B, and $h_2$ is

$$h_2 = mB/(a-1). \quad (6)$$

The boundary conditions are the usual specification of zero gauge pressures at the leading and trailing edge of the slider, i.e,

$$p(0) = p(B) = 0.$$

## III-2. Pressure Distribution

For a given slider bearing characterized by its physical dimensions (B, $H_c$, c) operating at a speed U with a given lubricant viscosity $\eta$, it is possible to obtain a solution to the Reynolds equation by direct numerical methods, providing that two of the three variables a, m, and $h_2$ are specified. It is emphasized that the appropriate expressions for the expectancy operators must be employed at each point in the integration, depending on whether the lubrication is purely hydrodynamic, or mixed at each point. The first integration is straightforward, and yields

$$dp/dx = 6\eta U\left[(E(H)/E(H^3) + C/E(H^3)\right] \tag{7}$$

where C is a constant of integration.

The second integration is performed by numerically calculating the expressions

$$p = 6\eta U\left[\int_o^x (E(H)/E(H^3))\,dx + C\int_o^x (1/E(H^3))\,dx\right],$$

whereupon, it results from the boundary conditions that

$$C = -\int_o^B (E(H)/E(H^3))\,dx \Big/ \int_o^B (1/E(H^3))\,dx.$$

## III-3. Bearing Load and Center of Pressure

Having performed the above integrations which give the pressure distribution that exists on the slider face, taking into account that some regions are in mixed lubrication, it is now necessary to introduce an ad hoc assumption regarding the manner in which the total load is developed. The simplest model of the contribution of the roughness asperities to the load assumes that in mixed lubrication regions, the metallic contact load is equal to the product of the

yield bearing stress of the weaker bearing material, multiplied by the fraction of area, per unit bearing width, over which such contact takes place. Thus, the load capacity (per unit bearing width) is represented as

$$w = \int_o^{l_1} \hat{p}dx + \int_{l_1}^{l_2} pdx + \int_{l_2}^{B} pdx, \tag{8}$$

where in the first and last integrals, p is the ordinary hydrodynamic pressure upstream and downstream of the interference region that exists between $l_1$ and $l_2$.

The second integral is the sum of the load carried by ordinary hydrodynamic pressure in the valleys between asperity peaks, and the load carried by the asperities; i.e.,

$$\int_{l_1}^{l_2} \hat{p}dx = \int_{l_1}^{l_2} r(x)pdx + p_y \int_{l_1}^{l_2} (1 - r)dx \tag{9}$$

where $p_y$ is the yield stress of the weaker bearing material, and r is the fraction of bearing area formed by the valleys between asperity elements, calculated from equation (4) to be

$$r = (1/32c^7)\{16c^7 + 35c^6h - 35c^4h^3 + 21c^2h^5 - 5h^7\},$$

per unit bearing width.

The center of pressure is obtained in a straightforward fashion by weighting the above integrands with x, performing the indicated integrations, and dividing by the load; i.e.,

$$C_p = \int_o^B pxdx / \int_o^B pdx, \tag{10}$$

where it is to be understood that the integrations follow the above rationale.

## III-4. Slider Friction

The shearing stress acting on each element of the slider surface is obtained from the expression[1]

$$\tau(x) = \eta UE(1/H) + 1/2\,(dp/dx)E(H), \tag{11}$$

where dp/dx is given by (7).

The total frictional force on the slider is determined in a manner similar to the method used in obtaining the load; i.e.,

$$F_s = \int_o^{l_1} \tau dx + \int_{l_1}^{l_2} \hat{\tau} dx + \int_{l_2}^{B} \tau dx, \tag{12}$$

where, here again,

$$\int_{l_1}^{l_2} \hat{\tau} dx = \int_{l_1}^{l_2} r\tau\, dx + \sigma \int_{l_1}^{l_2} (1 - r)\, dx, \tag{13}$$

and $\sigma$ is the yield shearing stress of the weaker bearing material.

The frictional moment about the pivot center is the integral of the shear acting on each surface element weighted by its distance from the y coordinate of the pivot center. Since the bearing surface is curved, this distance is not, strictly speaking, constant along the bearing surface. However, in our area of interest, the maximum ratio of crown height to slider length is of the order $10^{-3}$ and it is sufficiently accurate to assume that all shearing stresses act at constant distance from the y pivot coordinate, thus simplifying subsequent moment balance calculations.

In order to perform the indicated integrations to obtain the frictional force, the additional expectation function E(1/H) must be evaluated. In the pure hydrodynamic region, this is, from (3),

$$E(1/H) = (35/32c^7)\Big[(c^2 - h^2)^3 \ln\{(H + c)/(h - c)\}$$

$$+ (2/15)ch(15h^4 - 40c^2h^2 + 33c^4)\Big]$$

and, in the mixed region, the equivalent expression is

$$E(1/H) = 35/32c^7)\Big[(c^2 - h^2)^3 \ln\{(h + c)/(h - h^*)\} + (8h^3/3)(h + c)^3$$

$$-(1/6)(h + c)^6 - 4(c^2 - h^2)h(h + c)^3$$

$$+ 6(c^2 - h^2)^2h(h + c) + 6(c^2 - h^2)h^2)(c + h^2)$$

$$-(1/6)(h + c)^6 - 4(c^2 - h^2)h(h + c)^3$$

$$-3h^2(c + h)^4 + (6/5)h(h + c)^5 + (3/4)(c^2 - h^2)(h + c)^4$$

$$-(3/2)(c^2 - h^2)^2(h + c)^2\Big]$$

The term h* in the above expression appears in order to prevent the logarithmic term from becoming unbounded. Following Christensen, we set h - h* = mB/1000 in subsequent calculations. Numerical experimentation shows that the resulting solutions are not particularly sensitive to this assumption.

III-5. Coefficient of Friction

The frictional force indicated above acts on the slider surface. The total resistance to motion is this force, plus the component of load acting in the plane of rotation. A precise determination of this second contribution would involve an integration of the components of load in the direction of rotation that act on each element of the curved slider surface. Since, however, the radius of curvature of the curved surface is many orders of magnitude greater than the slider length, it is sufficiently accurate to write

$$F_r = F_s + mw,$$

where $F_r$ is the frictional force on the runner. Then the coefficient of friction $\mu$ is obtained by dividing $F_r$ by the load; i.e.,

$$\mu = F_s/w + m.$$

III-6. Moment Balance

Referring to Figure 2, it is seen by inspection that the condition that satisfies zero unbalanced moments about the pivot center is

$$F_s Y_p = (X_p - C_p)\, w, \text{ or}$$

$$C_p = X_p - (F_s/w) Y_p \qquad (14)$$

where $X_p$, $Y_p$ are fixed by design, and $C_p$, $F_s$, and w are functions of speed, load, etc. the term $F_s/w$ is recognized from the above as a first approximation to the friction coefficient which, for bearings operating in the pure hydrodynamic regimes, is a number approximating $10^{-3}$. In classical formulations, the second term is neglected. However, in the mixed regime, this simplification is not generally justified, and thus will not be adopted in this study.

This completes the basic formulation of the problem.

## IV COMPUTATION OF SPECIFIC BEARING PERFORMANCE

### IV-1. The Inverse Problem

Discounting obvious embellishments required to accommodate mixed lubrication and crowning considerations, the preceding analysis has followed the classical approach to bearing performance; i.e., the Reynolds equation is integrated to obtain the pressure distribution, which is then successively integrated to obtain the load and pressure center. A parallel integration gives the frictional force. Application of this approach depends upon practical assumptions regarding the mean film height (or the film height ratio, which amounts to the same thing) and the slider inclination angle. When this is done, the performance of a given bearing may be determined. In particular, the load and pressure center of a bearing operating under given conditions may be obtained from explicit relations (or, in the more complex case treated here, by direct numerical integrations) that take the form

$$w = w(a,m,U,\eta, \textit{dimensions}, \textit{material properties})$$

$$C_p = C_p(a, m,U,\eta, \textit{dimensions}, \textit{material properties})$$

where a and m are assumed known to reasonable approximation.

In the real situation, however, the pivot point is fixed by design, and the load and speed are independent variables. As these vary (often simultaneously, according to some speed-load schedule) the film height and inclination angle automatically adjust to accommodate the new operating conditions; we may thus think of a bearing as a computer that continuously solves the inverse problem according to functional relations of the form

$$a = a(w,\ X_p, U, etc.)$$

$$m = m(w, X_p, etc.)$$

where $X_p$ and w are specified.

The method by which the bearing performs this inversion cannot be duplicated by rational analysis. Thus, if a bearing's performance is to be determined across a spectrum of operating conditions, it must be done by trial-and-error, using the forward integration technique indicated above. It is evident that a dual iteration must be performed on the variables a and m, which, when acting in proper (and, one would hope, unique) combination, results in a correct load prediction, and at the same time gives assurance that the dual moments about the pivot center caused by load and friction will be effectively canceled.

Computational methods exist, of course, for dual iteration problems. However, such schemes usually owe their success to the fact that the values sought are single valued, and vary monotonically with the iteration variables. Considering the sizeable number of variables in the present problem, there is no assurance whatever that these conditions can always be met. It is clear that physical insights, leading to "intelligent guesses," must be sought.

## IV-2. Inverting the Plane Slider Bearing Problem

By way of illustrating the above considerations, as well as obtaining a highly useful means of arriving at an intelligent first guess needed to expedite the iteration process in the more complex case treated in this study, the plane slider bearing problem is inverted; i.e., given the load, speed, dimensions, viscosity, and pivot center, the problem is to obtain the inclination angle and film height ratio, for the case of the smooth plane slider bearing.

To begin, the Reynolds equation is solved for the pressure distribution. The result, expressed in partial fractions suitable for further integration, is:

$$p(x) = \frac{6\eta UB}{(a-1)h_2^2}\left\{\frac{1}{1+(a-1)x/B} - \frac{a}{(a+1)(1+(a-1)(x/B)^2} - \frac{1}{(a+1)}\right\}$$

which, when integrated on x between the limits O, B, gives

$$w = \frac{6\eta UB^2}{(a-1)^2h_2^2}\left\{ln(a) - \frac{2(a-1)}{(a+1)}\right\}$$

With the help of (6), this may be rewritten

$$w = \frac{6\eta U}{m^2}\left[ln(a) - \frac{2(a-1)}{(a+1)}\right] \tag{15}$$

$$= 6\eta U g(a)/m^2 \tag{16}$$

The center of pressure is obtained by a second integration to yield

$$c_p = C_p/B = \frac{2a(a+2)ln(a) - (5a+1)(a-1)}{2(a-1)[(a+1)ln(a) - 2(a-1)]}$$

$$= cp(a). \tag{17}$$

Now clearly, if it were possible to invert this last expression, yielding

$$a = a(c_p)$$

then m would immediately follow from (16), i.e.,

$$m = \sqrt{6\eta U f(a)/w}. \tag{18}$$

Unfortunately, the transcendental form of (17) prohibits a direct inversion; however, for reasons that are not readily apparent, an excellent correlation formula, good to 1% of the exact prediction given by (17) in the range $1 \leq a \leq 8$ is

$$c_p = .0919\, ln(a) + .504 \tag{19}$$

which is readily inverted to yield

$$a = exp\left[10.88(c_p - .504)\right] \tag{20}$$

Having now determined a, the value of m follows from (18), and $h_2$ from (6). The slider friction per unit bearing width is obtained from the expression

$$F_s = \frac{\eta UB}{h_2}\left[\frac{6}{a+1} - \frac{2\,ln(a)}{(a-1)}\right],$$

the runner friction is

$$F_r = F_s + mw,$$

and the coefficient of friction is $F_r/w$. Thus, the problem is inverted. Note that if the pivot coordinates are specified, it is possible to compute the actual pressure center required to nullify the load and frictional moments. Then, with the aid of (20), a new value of a is found, and the calculations are repeated. Study shows that one, or at the most two, iterations is all that is required to completely specify the frictional force, with full assurance that moment balance is achieved.

There is an interesting extension to this development that bears directly on the more complex cases being dealt with in this study. Returning to the expression for the slider friction given above, then, with the help of (6), this becomes

$$F_s = \frac{\eta U}{m}\left[\frac{6(a-1)}{(a+1)} - 2\,ln(a)\right] = \frac{\eta U}{m} f(a)$$

and so the runner friction is

$$F_r = \frac{\eta U}{m} f(a) + mw = \frac{\eta U}{m}\left[f(a) + 6g(a)\right] \text{ from (16).}$$

Thus the coefficient of friction is, again using (16),

$$\mu = m\left[f(a) + 6g(a)\right]/6g(a) = mF(a). \tag{21}$$

The full solution for this problem, given the load, speed, viscosity, and pivot center is thus

$$\mu = \left[\frac{2(a+1)ln(a) - 3(a-1)}{3(a+1)ln(a) - 6(a-1)}\right]\sqrt{\frac{6\mu U}{w}\left[ln(a) - \frac{2(a-1)}{(a+1)}\right]} \tag{22}$$

where a is obtained from the correlation formula

$$a = exp\left[10.88(c_p - .504)\right], \tag{20}$$

and the minimum film height is

$$h_2 = \frac{mB}{(a-1)} = \left\{\frac{6\eta U}{w(a-1)}2\left[ln(a) - \frac{2(a-1)}{a+1}\right]\right\}^{1/2} \tag{6, 23}$$

Note that (22) may be written

$$\mu = G(a)\left(\frac{\eta U}{w}\right)^{1/2}, \tag{24}$$

expressing the well-known fact that the coefficient of friction is proportional to the product of the speed and viscosity, divided by the load, all raised to the one-half power. Once again, if moment balance is considered important, the above relations offer a rapid iteration method.

## IV-3 Effects of Mixed Lubrication

In the preceding development, a simple strategy emerged for determining the friction coefficient while requiring moment balance. In the mixed lubrication

regime, there is no hope of duplicating this since more variables are introduced, and the equations do not admit closed form solutions. Thus, the problem of finding both the inclination angle and the ratio of film heights that deliver a given load, while assuring moment balance, is formidable.

But if we pause to consider that in general the primary interest is not so much in the determination of these parameters for a given load, but rather a range of loads, then the picture is somewhat brighter. In the pure hydrodynamic regime, (6) shows that for a given bearing operating at a given speed, the inclination angle and load exist in simple relationship. Thus, given the load, m is established, but one could just as well specify m and compute the load that this corresponds to. Therefore, in a numerical determination of bearing performance, a reasonable approach seems to be one in which the inclination angle is successively stepped, with film height iterations that produce moment balance being performed at every step along the way. This is in fact the approach eventually adopted after considerable experimentation with dual iteration schemes.

## V NONDIMENSIONAL SYSTEM

In order to facilitate computations and to illuminate certain consequences of mixed lubrication, it is convenient to normalize the relevant equations of motion. To do this, we note that

$$U \triangleq L/T, p \triangleq F/L^2, x \triangleq L, E(H^n) \triangleq L^n,$$

where F, L indicate the dimensions of force and length.

Defining

$$x' = x/B, H' = H/h_2, p' = ph_2^2/\eta UB, \text{ then}$$

d/dx = d/Bdx', and the Reynolds equation (2) becomes

$$\frac{d}{dx'}\left[\frac{dp'}{dx'}E(H'^3)\right] = 6\frac{dE(H')}{dx'}$$

which is now fully nondimensional.

The macroscopic height expression (5) may be normalized on $h_2$ and B to yield

$$h' = h/h_2 = a - \left[(1-a)\right]\left[(1 + 4H'_c/m)x' - (4H'_c/m)x'^2\right],$$

where $H'_c = H_c/B$.

Likewise, all expectation functions can be normalized on $h_2$, replacing c with $c' = c/h_2$ and $h' = h/h_2$. Then it follows that

$$E(H^n) = h_2^n \; E(H'^n), \text{ where n is any integer.}$$

Following this rationale, the load, given by (8) may be rewritten

$$w = \eta UB^2/h_2^2 \left[\int_o^{1'_1} p'dx' + \int_{1'_1}^{1'_2} rp'dx' + (p_y h_2^2/\eta UB^2)\int_{1'_1}^{1'_2}(1-r)dx' + \int_{1'_2}^{1'} p'dx'\right]$$

since r' = r from above.

The nondimensional shear stress $\tau' = \tau h_2/\eta U$ comes from (11) and is given by

$$\tau' = E(1/H') + 1/2(dp'/dx')E(H')$$

and the force on the slider is therefore written

$$F_s = \eta UB/h_2\left[\int_o^{1'_1} \tau'dx' + \int_{1_1}^{1_2} \tau'rdx' + (\sigma h_2/\eta UB)\int_{1_1}^{1'_2}(1-r)dx' + \int_{1'_2}^{1'} \tau'dx'\right]$$

With this nondimensionalization, it is possible to generalize and thereby greatly facilitate numerical integration of the above equation.

Another result of this development is the indication that bearing performance cannot be predicted by the simple relationship given by (24) in the mixed regime, owning to the introduction of the new parameters $p_y$ and $\sigma$.

## VI COMPUTATIONAL SCHEME

On the basis of the foregoing, a computer program was developed in the BASIC language for use on an interactive system such as the Tektronics 4052. The inputs required are the bearing dimensions, rotational speed, asperity and crown heights, the bearing material properties, and the pivot coordinates, all in the dimensions

indicated in the program. The program then calculates a reasonable first approximation to the value of a (= $h_1/h_2$) and a slope m, based on rationale previously presented. The equations are then successively integrated to obtain the friction and pressure moments. If the net unbalanced moment is greater than the load multiplied by one-tenth of one percent of the bearing length, a new value of a is tried, calculated from a "hunting" routine, and the process repeated until the moment balance criterion is met. Regarding the adoption of this criterion, it is noted that this particular standard appeared to represent the best compromise between reasonable moment balance and iteration time, which can be quite lengthy, especially in the mixed regime.

When the moment balance criterion has been met, the operator then receives a listing of pertinent bearing parameters such as the load and friction forces (broken down into contributions from pure hydrodynamic, mixed hydrodynamic, and asperity contact forces), the shear and pressure moments, and so on. The operator may then select a new slope, and the process is then repeated,. Operators who wish to change the initial inputs may access this routine by inputting a zero slope. Instructions are given throughout the program to assist the operator in selecting workable combinations. For example, if zero crown height is selected, and the pivot center is specified to lie at the midpoint of the bearing, the operator will be informed that this is an unworkable combination of parameters, and will be given the opportunity to try new, workable combinations.

As shown in Ref. 2, and borne out in this study, certain regions of crowned bearing operations lead to negative (gauge) pressures at some points on the slider face, which may in some applications result in cavitation, thus altering the pressure distribution. It was not, however, possible to pursue this aspect within

the scope of this study, and so it was decided to merely alert the operator to this possibility when negative pressures appear through the statement, "Bearing may cavitate." When this statement appears, the operator should exercise some caution in applying the results.

The requirement for continuous slope information requires continuous inputs from the operator. In an earlier version of this program, the slope was stepped successively through the program, but it was found that very small changes in slope bring about quite large variations in load and friction coefficient in the transition regime between pure hydrodynamic and mixed lubrication, and this scheme had to be abandoned because too much information was being "lost" with this routine.

As a matter of information to operators, it is noted that the program "remembers" the value of a that was found by iteration in a previous run, and uses this as the first estimate for the next run. Therefore, iterations are minimized if the operator takes relatively small "bites" in specifying new slopes. That is, the larger the increment in m for each succeeding run, the greater the number of iterations will be required.

A complete program listing is given in Appendix I.

## VII APPLICATION OF RESULTS

To illustrate the use of this effort, a bearing pad presently under study by the David W. Taylor Naval Research and Development Center was used as a prototype. The general characteristics of this slider are:

B = 5.87cm (2.31 in.), mean diameter = 13.2cm (5.2 in.), $\eta$ = 4.13 poise (6 x $10^{-6}$ reyns), $p_y = 1.22 \times 10^8$ N/m$^2$ (18,000 psi), $\sigma/P_y = 0.2$, $x_p = 0.5$, $y_p = 0.3$.

With these fixed inputs, several cases of asperity height, crown heights, and rotational speeds were chosen for study. These are summarized in the following table:

| Case | $H_c$ | c | RPM |
|---|---|---|---|
| I | 0.0002 in. | 0.0002 in. | 35 |
| II | 0.0002 in. | 0.0001 in. | 35 |
| III | 0.0002 in. | 0.0002 in. | 20 |
| IV | 0.0002 in. | 0.0002 in. | 50 |

Figure 3 shows the effect of asperity height. Characteristic of this class of problems, extremely small dimensional changes, as compared with the macroscopic dimensions of the bearing pad, lead to significant differences in the performance characteristic. This is reinforced in Figure 4, which shows the ratio of film heights plotted against the speed-load parameter.

Figure 5 shows the "nonsimilarity" of solutions in the mixed lubrication regime, as discussed in Section V. Finally, Figure 6 shows the level of agreement between the calculated values of shear and pressure moments, as discussed in Section VI. Here, it can be seen that the level of agreement increases at the higher loads, coresponding to the moments developed in the mixed regime, where such agreement is most important.

Many similar cases were explored during the course of this study, leading to the same essential conclusions. It is emphasized that the utility of this study cannot be realized without the aid of a computer, which allows a plethora of such examples to be considered.

C O P Y

## VIII SUMMARY

This study represents an extension of prior work by adapting the stochastic model of mixed lubrication due to Christensen to the problem of the curved slider bearing treated by Abramovitz. As a further refinement, the bearing pad is left free to seek the combination of parameters that causes the dual moments due to load and friction to balance, within a narrow margin. The results are presented in the form of an interactive computer program which offers the operator a wide range of parametric authority in the design or analysis of a family of roughened, crowned, tilt pad bearings.

As Christensen points out, no allowance is made for wear of the asperity contacts in the mixed regime, which almost certainly would exist to some greater or lesser extent in the real situation. The major consequence of this restriction is probably an overly-pessimistic prediction of the friction coefficient at the higher loads. Thus, the error introduced by this assumption is on the side of conservatism.

It may also be noted that the crown height and viscosity are considered constant in this model (although they may easily be changed from one run to another) whereas in the real situation they are also most probably time-dependent due to thermal effects. This effect cannot be accounted for, of course, unless heat transfer is introduced into the present model. This would seem to be the logical next extension of the present work.

## REFERENCES

1. Christensen, H., A Theory of Mixed Lubrication, Proceedings of the Institution of Mechanical Engineers, Vol. 186, pp. 421-430, 1972

2. Abramovitz, S., Theory for a Slider Bearing with a Convex Surface: Side Flow Neglected. Journal of the Franklin Institute, Vol. 259, 1955.

COPY

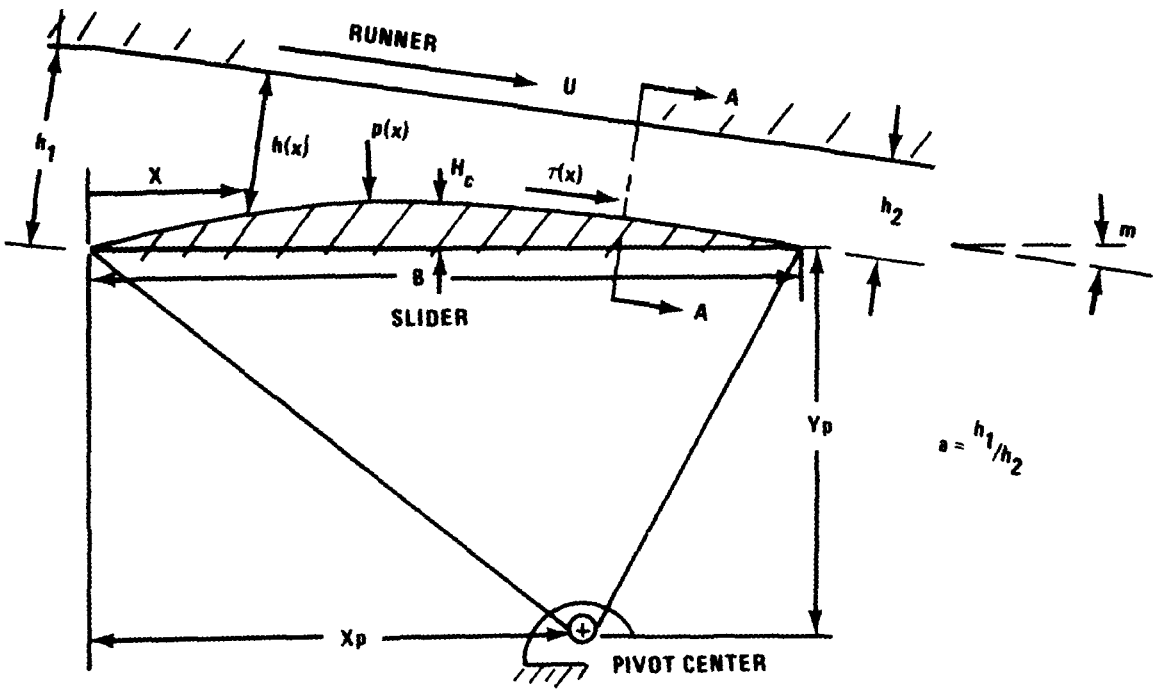


$$h = h_2 \left\{ a + (1-a)\left[(1+4Hc/mB)^{X}/B-(4H_c/mB)(^{X}/B)^2\right] \right\}$$

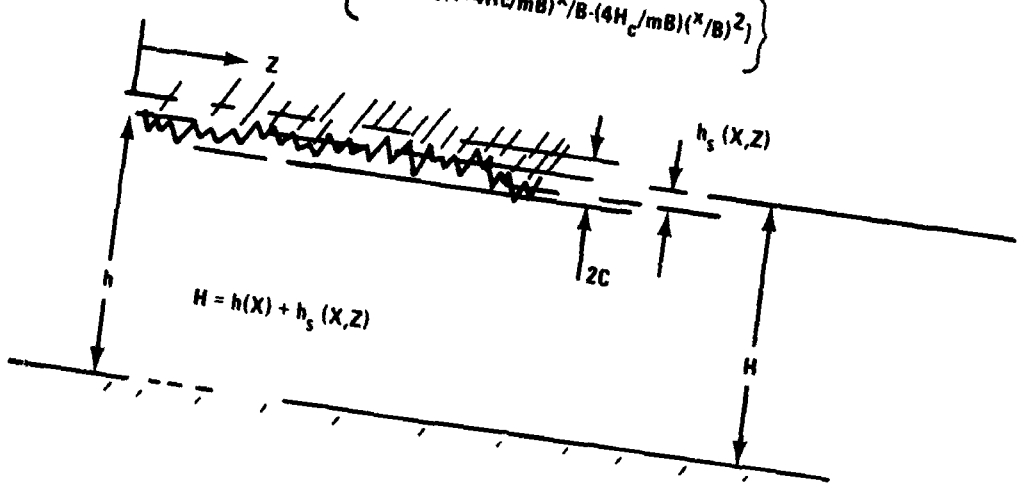


SECTION A-A
(NOTE: IF BOTH SURFACES ARE ROUGH, 2C IS THE COMBINED ROUGHNESS HEIGHT.)

CURVED SLIDER BEARING WITH SURFACE ROUGHNESS -- NOMENCLATURE

FIGURE 1

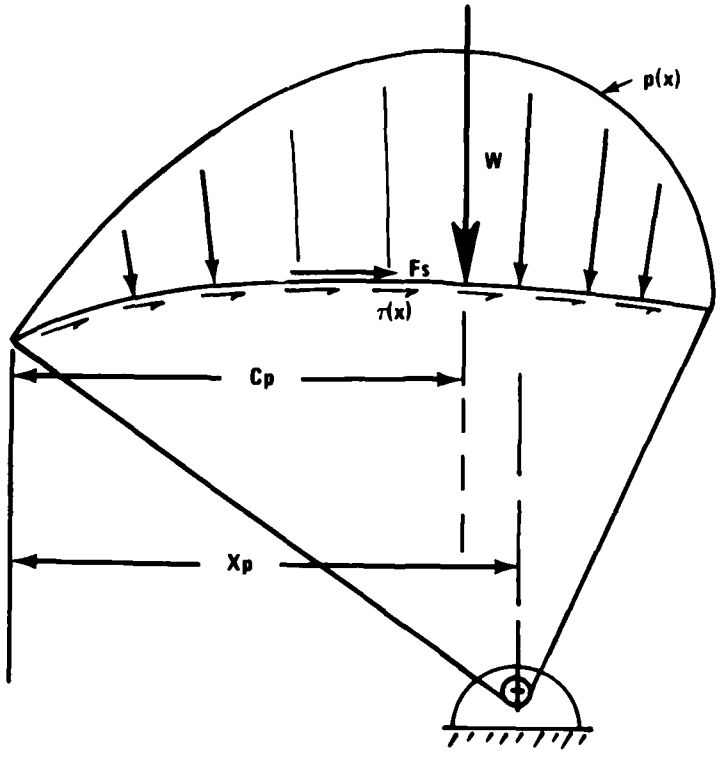


**NOMENCLATURE FOR MOMENT BALANCE DETERMINATION (NOTE: SEE EQUATION 14)**

FIGURE 2

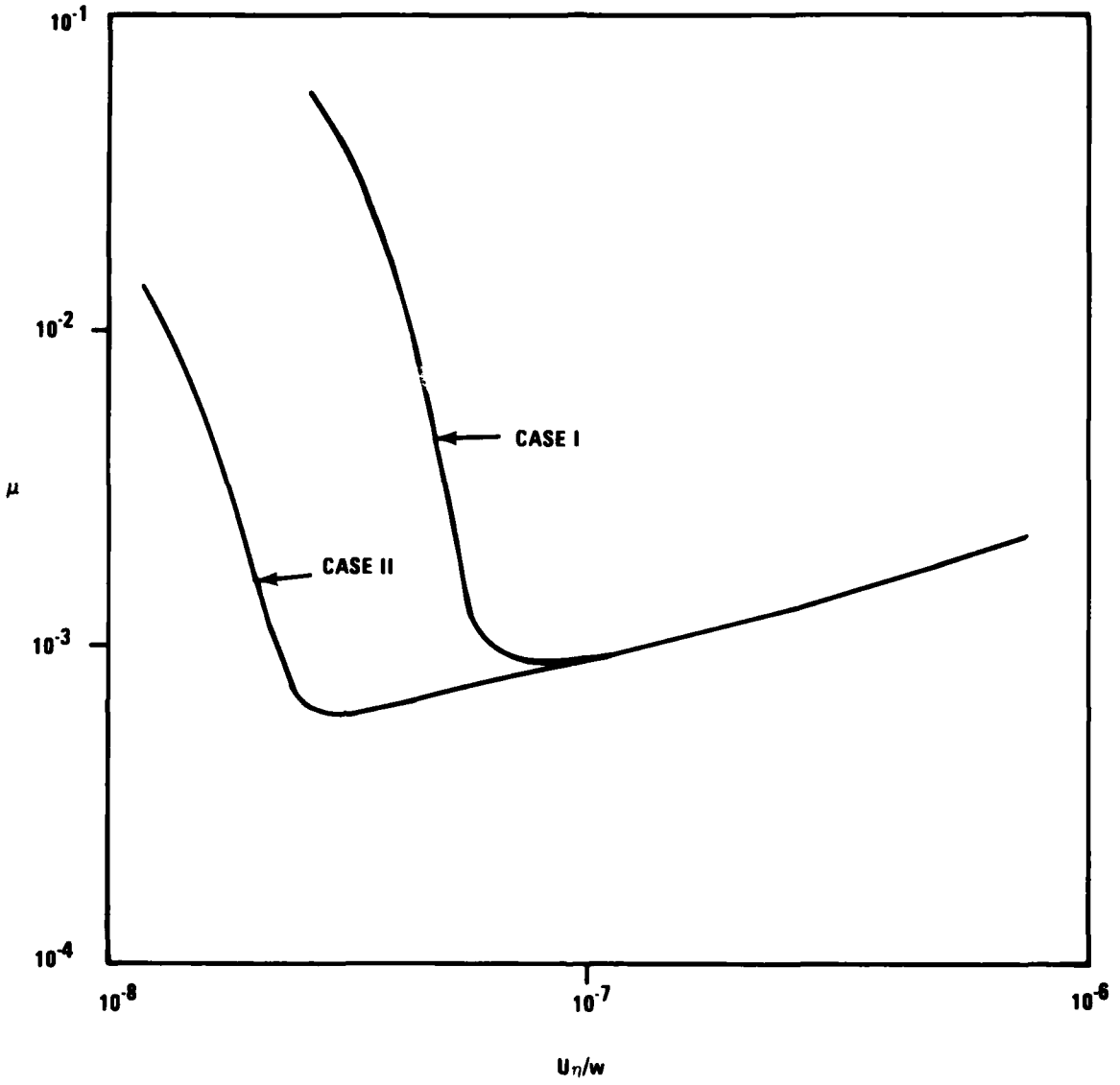


**COEFFICIENT OF FRICTION**
**VS**
**SPEED-LOAD PARAMETER**

FIGURE 3

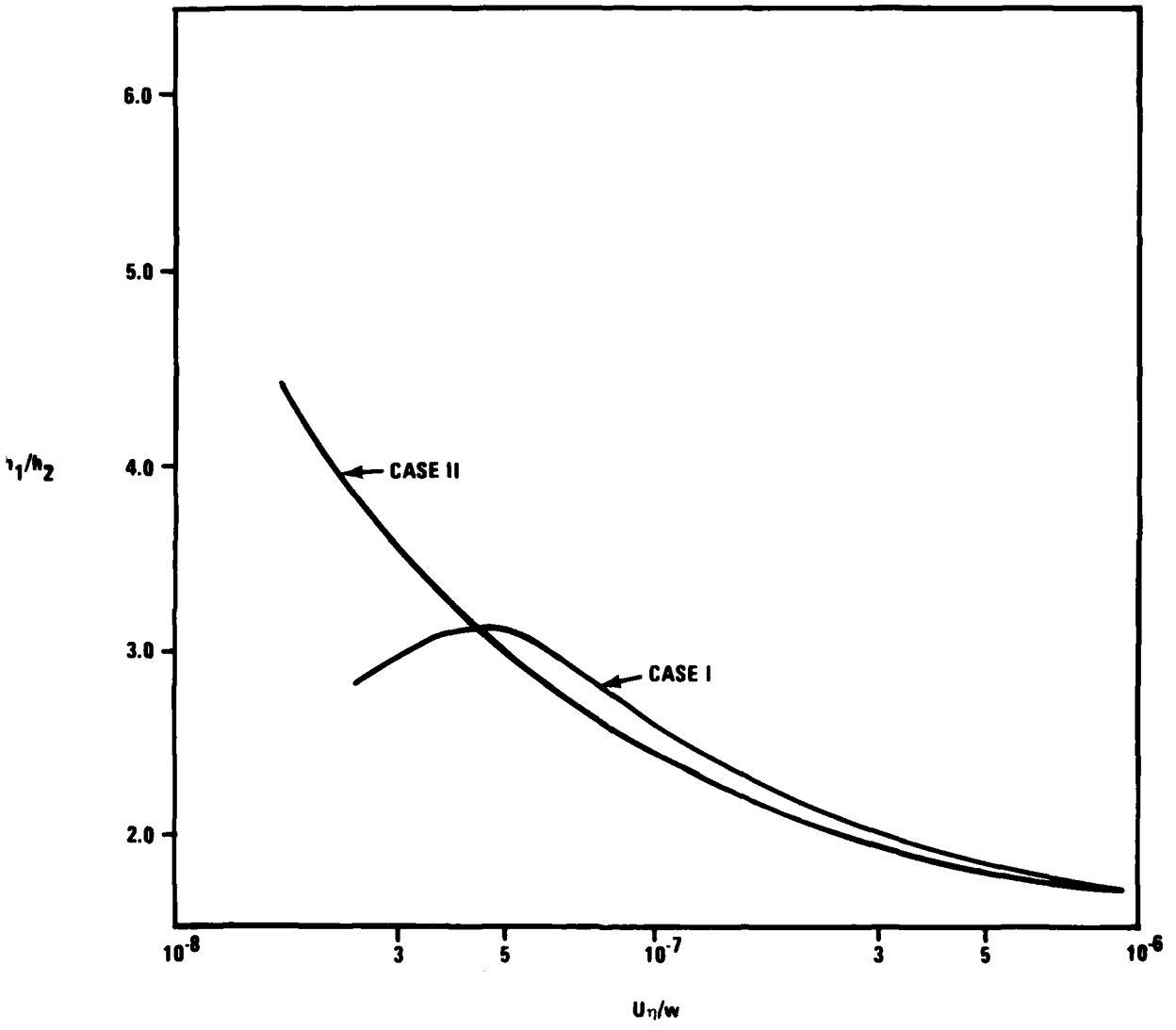


**LEADING/TRAILING EDGE HEIGHT RATIO**
**VS**
**SPEED-LOAD PARAMETER**

FIGURE 4

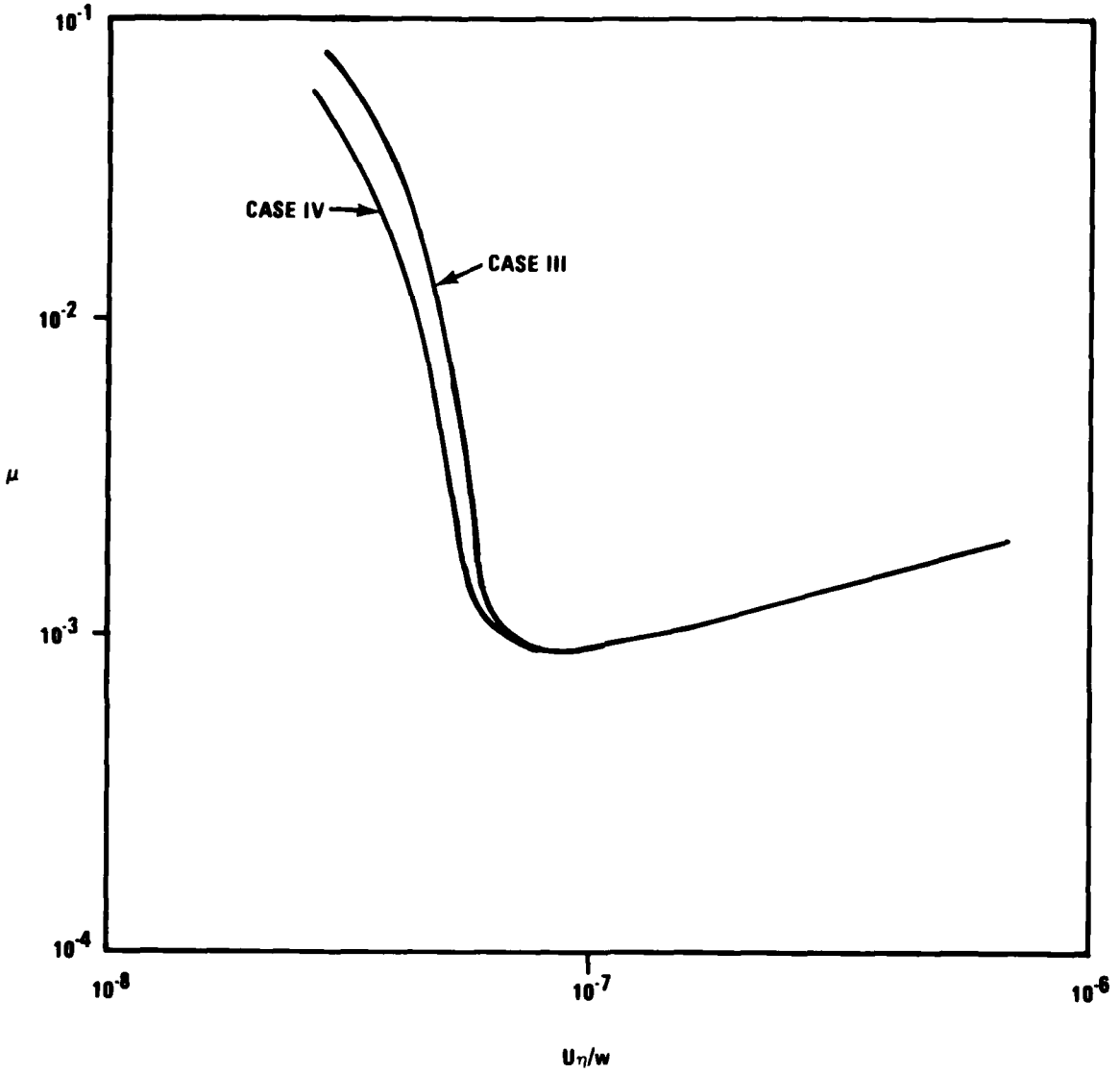


**COEFFICIENT OF FRICTION**
**VS**
**SPEED-LOAD PARAMETER**

FIGURE 5

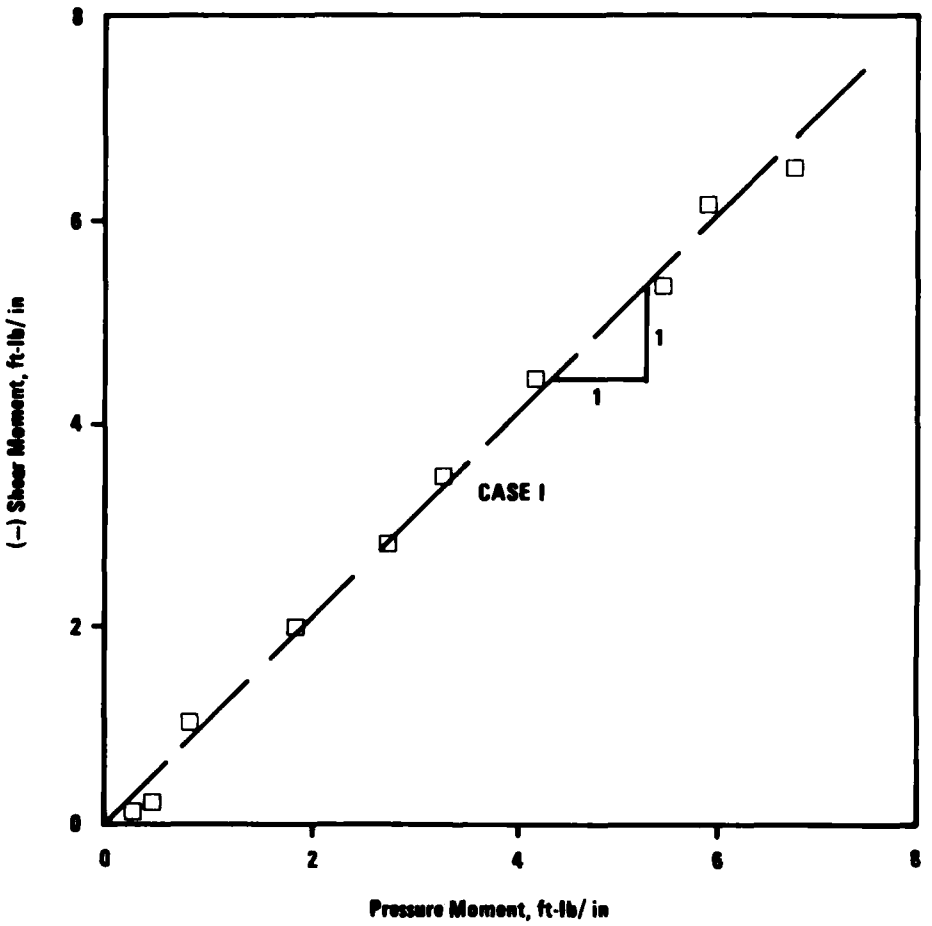


Typical Calculated Shear, Pressure Moments
(Case I)

FIGURE 6

C O P Y

# APPENDIX 1

## Program Listing

```
100   PRINT "DO YOU WANT AN EXPLANATION OF THIS PROGRAM?"
110   INPUT P$
120   IF SEG$ (P$, 1, 1) = "Y" THEN 3120
210   PRINT "INPUT RPM"
220   INPUT U1
230   PRINT "INPUT MEAN BEARING SURFACE DIAMETER, INCHES"
240   INPUT K1
250   PRINT "INPUT VISCOSITY, REYNS X 1E6"
260   INPUT M2
270   M2 = M2*1E-6
280   PRINT "INPUT SHOE LENGTH, INCHES"
290   INPUT B
300   PRINT "INPUT ASPERITY HEIGHT, INCHES"
310   INPUT C2
320   PRINT "INPUT YIELD BEARING STRESS, PSI X 1E-3"
330   INPUT P8
340   P8 = P8*1E3
350   PRINT "INPUT RATIO OF SHEAR TO YIELD STRESS"
360   INPUT M3
370   PRINT "INPUT CROWN HEIGHT, INCHES"
380   INPUT H4
390   PRINT "INPUT PIVOT CENTER, X, Y, FRACTION OF SHOE LENGTH"
400   INPUT P2, P3
410   U2 = U1*(3. 1416/60)*K1
440
450   K5 = 0
460   A = .0042*EXP(10.88*P2)
470   A = A + (H4/B) * 1E4
480   IF A > 1 THEN 500
490   A = 1. 001
500   Z1 = . 005
510   M5 = . 00025*(P2 + . 5)
520   K9 = 0
530   K8 = 0
540   N8 = 0
560   K7 = 0
570   PRINT
580   L1 = 0
590   I6 = 0
600   I7 = 0
605   X4 = 0
606   X5 = 0
610   I8 = 0
620   J1 = 0
630   J6 = 0
640   J7 = 0
650   J8 = 0
660   N9 = 0
670   I1 = 0
680   I2 = 0
690   I3 = 0
```

```
700   I4=0
704   X4=0
705   X4=0
710   T1=0
720   T2=0
730   T3=0
740   H2=M5*B/(A-1)
750   M6=H2/B
760   H7=H4/B
796   X5=0
810   G=P8*M6^2/(M2*U2)
820   H=G*M3/M6
830   M1=M5*B/1000
840   M1=M1/H2
850   FOR X= Z1 TO1 STEP Z1
860   F=H4/H2
870   F1=A+(1-A)*((1+4*H4/(M5*B))*X-(4*H4/(M5*B))*X^2)
880   C1=C2/H2
890   IF C1/F1<1 THEN 1000
900   N1=(C1^8)/8 +(16/35)*C1*(C1^6)*F1+ 5*F1*(C1^6)*F1
910   N1=N1 -(.25)*(C1*F1)^4 + (C1^2)*(F1^6)* 1-(F1^8)/56
920   N1=N1*35/(32*C1^7)
930   D2=(C1^10)/40 +(16/105)*F1*C1^9 +(3/8)*(C1^8)*(F1^2)
940   D2=D2+(16/35)*(C1^7)*F1^3
950   D2=D2+.25*(C1^6)*F1^4 - (1/20)*C1^4*F1^6 +3/280
960   D2=D2-3/280 +(3/280)*(C1^2)*(F1^8)-(1/840)*(F1^10)
970   D2=35*D2/(32*C1^7)
980   D1=D2/N1
990   GO TO 1020
1000  D1=F1 * (F1 ↑ 2 + C1 ↑ 2/3)
1010  D2= F1*D1
1020  I1=I1+ Z1/(D1)
1030  I2=I2+Z1/(D2)
1040  NEXT X
1050  C=I1/I2
1060  FOR X =Z1 TO 1 STEP Z1
1070  F1=A+(1-A)*((1+4*H4/(M5*B))*X-(4*H4/(M5*B))*X^2)
1080  C1=C2/H2
1090  IF C1/F1<1THEN 1460
1100  L1=L1+Z1
1110  N9=N9+1
1120  X4=X+Z1*(1-N9)
1130  R1=(1/(32*C1^7))*(16*C1^7 +35*(C1^6)*F1-35*(C1^4)*F1^3)
1140  R1=R1+ (1/(32*C1^7))*(21*(C1^2)*F1^5 -5*F1^7)
1150  I6=I6+(1-R1)*Z1
1160  J6=J6+(1-R1)*X*Z1
1170  N1=(C1^8)/8+(16/35)*(C1^7)*F1+.5*(C1^6)*(F1^2)
1180  N1=N1-.25*(C1^4)*F1^4+.1*(C1^2)*(F1^6)-(1/56)*(F1)^8
1190  N1=35*N1/(32*C1^7)
1200  D2=(C1^10)/40+(16/105)*(C1^9)*F1 +(3/8)*(C1^8)*F1^2
1210  D2=D2+ (16/35)*(C1^7)*(F1^3)+. 25*(C1^6)*F1^4
```

```
1220  D2=D2-.05*(C1^4)*(F1^6) +(3/280)*(C1^2)*(F1^8)-(1/840)*(F1^10)
1230  D2=35*D2/(32*C1^7)
1240  D1=D2/N1
1250  N3=((C1^2-F1^2)^3)*LOG((F1+C1)/M1)+(8*F1^3/3)*(F1+C1)^3
1260  N3=N3-(1/6)*F1+C1)^6-4*(C1^2-F1^2)*F1*(C1+F1)^3
1270  N3=N3+6*(C1^2-F1^2)^2*F1*(F1+C1)+6*(C1^2-F1^2)*F1^2*(C1+F1)^2
1280  N3=N3-3*(F1^2)*(C1+F1)^4+(6/5)*F1*(C1+F1)^5
1290  N3=N3+(3/4)*(C1^2-F1^2)*((F1+C1)^4)
1300  N3=N3-(3/2)*(C1^2-F1^2)*(C1^2-F1^2)*(F1+C1)^2
1310  N3=N3*(35/(32*C1^7))
1320  T1=T1+R1*Z1*(N3+3*N1*(N1-C)/D2)
1330  I3=I3+Z1/D1
1340  I4=I4+Z1/D2
1350  Q=I3-C*I4
1360  IF Q>-1E-4 THEN 1410
1370  N8=N8+1
1410  Q=Q*6
1420  I7=I7+Q*Z1*R1
1430  J7=Q*Z1*R1*X+J7
1440  X5=X
1450  GO TO 1710
1460  D1=F1*(F1↑2 + C1↑2/3)
1470  D2=D1*F1
1480  N1=F1
1520  IF C1<1E-3 THEN 1570
1521  IF F1>0 THEN 1530
1522  PRINT "YOU WILL HAVE TO INCREASE SLOPE FOR A SOLUTION"
1523  GO TO 2506
1530  N3=((C1^2-F1^2)^3)*LOG((F1+C1)/(F1-C1))
1540  N3=N3+ (2/15)*(C1*F1)*(15*F1^4-40*(C1*F1)^2+33*C1^4)
1550  N3=N3*(35/(37*C1^7))
1560  GO TO 1580
1570  N3=1/F1
1580  I3=I3+Z1/(D1)
1590  I4=I4 +Z1/(D2)
1600  Q=I3-C*I4
1610  IF Q>-1E-4 THEN 1660
1620  N8=1
1660  LET Q=Q*6
1670  N3=1/F1
1680  T2=T2+(3*N1*(N1-C)/D2+N3)*Z1
1690  I8=I8+Z1*Q
1700  J8=J8+Z1*Q*X
1710  NEXT X
1720  W=I7+I8+G*I6
1730  W1=W*U2*M2/M6^2
1740  W2=I7*U2*M2/M6^2
1750  W3=I8*U2*M2/M6^2
1760  W4=G*I6*U2*M2/M6 2
1780  T3=T1+T2+I6*H
1790  T5=T2*U2*M2/M6
```

```
1800  T6=T1*U2*M2/M6
1810  T7=I6*H*U2*M2/M6
1820  T4=T3*U2*M2/M6
1830  U3=U2*M2/W1
1840  IF U3>0 THEN 1860
1850  GO TO 1990
1860  R3=(T4/W1)/(U3^.5)
1870  M=J7+J8+J6*G
1880  P1=M/W
1890  M8=W1*(P1-P2)+T4*P3
1900  IF ABS(M8/W1)<.001 THEN 2150
1910  IF M8>0 THEN 2030
1920  A=A*(1+.1/(1+K8))^5
1930  K7=K7+1
1940  IF K7>40 THEN 2505
1950  IF K7<15 THEN 1970
1960  K7=1.5
1970  IF P1>0 THEN 2000
1990  GO TO 1522
2000  K9=K9+1
2010  K5=K5+1
2020  GO TO 570
2030  A=A*(1-.1/(1+K7))^.5
2031  IF A>1 THEN 2040
2032  PRINT "YOU WILL HAVE TO DECREASE SLOPE FOR A SOLUTION"
2033  A=2
2034  PRINT "CURRENT SLOPE =";M5
2035  GO TO 2506
2040  K8=K8+1
2050  IF K8>30 THEN 2505
2060  IF K8<15 THEN 2080
2070  K8=1.5
2080  IF P1>0 THEN 2110
2100  GO TO 1522
2110  K9=K9+1
2120  K5=K5+1
2130  IF K9>30 THEN 2505
2140  GO TO 570
2150  PRINT "SLOPE =";M5;"PIVOT =";P2;",";P3
2160  PRINT
2170  PRINT "CENT. PRESS=";P1
2180  PRINT "PURE HYDRO LOAD=";W3/B
2190  PRINT "MIXED HYDRO LOAD=";W2/B;"PSI"
2200  PRINT "CONTACT LOAD=";W4/B;" PSI"
2210  PRINT "TOT. LOAD=";W1/B;" PSI"
2220  PRINT "PURE HYDRO FRICT=";T5/B;"PSI"
2230  PRINT "MIXED HYDRO FRICT=";T6/B;" PSI"
2240  PRINT "CONTACT FRICT. =";T7/B;" PSI"
2250  PRINT "TOT. FRICT=";T4/B;"PSI"
2260  PRINT "U-ETA/W=";U3
2270  PRINT "COEF. OF FRICTION=";T4/W1+M5
```

C O P Y

```
2280  PRINT "SHOE SPEED = "; U2; " IN/S"
2290  PRINT "PRESS. MOM. = "; W1*B*(P1-P2)/12; "FT LB/IN"
2300  PRINT "SHEAR MOM. = "; T4*P3*B /12; "FT-LB/IN"
2310  PRINT "H1/H2 RATIO = "; A
2320  PRINT "H2 = "; H2
2330  PRINT "C/H2"; C1
2340  PRINT "ABRAMOVITZ'S PHI = "; F
2350  PRINT
2360  PRINT  "NO. ITERATIONS = "; K9
2361  IF N8 < .5 THEN 2370
2362  PRINT "BEARING MAY CAVITATE"
2370  PRINT
2380  IF X4 = 0 THEN 2410
2390  PRINT "MIXED LUBRICATION BETWEEN"; X4*100; "AND"; (X5 + . 00001)*100; "%"
2400  GO TO 2420
2410  PRINT "NO MIXED LUBRICATION"
2420  PRINT
2505  PRINT "FOR HIGHER LOAD, DECREASE SLOPE, AND VICE-VERSA"
2506  PRINT "NEW SLOPE? (INPUT ZERO TO END THIS SEQUENCE)"
2507  INPUT M5
2508  IF M5 < 1E-6 THEN 2560
2510  GO TO 520
2560  PRINT "TOTAL ITERATIONS THIS RUN = "; K5
2570  PRINT "CURRENT VALUES:  RPM = "; U1; "DIA = "; K1; "IN. , VISCOSITY = "; M2; "REYNS,
2580  PRINT "LENGTH = "; B; "IN." ; "ASP HEIGHT = "; C2; "IN. , YIELD STRESS = "; P8
2590  PRINT  "RATIO, SHEAR/YIELD = "; M3; "CROWN HEIGHT = "; H4; "IN."
2600  PRINT "PIVOT CENTER = "; P2;", ";P3
2610  PRINT "DO YOU WANT TO CHANGE A PARAMETER AND RERUN?"
2620  INUT E$
2630  IF SEG$ (E$, 1, 1) = "Y" THEN 2670
2640  IF SEG$ (E$, 1, 1) = "N" THEN 3370
2650  PRINT "INCORRECT RESPONSE, ANSWER YES OR NO"
2660  GO TO 2620
2670  PRINT "NEW PARAMETER?"
2680  INPUT D$
2690  IF SEG$ (D$, 1, 2) = "RP" THEN 2820
2700  IF SEG$ (D$, 1, 1) = "D" THEN 2850
2710  IF SEG$ (D$, 1, 1) = "V" THEN 2880
2720  IF SEG$ (D$, 1, 1) = "L" THEN 2920
2730  IF SEG$ (D$, 1, 1) = "A" THEN 2950
2740  IF SEG$ (D$, 1, 1) = "Y" THEN 2980
2750  IF SEG$ (D$, 1, 2) = "RA" THEN 3020
2760  IF SEG$ (D$, 1, 1) = "C" THEN 3050
2770  IF SEG$ (D$, 1, 1) = "P" THEN 3080
2780  IF SEG$ (D$, 1, 2) = "RU" THEN 410
2790  PRINT "OPTIONS ARE RPM, DIAMETER, VISCOSITY, LENGTH, ASPERITY,"
2800  PRINT "YIELD, RATIO, CROWN, PIVOT, RUN"
2810  GO TO 2670
2820  PRINT "NEW RPM?"
2830  INPUT U1
2840  GO TO 2670
```

```
2850  PRINT "NEW DIAMETER, INCHES?"
2860  INPUT K1
2870  GO TO 2670
2880  PRINT "NEW VISCOSITY, REYNS X 1E6?"
2890  INPUT M2
2900  M2 = M2*1E-6
2910  GO TO 2670
2920  PRINT "NEW LENGTH, INCHES?"
2930  INPUT B
2940  GO TO 2670
2950  PRINT "NEW ASPERITY HEIGHT, IN.?"
2960  INPUT C2
2970  GO TO 2670
2980  PRINT "NEW YIELD STRESS, PSI X 1E-3?"
2990  INPUT P8
3000  P8 = P8*1E3
3010  GO TO 2670
3020  PRINT "NEW RATIO, SHEAR/YEILD?"
3030  INPUT M3
3040  GO TO 2670
3050  PRINT "NEW CROWN HEIGHT, INCHES?"
3060  INPUT H4
3070  GO TO 2670
3080  PRINT "NEW PIVOT CENTER, X, Y, FRACTION OF SHOE LENGTH?"
3090  INPUT P2,P3
3100  GO TO 2670
3120  PRINT
3130  PRINT "THIS PROGAM WILL CALCULATE THE PERFORMANCE CHARACTERISTICS"
3140  PRINT "FOR A CROWNED SLIDER BEARING OPERATING IN THE MIXED"
3150  PRINT "LUBRICATION REGIME.  THE INPUTS REQUIRED ARE THE ROTATIONAL"
3160  PRINT "SPEED, THE SHOE LENGTH, THE VISOCITY OF THE LUBRICANT,"
3170  PRINT "THE MEAN BEARING SURFACE DIAMETER, THE ROUGHNESS ASPERITY"
3180  PRINT "HEIGHT, THE BEARING YIELD STRESS, THE RATIO OF THE SHEAR"
3190  PRINT "STRESS TO YIELD STRESS, THE CROWN HEIGHT, AND THE PIVOT"
3200  PRINT "COORDINATES, MEASURED FROM THE LEADING EDGE OF THE SHOE,"
3210  PRINT "AND EXPRESSED IN FRACTION OF SHOE LENGTH.  ALL OTHER"
3220  PRINT "DIMENSIONS ARE INDICATED IN APPROPRIATE INPUT STATEMENTS"
3230  PRINT
3240  PRINT "AT THE END OF EACH RUN, ANY OF THE ABOVE PARAMETERS MAY BE "
3250  PRINT "CHANGE FOR A RERUN.  DURING EACH RUN, THE OPERATOR"
3260  PRINT "WILL OBTAIN A TABULATION OF THE SPEED-LOAD PARAMETER"
3270  PRINT "(SHOE SPEED X VISCOSITY/(BEARING PRESSURE X LENGTH)"
3280  PRINT "VERSUS COEFFICIENT OF FRICTION AND THE RATIO OF LEADING"
3290  PRINT "AND TRAILING EDGE HEIGHTS."
3300  PRINT
3310  PRINT "THE OPERATOR WILL BE ADVISED IF HE HAS SELECTED AN"
3320  PRINT "UNWORKABLE COMBINATION OF PARAMETERS.  NORMALLY, CROWN"
3330  PRINT "HEIGHT/SHOE LENGTH RATIOS GREATER THAN 0. 0001 WILL LEAD"
3340  PRINT "TO BEARING INTERFERENCE, DEPENDING ON THE PIVOT POINT."
3350  PRINT
3360  GO TO 210
```

```
3370    PRINT "PROGRAM TERMINATED"
3380    END
```

## APPENDIX B

## INTEGRALS FOR CIRCUMFERENTIAL AND AXIAL COMPUTATION

Integral formula is to be developed for

$$A_k(\xi) = \int \frac{\xi^k \, d\xi}{H(\xi)^3}; \quad H(\xi) = b_0 + b_1 \xi + b_2 \xi^2/2 \tag{B-1}$$

First, special characteristics of the second order polynomial will be considered.

(i) Degenerate Constant $b_1 = b_2 = 0$

$$A_k(\xi) = \frac{\xi^{k+1}}{(k+1)\, b_o^3} \tag{B-2}$$

(ii) Degenerate Linear Function $b_2 = 0, \; b_1 \neq 0$

$$A_0(\xi) = -\frac{1}{2\, b_1 H^2} \tag{B-3}$$

$$A_1(\xi) = -\frac{1}{b_1}\left\{\frac{1}{b_1 H} + b_0 A_0\right\} \tag{B-4}$$

(iii) General Case $(b_1, b_2) \neq 0$

Write

$$\lambda^2 = b_1^2 - 2\, b_0 b_2 \tag{B-5}$$

then

$$H = \left\{(b_2\xi + b_1)^2 - \lambda^2\right\} / (2\, b_2) \tag{B-6}$$

$$\frac{1}{H} = \frac{b_2}{\lambda}\left\{\frac{1}{b_2\xi + b_1 - \lambda} - \frac{1}{b_2\xi + b_1 + \lambda}\right\} \tag{B-7}$$

$$\int d\xi/H = \left\{ln\left(\frac{b_2\xi + b_1 - \lambda}{b_2\xi + b_1 + \lambda}\right)\right\} / \lambda \tag{B-8}$$

$$H^{-2} = (b_2/\lambda)^2 \left\{ \frac{1}{(b_2\xi + b_1 - \lambda)^2} - \frac{2}{\{(b_2\xi + b_1)^2 - \lambda^2\}} + \frac{1}{(b_2\xi + b_1 + \lambda)^2} \right\}$$

$$= (b_2/\lambda)^2 \left\{ \frac{1}{(b_2\xi + b_1 - \lambda)^2} + \frac{1}{(b_2\xi + b_1 + \lambda)^2} - \frac{1}{b_2 H} \right\}$$

$$\int H^{-2} d\xi = - \frac{b_2\xi + b_1}{\lambda^2 H} - \frac{b_2}{\lambda^2} \int H^{-1} d\xi \qquad \text{(B-9)}$$

$$H^{-3} = (b_2/\lambda)^3 \left\{ \frac{1}{(b_2\xi + b_1 - \lambda)^3} - \frac{6\lambda}{\{(b_2\xi + b_1)^2 - \lambda^2\}^2} - \frac{1}{(b_2\xi + b_1 - \lambda)^3} \right\}$$

$$= (b_2/\lambda)^3 \left\{ \frac{1}{(b_2\xi + b_1 - \lambda)^3} - \frac{1}{(b_2\xi + b_1 + \lambda)^3} - \frac{3\lambda}{2 b_2^2 H^2} \right\}$$

$$A_0(\xi) = - \frac{(b_2\xi + b_1)}{2\lambda^2 H^2} - \frac{3 b_2}{\lambda^2} \int H^{-2} d\xi \qquad \text{(B-10)}$$

$$A_1(\xi) = - \frac{1}{2 b_2 H^2} - (b_1/b_2) A_0(\xi) \qquad \text{(B-11)}$$

In the event that $b_1^2 - 2b_0b_2 < 0$, instead of Equation (B-5), write

$$\gamma^2 = -\lambda^2 = 2b_0b_2 - b_1^2 \qquad \text{(B-12)}$$

Then Equation (B-8) can be rewritten as

$$\int H^{-1} d\xi = - (2/\gamma) \tan^{-1} \{\gamma/(b_2\xi + b_1)\} \qquad \text{(B-13)}$$

## APPENDIX C

## INTEGRALS FOR RADIAL COMPUTATION

Integral formula is to be developed for

$$B_k(\xi) = \int \frac{\xi^k \, d\xi}{(\xi+\xi_o) H^3}; H(\xi) = c_0 + c_1 \xi + \frac{1}{2} c_2 \xi^2 \tag{C-1}$$

(i) Degenerate Constant $c_1 = c_2 = 0$

$$B_0(\xi) = \frac{1}{c_0^3} \ln(\xi + \xi_o) \tag{C-2}$$

$$B_1(\xi) = \frac{1}{c_0^3} [\xi - \xi_o \ln(\xi - \xi_o)] \tag{C-3}$$

(ii) Degenerate Linear Function $c_2 = 0$, $c_1 \neq 0$

$$\frac{1}{(\xi + \xi_o) H^3} = \frac{1}{(\xi + \xi_o) H_o^3} - c_1 \left\{ \frac{1}{H_o^3 H} + \frac{1}{H_o^2 H^2} + \frac{1}{H_o H^3} \right\}; \text{where } H_o = c_o - c \tag{C-4}$$

$$B_0(\xi) = \frac{1}{H_o^3} \ln\left( \frac{\xi + \xi_o}{H} \right) + \frac{1}{H_o^2 H} + \frac{1}{2 H_o H^2}$$

$$B_1(\xi) = \xi_o \left[ \frac{1}{H_o^3} \ln\left( \frac{H}{\xi + \xi_o} \right) - \frac{1}{H_o^2 H} \right] - \frac{c_o}{2 c_1 H_o H^2} \tag{C-5}$$

(iii) General Case $(c_1, c_2) \neq 0$

Write

$$\lambda^2 - c_1^2 - 2 c_0 c_2 \tag{C-6}$$

$$H = \frac{1}{2 c_2} \left[ (c_2 \xi + c_1)^2 - \lambda^2 \right]; H_o = H(-\xi_o) \tag{C-7}$$

$$\frac{1}{H} = \frac{c_2}{\lambda}\left[\frac{1}{c_2\xi + c_1 - \lambda} - \frac{1}{c_2\xi + c_1 + \lambda}\right] \tag{C-8}$$

$$\frac{1}{(\xi+\xi_o)H} = \frac{1}{H_o(\xi+\xi_o)} + \frac{c_2^2}{\lambda}\left\{\frac{1}{(c_2\xi_o - c_1 + \lambda)(c_2\xi + c_1 - \lambda)} - \frac{1}{(c_2\xi_o - c_1 - \lambda)(c_2\xi + c_1 + \lambda)}\right\}$$

$$\int \frac{d\xi}{(\xi+\xi_o)H}$$

$$= \frac{1}{2H_o}\left\{ln\left[\frac{(\xi+\xi_o)^2}{H}\right] - \frac{(c_2\xi_o - c_1)}{\lambda} ln\left[\frac{c_2\xi + c_1 - \lambda}{c_2\xi + c_1 + \lambda}\right]\right\} \tag{C-9}$$

$$\frac{1}{H^2} = \left(\frac{c_2}{\lambda}\right)^2\left\{\frac{1}{(c_2\xi + c_1 - \lambda)^2} - \frac{1}{c_2 H} + \frac{1}{(c_2\xi + c_1 + \lambda)^2}\right\}$$

$$\frac{1}{(\xi+\xi_o)H^2} = \left(\frac{c_2}{\lambda}\right)^2\left\{\frac{1}{(\xi+\xi_o)(c_2\xi + c_1 - \lambda)^2} + \frac{1}{(\xi+\xi_o)(c_2\xi + c_1 + \lambda)^2} - \frac{1}{c_2(\xi+\xi_o)H}\right\}$$

$$\frac{1}{(\xi+\xi_o)(c_2\xi + c_1 \mp \lambda)^2} = \frac{1}{(c_2\xi_o - c_1 \pm \lambda)^2}\left\{\frac{1}{\xi+\xi_o} - \frac{c_2}{c_2\xi + c_1 \mp \lambda}\right\} + \frac{c_2}{(c_2\xi_o - c_1 \pm \lambda)(c_2\xi + c_1 \mp \lambda)^2}$$

$$\int \frac{d\xi}{(\xi+\xi_o)H^2} = \frac{1}{2H_o}\left\{\frac{1}{H_o}\left[\frac{(c_2\xi_o - c_1)^2 + \lambda^2}{2\lambda^2}\right] ln\,\frac{(\xi+\xi_o)^2}{H} + \frac{(c_2\xi_o - c_1)}{\lambda} ln\left(\frac{c_2\xi + c_1 - \lambda}{c_2\xi + c_1 + \lambda}\right)\right|$$

$$- \frac{[(c_2\xi_o - c_1)(c_2\xi + c_1) - \lambda^2|}{\lambda^2 H}\}$$

$$- \frac{c_2}{\lambda^2}\int \frac{d\xi}{(\xi+\xi_o)H} \tag{C-10}$$

$$\frac{1}{H^3} = \left(\frac{c_2}{\lambda}\right)^3 \left\{ \frac{1}{(c_2\xi + c_1 - \lambda)^3} - \frac{1}{(c_2\xi + c_1 + \lambda)^3} - \frac{3\lambda}{2\,c_2^2 H^2} \right\}$$

$$\frac{1}{(\xi + \xi_o) H^3} = \left(\frac{c_2}{\lambda}\right)^3 \left\{ \frac{1}{(\xi + \xi_o)(c_2\xi + c_1 - \lambda)^3} - \frac{1}{(\xi + \xi_o)(c_2\xi + c_1 + \lambda)^3} - \frac{3\lambda}{2\,c_2^2 (\xi + \xi_o) H^2} \right\}$$

$$\frac{1}{(\xi + \xi_o)(c_2\xi + c_1 \mp \lambda)^3} = \frac{1}{(c_2\xi_o - c_1 \pm \lambda)^3} \left( \frac{c_2}{c_2\xi + c_1 \mp \lambda} - \frac{1}{\xi + \xi_o} \right)$$

$$- \frac{c_2}{(c_2\xi_o - c_2 \pm \lambda)(c_2\xi + c_1 \mp \lambda)^2} \left( \frac{1}{c_2\xi_o - c_1 \pm \lambda} - \frac{1}{c_2\xi + c_1 \mp \lambda} \right)$$

$$B_0(\xi) = \frac{1}{4H_o} \left\{ \frac{1}{H_o^2} \left[ \frac{3(c_2\xi_o - c_1)^2 + \lambda^2}{2\lambda^2} \ln \frac{(\xi + \xi_0)^2}{H} - \frac{(c_2\xi_o - c_1)[(c_2\xi_o - c_1)^2 + 3\lambda^2]}{2\lambda^3 H_c} \ln \left( \frac{c_2\xi + c_1 - \lambda}{c_2\xi + c_1 + \lambda} \right) \right. \right.$$

$$\left. \left. + \frac{1}{\lambda^2 H_o H} \left[ 3c_2 - (c_2\xi_o - c_1)(c_2\xi + c_1) \left( \frac{2}{H_o} + \frac{1}{H} \right) \right] \right] \right\} \qquad \text{(C-11)}$$

$$B_1(\xi) = -\xi_o B_0(\xi) - \left( \frac{c_2\xi + c_1}{2\lambda^2 H^2} \right) + \left( \frac{3c_2}{\lambda^2} \right) \left\{ \left( \frac{c_2\xi + c_1}{\lambda^2 H} \right) + \frac{c_2}{\lambda^3} \ln \left( \frac{c_2\xi + c_1 - \lambda}{c_2\xi + c_1 + \lambda} \right) \right\} \qquad \text{(C-12)}$$

If $\lambda^2 = -\gamma^2 < 0$, then both $\lambda$ and $\ln [(c_2\xi + c_1 - \lambda)/(c_2\xi + c_1 - \lambda)]$ would be imaginary. However

$$\frac{1}{\lambda} \ln \left( \frac{c_2\xi + c_1 - \lambda}{c_2\xi + c_1 + \lambda} \right) \equiv - \frac{2}{\gamma} \tan^{-1} \left( \frac{\gamma}{c_2\xi + c_1} \right) \qquad \text{(C-13)}$$

remains real and should be used in computing Equations (C-9), (C-10), (C-11) and (C-12).

## INITIAL DISTRIBUTION

| Copies | | CENTER DISTRIBUTION | | |
|---|---|---|---|---|
| | | Copies | Code | Name |
| 2 | ONR | | | |
| | 1 Code 431/Mr. K. Ellingsworth | | | |
| | 1 Code 621/Dr. R. Miller | 2 | 0123 | Dr. Jewell |
| 7 | NAVSEA | 1 | 15 | Dr. Bai |
| | 2 SEA 05R25/Dr. Vanderveldt | | | |
| | 5 SEA 56X4 | 1 | 17 | Dr. Ma |
| 12 | DTIC | 2 | 2723 | Dr. E. Quandt |
| 15 | COLUMBIA UNIVERSITY | 1 | 28 | J. R. Belt |
| | Dr. Coda Pan | | | |
| | | 1 | 2809 | C. DeLashmet |
| | | 1 | 283 | H. Singerman |
| | | 10 | 2832 | J. F. Dray |
| | | 10 | 2832 | T. L. Daugherty |
| | | 10 | 5211.1 | Reports Distribution |
| | | 1 | 522.1 | Unclass. Library (C) |
| | | 1 | 522.2 | Unclass. Library (A) |

DTNSRDC ISSUES THREE TYPES OF REPORTS

1. DTNSRDC REPORTS, A FORMAL SERIES, CONTAIN INFORMATION OF PERMANENT TECHNICAL VALUE. THEY CARRY A CONSECUTIVE NUMERICAL IDENTIFICATION REGARDLESS OF THEIR CLASSIFICATION OR THE ORIGINATING DEPARTMENT.

2. DEPARTMENTAL REPORTS, A SEMIFORMAL SERIES, CONTAIN INFORMATION OF A PRELIMINARY, TEMPORARY, OR PROPRIETARY NATURE OR OF LIMITED INTEREST OR SIGNIFICANCE. THEY CARRY A DEPARTMENTAL ALPHANUMERICAL IDENTIFICATION.

3. TECHNICAL MEMORANDA, AN INFORMAL SERIES, CONTAIN TECHNICAL DOCUMENTATION OF LIMITED USE AND INTEREST. THEY ARE PRIMARILY WORKING PAPERS INTENDED FOR INTERNAL USE. THEY CARRY AN IDENTIFYING NUMBER WHICH INDICATES THEIR TYPE AND THE NUMERICAL CODE OF THE ORIGINATING DEPARTMENT. ANY DISTRIBUTION OUTSIDE DTNSRDC MUST BE APPROVED BY THE HEAD OF THE ORIGINATING DEPARTMENT ON A CASE-BY-CASE BASIS.